





**LIBRARY**  
**Michigan State**  
**University**

This is to certify that the

thesis entitled

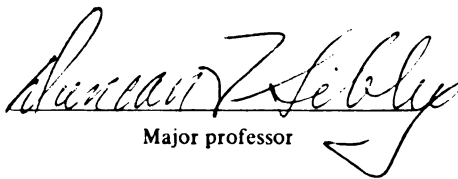
CRYSTAL SIZE DISTRIBUTION COMPARISON  
IN ORDOVICIAN DOLOMITES

presented by

ROBERT CRAIG BROWN

has been accepted towards fulfillment  
of the requirements for

MASTER degree in SCIENCE

  
Major professor

Date July 21, 1994



**PLACE IN RETURN BOX** to remove this checkout from your record.  
**TO AVOID FINES** return on or before date due.

DATE DUE	DATE DUE	DATE DUE
_____	_____	_____
_____	_____	_____
_____	_____	_____
_____	_____	_____
_____	_____	_____
_____	_____	_____
_____	_____	_____

**CRYSTAL SIZE DISTRIBUTION COMPARISON  
IN ORDOVICIAN DOLOMITES**

**by**

**Robert Craig Brown**

**A THESIS**

**Submitted to  
Michigan State University  
in partial fulfillment of the requirements  
for the degree of**

**MASTER OF SCIENCE**

**Department of Geological Sciences**

**1994**

## **ABSTRACT**

### **CRYSTAL SIZE DISTRIBUTION COMPARISON IN ORDOVICIAN DOLOMITES**

**By**

**Robert Craig Brown**

Crystal size distributions (CSDs) vary according to nucleation and growth. CSDs are compared within and between the Trenton Formation (Middle Ordovician) and the Saluda Formation (Upper Ordovician) dolomites, and to theoretical models (site-saturation, Johnson-Mehl). Comparisons are made by 1) t-test of standard deviations of normalized CSDs, 2) Kolmogorov-Smirnov goodness-of-fit (K-S) test between CSDs, 3) K-S test of CSDs to normal, lognormal, and gamma distributions, and 4) t-test of the gamma distribution shape factor, alpha. Dolomite CSDs are more closely represented by the gamma distribution than the normal or lognormal distributions. Trenton CSDs are not significantly different from each other despite significant differences in mean grain size. The pattern of CSD shape does not change relative to mean grain size. Saluda CSDs are not different from each other, but are different from Trenton CSDs. Theoretical models do not resemble the dolomite CSDs.

## Acknowledgements

Many thanks go to the MSU Geology Department Faculty and Staff, for their assistance, encouragement, and financial support. I appreciate the opportunity to study under the guidance of Duncan F. Sibley, Michael A. Velbel, and David T. Long. I appreciate being able to meet and talk with Aureal T. Cross, John T. Wilband, Thomas A. Vogel, Graham Larson, F.W. Cambray, Hugh Bennett, and Bob Anstey.

My thanks goes to Jill and Tom Stebbins for welcoming me into their busy and wonderful household in Okemos. I would like to acknowledge my friends (whose advice to finish as soon as possible was promptly ignored, yet they remain good friends) Myung Yi, Abdule Muhanna, Mohammad Ghavidal-Syooki, Mounir Saad, and Soo Meen Wee. Acknowledgement should also go to Sgt. McCloud (Dave Cook) and his sidekick crony in crime, Chester (Erin Lynch) for welcoming me to MSU. I want to thank my family for their humor throughout this ordeal.

## TABLE OF CONTENTS

<b>LIST OF TABLES .....</b>	<b><i>vi</i></b>
<b>LIST OF FIGURES .....</b>	<b><i>viii</i></b>
<b>INTRODUCTION .....</b>	<b>1</b>
<b>GENERAL GEOLOGIC SETTINGS OF SAMPLE DOLOMITES .....</b>	<b>3</b>
Trenton Formation Dolomite .....	3
Saluda Formation Dolomite .....	7
<b>COMPUTER - GENERATED MICROSTRUCTURES AND ANALYSES .....</b>	<b>12</b>
<b>METHODS .....</b>	<b>18</b>
Method of Crystal Size Distribution Measurement .....	18
Stereology of CSD Determination .....	18
Statistical Analyses .....	24
Method Reproducibility .....	32
<b>CSD DATA .....</b>	<b>43</b>
Trenton Formation .....	43
Saluda Formation .....	50
Theoretical Computer - Generated Microstructures .....	53
Analysis and Comparison Between Formation and Theoretical CSDs .....	55
<b>DISCUSSION .....</b>	<b>58</b>
<b>CONCLUSIONS .....</b>	<b>63</b>
<b>APPENDIX A</b>	
Thin-Section Description, Photographs And Drawing .....	65
<b>APPENDIX B</b>	
Two-Sample Kolmogorov-Smirnov Goodness-Of-Fit Tests .....	82



**TABLE OF CONTENTS (cont'd)**

**APPENDIX C**  
    **Normalized Crystal Size Distribution Frequency Histograms And**  
    **Crystal Size Distribution To Thin-Section Sample Key ..... 88**

**BIBLIOGRAPHY ..... 127**

## LIST OF TABLES

<b><u>TABLE</u></b>	<b><u>PAGE</u></b>
1      Two-Sample Kolmogorov-Smirnov Test Evidence of Reproducibility On Measured Crystal Size Distribution Data.....	41
2      Comparison of Statistical Values of Duplicate CSD Counts and Thin-Section Samples.....	42
3      Trenton Formation CSD Statistical Values .....	44-45
4      Two Sample K-S Tests Between Thin-Section TL1 Clasts .....	47
5      Two Sample K-S Tests Between Thin-Section TL2 Clasts .....	47
6      Two Sample K-S Tests Between Thin-Section TL3 Clasts .....	48
7      Two Sample K-S Tests Between Thin-Section TL7 Clasts .....	48
8      Two Sample K-S Tests Between Thin-Section TL8 Clasts .....	49
9      Two Sample K-S Tests Between Thin-Section TL9 Clasts .....	49
10     Two Sample K-S Tests Between Thin-Section TL11 Clasts.....	49
11     Saluda Formation CSD Statistical Values .....	52
12     Two-Sample Kolmogorov-Smirnov Goodness-Of-Fit Tests Between Saluda Formation Samples .....	53
13     Theoretical Computer-Generated Microstructure CSD Statistical Values .....	54
14     Two-Sample Kolmogorov-Smirnov Goodness-Of-Fit Tests Between Normalized Theoretical Computer-Generated Microstructure CSDs .....	55

## LIST OF TABLES (cont'd)

<b><u>TABLE</u></b>		<b><u>PAGE</u></b>
15	Comparison of Mean and Standard Deviations of the Means and Standard Deviations of the Alpha, Normalized Standard Deviation, Skewness, and Inclusive Graphic Skewness Values for the Saluda and Trenton Formations .....	56

## LIST OF FIGURES

<b><u>FIGURE</u></b>	<b><u>PAGE</u></b>
1      Regional sample location map of the Trenton Formation (middle Ordovician) core samples within the Michigan Basin and the Saluda Formation (upper Ordovician) outcrop samples on the western flank of the Cincinnati Arch. ....	4
2      Detail map of the Trenton Formation core sample location with the well lease names listed. The wells from which core samples were investigated in this study are circled (after Miller, 1988). ....	6
3      Photomicrograph of Trenton Formation limestone conglomerate showing rounded quartz grain matrix .....	7
4      Detail map of the Saluda Formation (upper Ordovician) outcrop sample location (after Walters, 1988). ....	8
5      General stratigraphy of the Cincinnati Series as determined by various authors (from Davis, 1986). ....	9
6      Computer generated microstructures (from Fridy et al. 1992) with corresponding CSD frequency histograms. Nucleation and growth models are a) Johnson-Mehl, b) Site-Saturation (cellular), and c) Site- Saturation with weakly clustered nuclei. ....	13
7      Size histogram of circles measured from intersections on several sphere sizes is the sum of the individual distributions shown by the differently shaded bars (after Russ, 1986). ....	20
8      CSD frequency histograms of Boi Doi dolomite from Aruba, Netherlands Antilles. Histograms are from a) thin-section, and b) disaggregated grain-mount. ....	21

## LIST OF FIGURES (cont'd)

<u>FIGURE</u>	<u>PAGE</u>
9      a) Shaded grains show those measured in a line point count, and b) the corresponding CSD frequency histogram. ....	23
10     Densities of the gamma and lognormal distributions with parameters selected to give the maximum value .54 at $x=1$ (after Breiman, 1973). ....	28
11     a) frequency histograms, and b) cumulative relative frequency distributions of Gamma distributions using a constant $\beta$ (scale) value and different $\alpha$ (shape) values. ....	29
12     a) frequency histograms, and b) cumulative relative frequency distributions of Gamma distributions using a constant $\alpha$ (shape) value and different $\beta$ (scale) values. ....	30
13     a) frequency histograms, and b) cumulative relative frequency distributions of Gamma distributions using equal $\alpha$ (shape) and $\beta$ (scale) values. ....	31
14     Two of the three frequency histograms of line point counts of Trenton clast TL1A. (Note: size data is measured data and not normalized.) ....	33
15     Respective cumulative relative frequency distributions of the frequency histograms of Trenton clast TL1A shown in Figure 14. ....	34
16     Two of the three frequency histograms of line point counts of Trenton clast TL1B. The solid line is a fitted gamma distribution. (Note: size data is measured data and not normalized.) ....	35



## LIST OF FIGURES (cont'd)

<b><u>FIGURE</u></b>	<b><u>PAGE</u></b>
17      Respective cumulative relative frequency distributions of frequency histograms of Trenton clast TL1B shown in Figure 16. ....	36
18      Frequency histograms of duplicate line point counts of Boi Doi dolomite from Aruba, Netherlands Antilles. The solid line is a fitted gamma distribution. (Note: size data is measured data and not normalized.) .....	37
19      Respective cumulative relative frequency distributions of the frequency histograms of the Boi Doi dolomite shown in Figure 18. ....	38
20      Frequency histograms of line point counts of duplicate thin-section samples of the same clast from the Trenton Formation. (Note: size data is measured data and not normalized.) .....	39
21      Respective cumulative relative frequency distributions of the frequency histograms shown in Figure 20. ....	40
22      Two of the eight frequency histograms of the Saluda dolomite samples. ....	51
23      Kolmogorov-Smirnov goodness-of-fit test cumulative relative frequency distribution showing the consistent differences between the Saluda and Trenton Formation CSDs. ....	58

## **INTRODUCTION**

The crystal size distribution (CSD) of a single phase, polycrystalline solid will vary according to the nucleation and crystal growth behavior during the transformation, or recrystallization, of that solid. Friedman (1965) recognized the importance of CSDs in describing the character of carbonate rocks such as dolomite, by classifying those with a relatively uniform CSD as equigranular and those with a polymodal CSD as inequigranular. Sibley and Gregg (1987) suggested that unimodal (equigranular) distributions result from a single nucleation event in a homogeneous substrate, and that polymodal (inequigranular) distributions result from nucleation in an inhomogeneous substrate, or multiple nucleation events. Marsh (1988) used CSDs to study the kinetics of crystallization in metamorphic and plutonic rocks. Marsh's basis for using CSD data was that it yields quantitative kinetic data that can be applied to understanding geochemical systems independent of the development of exact kinetic theory for the system under consideration (Marsh, 1988, p.278).

Many experimental CSDs have been observed, particularly in the material science field, often showing coarsely skewed, lognormal shapes to the distributions. This fact, and the effect of nucleation and crystal growth behavior on the crystal size distribution, has been investigated using a number of computer models in which varying nucleation and crystal growth processes can be chosen to generate a polycrystalline solid (Mahin, Hanson, and Morris, 1976, 1980; Saetre, Hunderi, and Nes, 1986; Marthinsen et al., 1989). A range of computer generated CSDs with specific crystal

nucleation and growth processes can be compared to experimentally derived CSDs to assess the nucleation and growth characteristics of these systems. In this study, three computer-generated CSDs are used to evaluate experimental size distributions measured in dolomites. Dolomite from the Trenton Formation, Middle Ordovician, of Michigan, and the Saluda Formation, Cincinnati Series, Upper Ordovician, of Indiana were investigated in this study. Rocks from these formations were chosen because of the different mean grain sizes within the formations and different temperatures of dolomitization between the formations.

The major limit of CSD data is that there is more than one way (nucleation and growth kinetics) of generating a given size distribution. For example, a transformation with an increasing nucleation rate and a constant growth rate may have a similar CSD to one with a constant nucleation rate and decreasing growth rate. Alternatively, differing CSD characteristics will result if a constant growth rate is maintained and the nucleation rate is varied. This is illustrated by several computer generated CSDs (Saetre et al., 1986; Marthinsen et al., 1989; Frost & Thompson, 1987). Similarly, Larikov (1986) generated nearly identical percent transformation sigmoidal graphs using a constant growth rate, but using different nucleation frequencies.

The purpose of this study is to compare the shape of CSDs from within a given population (formation), between populations (formations), and to theoretical CSDs, to place constraints on the interpretation of CSDs, thereby illuminating the influences of the differing conditions under which dolomites form.

## **GENERAL GEOLOGIC SETTINGS OF SAMPLE DOLOMITES**

Samples from two locations were investigated for this study. The first sample location is the epigenetic, fracture-related dolomite from the Trenton Formation, Middle Ordovician, within the Michigan Basin. The Trenton Formation samples are cored intervals from wells located in Jackson County, Michigan. Figure 1 shows the sample location in reference to the Michigan Basin. The second sample location is the Saluda Formation, Upper Ordovician, located in Jefferson County of southeastern Indiana. Figure 1 shows the Saluda Formation sample location in reference to the Cincinnati Arch and Illinois Basin..

### **Trenton Formation Dolomite**

The Trenton Formation overlies the St. Peter Sandstone (Lower Ordovician) and generally grades into the overlying Utica Shale (Upper Ordovician). The thickness of the Trenton Formation ranges from about 50 meters in the northeast to about 150 meters in the southeast of Michigan. The southeastward thickening of the formation probably represents carbonate platform development in that area. The top of the Trenton appears to be a regionally extensive hardground (Keith, 1985). The Trenton Formation is approximately 110 meters thick in the study sample location of Jackson County, Michigan. The Trenton Formation in this location is probably deposited in a deep subtidal environment (Wilson and Sungepta, 1985).

Three types of dolomites have been recognized in the Trenton Formation of the Michigan

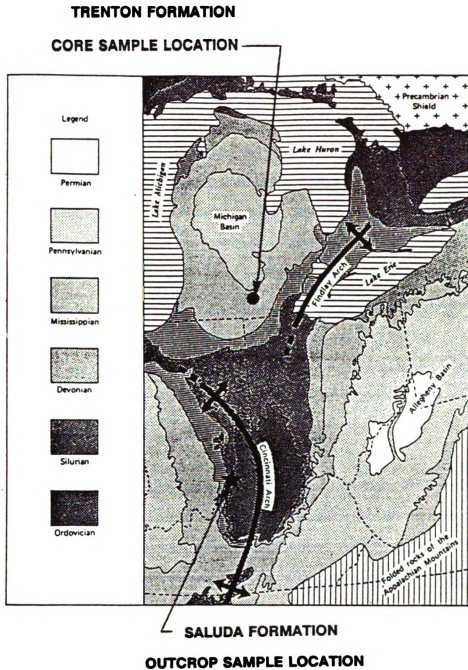


**Figure I** Regional sample location map of the Trenton Formation (middle Ordovician) core samples within the Michigan Basin and the Saluda Formation (upper Ordovician) outcrop samples on the western flank of the Cincinnati Arch.



Basin (Taylor and Sibley, 1986). A 'cap' dolomite exists at the upper few meters of the Trenton that is in contact with the Utica Shale and is distinctly ferroan (approximately 7 mole %  $\text{FeCO}_3$ ). A 'fracture-related' dolomite exists which is related to subsurface fractures, and structures of the basin. It is characterized by linear trends of epigenetic dolomites such as that found along the northwest-trending Albion-Scipio Trend which transects southeastern Jackson County, Michigan. A 'regional' dolomite is confined to the southwestern and western edges of the basin and does not extend into the study area. The Trenton core samples used in this study are considered to be part of the fracture-related dolomites taken from Jackson County, Michigan (depths of approximately 4850 to 4930 feet below sea level). Most of the formation in the study area is limestone, but the cored intervals for this study contain partially and completely dolomitized strata. Figure 2 is a local area map showing the well locations (from Miller, 1988). Much of the Trenton Formation in the study area consists of a mudstone or wackestone clast limestone. The dolomite is slightly calcium rich having a mean of 51 mole % Ca [based on position of  $d(104)$ ], (Miller, 1988). Taylor and Sibley (1986) calculated a temperature of precipitation of approximately  $80^\circ\text{C}$  by using oxygen isotope data.

The samples from these locations and depths were chosen for study because they are dolomitized intraclastic limestones which show significant textural variations between the clasts of the conglomerate. The textural variations of clasts in close proximity eliminates differences in overall solution chemistry or temperature as a control on the resulting dolomite textures.

The clasts range in size from a few millimeters to several centimeters in diameter. The clasts are generally surrounded by a matrix of carbonate mud and quartz silt. The silt is not found within the clasts, or within cemented fractures of some clasts, which shows the rocks to be true conglomerates, not collapse breccias. Dolomitization followed the lithification and subsequent deposition of the conglomerate as evidenced by the fact that the

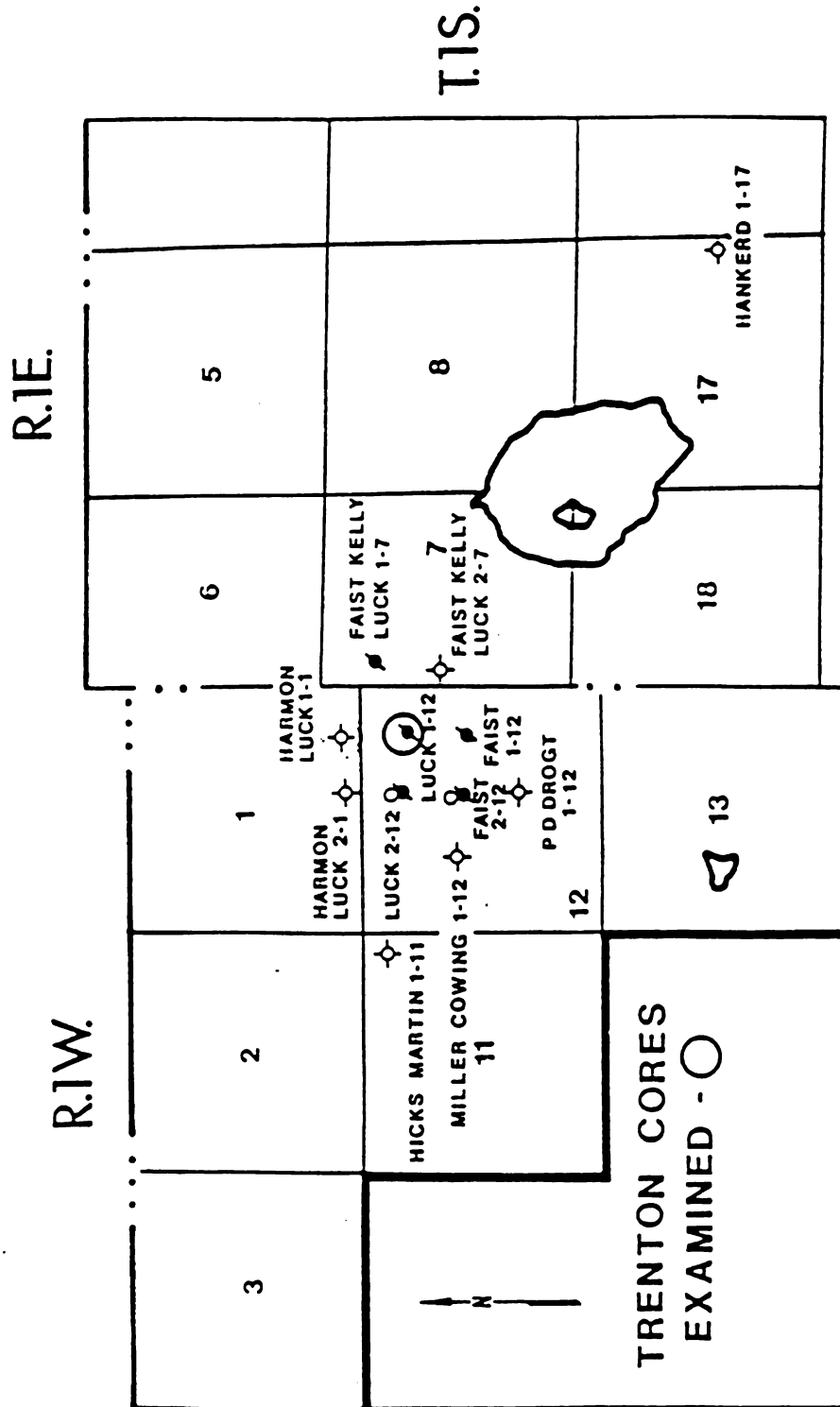


**Figure 2** Detail map of the Trenton Formation core sample location with the well lease names listed. The wells from which core samples were investigated in this study are circled (after Miller, 1988).

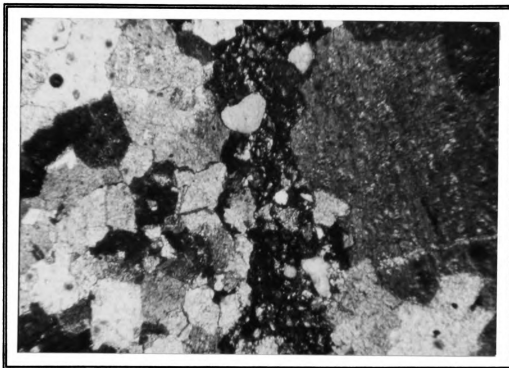


**Figure 3** Photomicrograph of Trenton Formation limestone conglomerate showing rounded quartz grain matrix.

Photographs of the thin-section, and drawings outlining and labeling the clasts are shown in Appendix A. A brief description of each clast studied in this investigation is also given in Appendix A.

### **Saluda Formation Dolomite**

The Saluda Formation samples analyzed in this study were obtained from a road cut along Highway 421, in Jefferson County of southeastern Indiana, approximately 3 miles north of Madison, Indiana, near the Kentucky-Indiana border. Figure 4 is a detail sample location map showing the location of the road cut. This site is located on the western flank of the Cincinnati dome/arch, toward the Illinois basin. The Saluda Formation is Upper Ordovician and part of the Richmond Group of the Cincinnati Series.

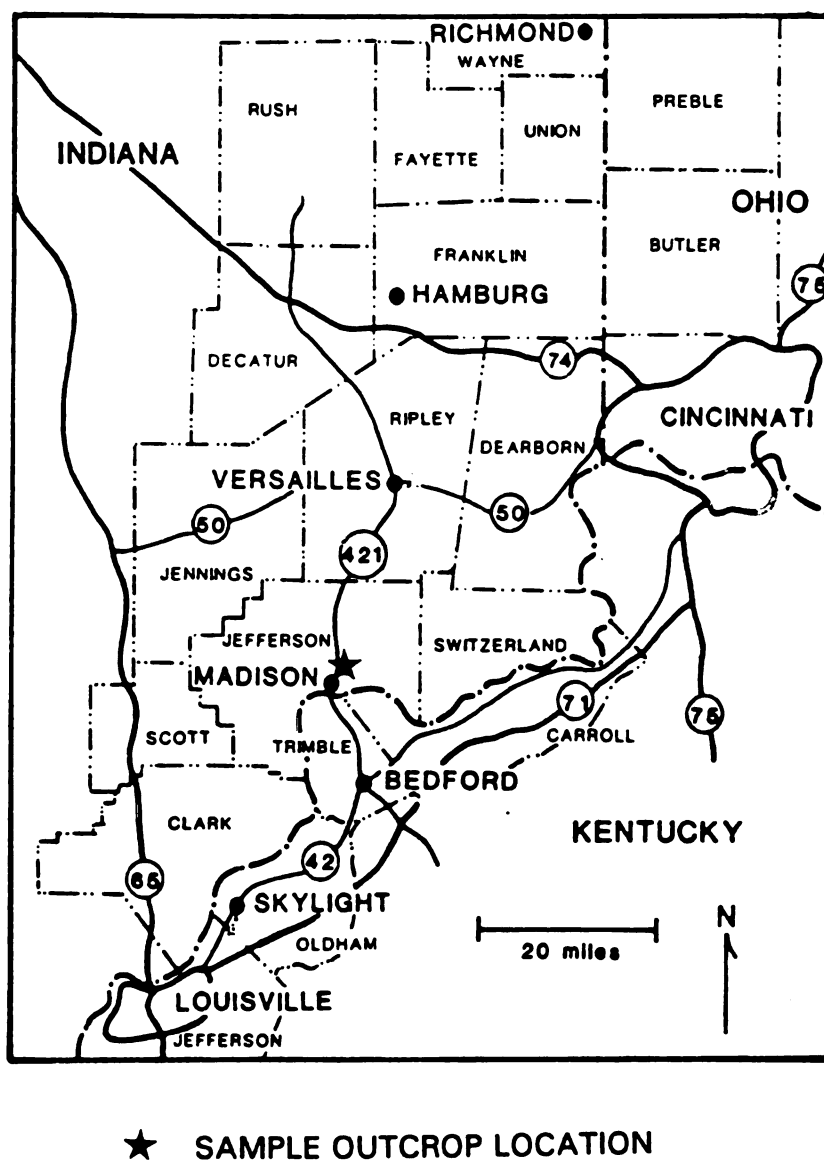


**Figure 4** Detail map of the Saluda Formation (upper Ordovician) outcrop sample location (after Walters, 1988).

dolomite in the partially dolomitized samples tends to form around the edges of the clasts. Figure 3 is a photomicrograph showing the edge of a clast and the rounded quartz in the matrix.

Figure 5 shows the general stratigraphy of the Cincinnati Series as determined by various authors (from Davis, 1986). Following the work of Walters (1988), the Saluda lies above the Liberty Formation and generally lies below, but interfingers with the Whitewater Formation above it. The Saluda thickens to the south and the Whitewater thickens to the north. The thickness of the Saluda is approximately 60 feet in the study area (Brown & Lineback, 1966).

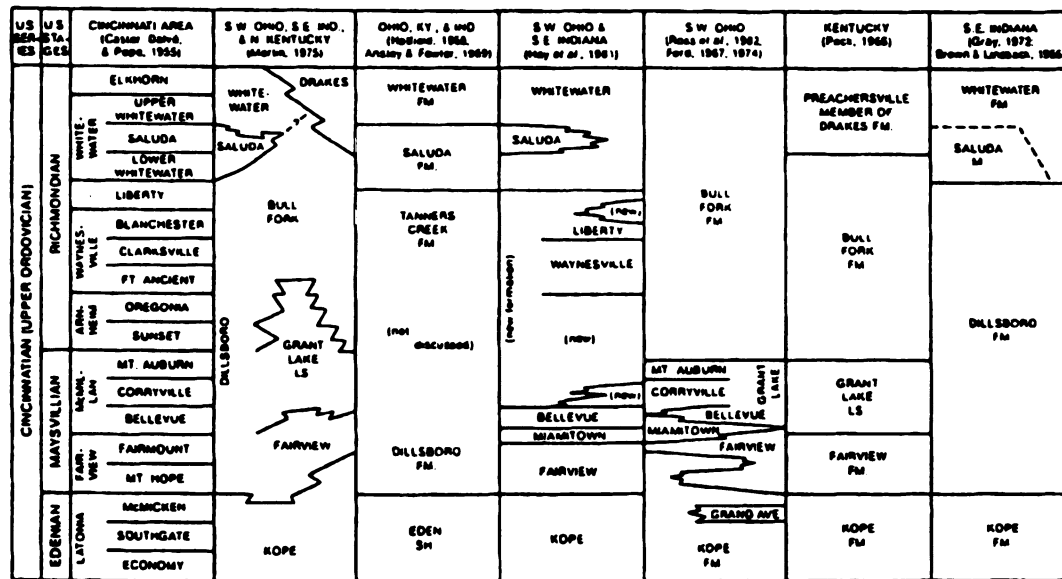


**FIGURE 5** General stratigraphy of the Cincinnati Series as determined by various authors (from Davis, 1986).

The Saluda is predominantly dolomite. Brown and Lineback (1966) indicate a distinctive contact at the base of the Saluda with the underlying strata. However, other authors describe the base of the Saluda to be gradational with the underlying strata, which is the



case at the sample location for this work. A distinctive zone of colonial corals exists near the base of the Saluda. The Saluda is predominantly overlain by, and grades into, the Whitewater Formation, which also contains a variety of limestone types interbedded with calcareous shales. In much of Jefferson County and Clark County to the south, the Saluda is disconformably overlain by the Silurian Brassfield Limestone (Brown & Lineback, 1966). Post-Ordovician erosion removed the uppermost Ordovician and lowermost Silurian strata, and in places the Saluda and Whitewater formations are overlain by upper lower Silurian strata (Walters, 1988 ref. of Hattin, 1961) .

At Madison, Indiana the Saluda consists of a section of thinly to thickly-bedded, bioturbated, dolomitized mudstones and wackestones, that is interbedded with lime grainstone lenses and overlain by approximately 15 meters of laminated, dolomitized mudstone. All the samples obtained for this study are mudstones from interbedded grainstones and mudstones.

Overlying the interbedded grainstones and mudstones are laminated, dolomitized mudstones which contain occasional mudcracks and rip-up clasts, but show no evidence of evaporite deposition. The laminated, mudstone section is completely dolomitized, as is the upper bioturbated mudstone portion of the mudstone-grainstone facies. The dolomite contains 44-48 mole % Mg [based on position of d(104)]. The amount of dolomite in the mudstone decreases down section, however, and partially dolomitized bioturbated mudstones are found approximately 10 meters below the base of the laminated mudstone facies. Mudstones with 50% dolomite occur as much as 20 meters below the base of the laminated mudstone facies.

The grainstone lenses contain fragments of brachiopods, bryozoans, trilobites, and crinoids. The wackestones contain fragments of bryozoans and brachiopods. The

grainstone lenses are also limestones or partially dolomitized, and the dolomite is generally confined to the mud found within the sheltered pores of the grainstone. The grainstone lenses are approximately 5 to 30 cm thick. They appear to be storm-washed deposits, as indicated by typically undulating bases with stacked and concave down brachiopods, overlain by crinoidal and bryozoan fragments, and terminate with relatively flat tops. The grainstones often pinch out laterally within a few meters. Deeper in the section, the grainstones are thinner and laterally more continuous.

The dolomite is unimodal planar and either does not replace allochems, or replaces them non-mimetically. Dolomite cement partially fills fossil molds (formerly aragonite), the remainder of which is filled with coarse, equant, orange cathodoluminescent (CL) calcite spar. The dolomite crystals have thin CL zones, and often have corroded interiors. The CL zones can be correlated through the upper 20 meters of the section, including the grainstone-mudstone facies. The zones in the dolomite deeper in the section are too faint to correlate, but those in the upper section indicate that the dolomitizing solutions were the same for the grainstones as for the mudstones.

The facies control on dolomite distribution in the Saluda is consistent with early diagenetic dolomitization. Hatfield (1965) suggested brines. Regardless of the water chemistry, the lack of deep burial in the area (Beaumont et al., 1988) is consistent with dolomitization at low temperatures.

## **COMPUTER - GENERATED MICROSTRUCTURES AND ANALYSES**

Mahin, Hanson and Morris (1976), developed a computer model to construct single-phase, polycrystalline microstructures for the purpose of characterizing the generation of grain shape. The model is sufficiently general to treat any nucleation and growth process in a one-phase solid. Because most crystal size distribution analyses are conducted in two dimensions, a planar section from the computer-generated microstructure unit cube was also generated. Two nucleation and growth models were used to illustrate the technique (Figure 6). The site saturation model, also referred to as the cellular model, begins with randomly-distributed nucleation sites in an isotropic, one-phase solid, which all nucleate simultaneously and grow uniformly as equi-sized spheres until impingement. Following impingement, the grains have planar boundaries to each other and grow according to the free space available. In the Johnson-Mehl model, nuclei are randomly distributed, form at a constant rate within the unit cube, and grow uniformly until impingement. The nucleation sites and times are random. This results in the unit cube being filled with grains of varying sizes and ages throughout the transformation, and in grain boundaries which are hyperboloids of revolution. In both models the growth rate is constant. A third microstructure, included in Figure 6, is a site saturation model with the nucleation sites being weakly clustered. The corresponding CSD frequency histograms are also presented with each microstructure in Figure 6. These microstructure prints are provided by Dr. Knut Marthinsen, Department of Physics and Mathematics, Norwegian Institute of Technology, Trondheim, Norway, (Fridy, Marthinsen, Rouns, Lippert, Nes, and Richmond, 1992).

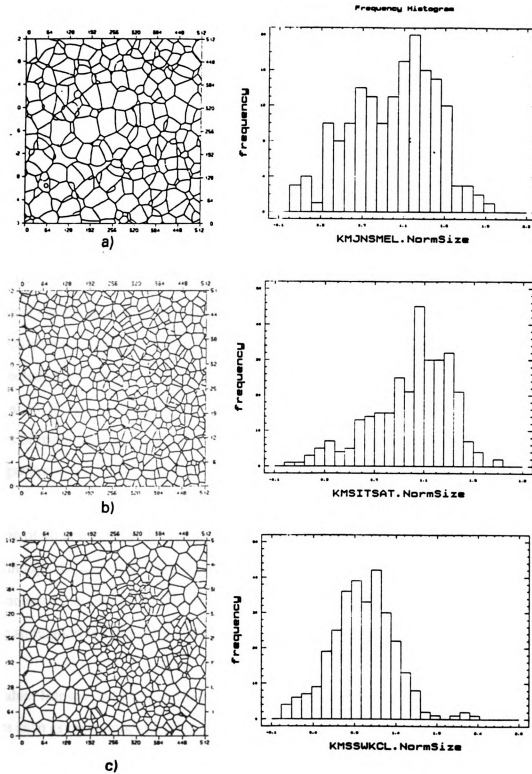


**Figure 6** Computer generated microstructures (from Fridy et al. 1992) with corresponding CSD frequency histograms. Nucleation and growth models are a) Johnson-Mehl, b) Site-Saturation (cellular), and c) Site-Saturation with weakly clustered nuclei.

The goal of Mahin, Hanson and Morris (1976) was to relate the topological features of well-defined microstructures to the nucleation and growth laws which generated them. "Physical experiments are limited by reproducibility, and the lack of total environmental control. The theoretical analysis, based on known statistical theorems, provides the ability to reproduce the sections and transformation control, but is limited by the scarcity of well defined models and theorems. Valid computer simulation, on the other hand, is able to extend the attributes of the theoretical work to include highly detailed two-dimensional representations of the progression of a transformation in time and space, as well as detailed three-dimensional information for any time or space." (Mahin, Hanson and Morris, 1976, page 39-40). For example, serial sections through microstructures of theoretical nucleation and growth models are useful aspects of computer-generated microstructures for crystal size and shape analyses. Mahin, Hansen and Morris (1976) concluded that it is possible to demonstrate theoretically that microstructures of a given model type (site saturation, Johnson-Mehl, etc.) will be geometrically equivalent, regardless of the nucleation/growth ratio ( $N_v/G$ ). They generated nearly identical, logarithmic-like, CSD frequency histograms for two Johnson-Mehl model microstructures. One of the Johnson-Mehl microstructures had a nucleation-to-growth ratio of 40 grains per unit volume, and the other had 244 grains per unit volume. Although the mean grain size changed, the shape of the CSDs remained the same. They concluded that the results followed the theoretical predictions in all cases, indicating that the simulation is valid at least for simple processes.

Mahin, Hanson and Morris (1980) investigated the nature of the distributions of quantities such as the number of sides, grain areas, and intercept lengths of a line transecting the grains on a planar section of site saturation, and Johnson-Mehl model microstructures. The frequency distributions of normalized grain areas and grain diameters did reveal qualitative differences between the site saturation and Johnson-Mehl

microstructures. The distribution of intercept lengths did not show as distinct a difference in the frequency histograms of the CSDs of the two microstructures.

Saetre, Hunderi and Nes (1986), constructed microstructures from the site saturation and Johnson-Mehl nucleation and growth models as well, and studied three additional models. A third model consisted of a decreasing nucleation rate accompanied by a constant growth rate. A fourth model incorporated an increasing nucleation rate with a constant growth rate, and a fifth model was composed of a constant nucleation rate and a decreasing growth rate. By holding the growth rate the same in the first four models, the effect of nucleation frequency on crystal size distribution can be seen. The models with an increasing nucleation rate or a decreasing growth rate were quite similar, and were the ones resulting in the most lognormal-like distributions.

An increasing nucleation frequency, and consequently the relative nucleation rate, results in a more coarsely skewed CSD than the site saturation model because younger, smaller grains will develop before all available space is consumed by the growth of the older grains. Generally, as the nucleation frequency increases, the nucleation density increases, and greater number of younger, smaller grains will be allowed to form in the unconsumed space of the unit cube. The resulting grain size distribution will contain a smaller mean grain size, a smaller mode, and a more coarsely-skewed distribution than a Johnson-Mehl model with the same growth rate. By holding nucleation frequency constant, the effect of varying growth rates may be viewed. An increasing growth rate, relative to a constant growth rate, would shorten the completion time of the transformation, and decrease the time and space available for new nucleation sites to form throughout the transformation. The space will be consumed at a relatively faster pace by the growing grains, thereby decreasing the number of subsequent nucleation events which can take place during the transformation. The resulting CSD would show a slightly less

coarsely-skewed distribution than a transformation with the same nucleation frequency and a constant growth rate. The opposite would be true for a corresponding decreasing growth rate. It would seem unlikely that nucleation would continue at a constant rate/frequency if the growth of existing grains is decreasing, unless the growth rates were somehow a surface-reaction-controlled process. Saetre, Hunderi & Nes (1986) produce several CSD histograms from the models described above which show that an increase in the nucleation rate serves to increase the number and peak frequency of small grains. This will lower the mean crystal size, and, generally, increase the size to mean-size ratio. This subsequently spreads out the distribution of the intermediately-sized grains, and produces a more lognormal-like normalized CSD.

Marthinsen, Lohne and Nes (1989) produced similar frequency histograms for both partially- and fully-recrystallized microstructures in both the site saturation and Johnson-Mehl models. The partially-recrystallized structures were investigated because the other simulated microstructures did not allow for any grain competition or grain growth after impingement, which would happen in real structures. The comparison of partially- and fully-recrystallized microstructures shows that the shape of the distribution remains essentially the same, and that the effect of impingement serves only to lower the peak frequency and consequently broaden the distribution. However, the effect of impingement appeared to show a greater influence on the site-saturation model CSD than on the Johnson-Mehl model CSD.

Marthinsen, Lohne and Nes (1989) also introduced non-uniformity with respect to the distribution of recrystallization nuclei and to the growth of new grains. This was done because experiments have shown that the recrystallization process is exceedingly inhomogeneous. Two methods of introducing non-uniformity were used in their study. The first method introduced non-uniformity by dividing a Johnson-Mehl model unit cube into

two areas, with one area having a much higher nucleation density than the other. The other method divided the recrystallized nuclei into classes, each of which was associated with a different decreasing growth rate. This second method was simulated using site saturation (instantaneous nucleation), Johnson-Mehl (constant nucleation), and increasing nucleation rates. The nuclei were distributed among the classes lognormally, in that the highest growth rate was assigned to the class with the fewest nuclei. The model of classes with different decreasing growth rates is based on a model for particle-stimulated nucleation of recrystallization in which it is assumed that the nucleation of recrystallization is restricted to the deformation zones surrounding large particles. The deformation zones and the amount of stored deformational energy is proportional to the particle size. The stored deformational energy is the driving force for the growth of the recrystallized grain. It is largest at the particle, and decreases throughout the deformation zone. Thus, the initial growth rate is largest at the largest particles. The modeling of lognormally distributed nuclei growth rates is based on the lognormal grain size distribution often observed in commercial alloys. The relevant aspect of the simulations to this study is the modeling of many different growth rates for many grains within the same microstructure, such as in flux-limited growth. The effect of altering the nucleation rates by creating the two zones with different nucleation densities did not significantly change the resulting CSD from that of a straight Johnson-Mehl nucleation and growth model. For the models with the introduction of classes of grains with different decreasing growth rates, none of the CSDs closely simulated the lognormal CSD. The CSDs with site saturation and Johnson-Mehl nucleation kinetics were broader, and subsequently had slightly lower peak frequencies, than their counterparts with isotropic, constant growth rates. The model with increasing nucleation rate was most similar to the lognormal distribution, and compared favorably to the increasing nucleation rate and decreasing growth rate models developed by Saetre, Hunderi & Nes. Again, it seems unlikely that an increasing nucleation rate would occur with a constant growth rate, or in this case classes with different decreasing growth rates, without a surface-reaction-controlling factor.



## **METHODS**

### **Method of Crystal Size Distribution Measurement**

In this study the CSDs of the thin-sections from the Trenton and Saluda were determined by taking line point count measurements. The line point counting method is conducted by traversing across a thin-section (or dolomite clast in the case of the Trenton) in which all of the crystals which touch the cross-hairs of the ocular along that traverse are included in the count. The longest diameter of each crystal encountered during the traverse of the thin section is measured and recorded. The grains on the edges of the clast or thin section were not measured to eliminate boundary effects. At the end of the traverse, the thin-section or clast is off-set approximately 1.5 to 2 times the size of the larger-sized grains measured in the first traverse, and a second traverse is begun. Those grains large enough to cross two traverses were counted only once. The number of grains measured per sample ranged from 199 to 300. The purpose of the line point counting method of CSD measurement described above is to minimize the bias toward the larger grains, in comparison to the normal point counting method. The method does not completely eliminate the large grain bias.

### **Stereology of CSD Determination**

The two-dimensional view of a microstructure obtained by slicing a planar section through the unit cube will show a different size distribution than would be observed for the true grain diameters viewed in 3-dimension. The resulting distribution is generally

coarsely-skewed; that is, fewer large grains are observed. This occurs because the probability of obtaining a longest-axis cross section of all crystals encountered by a planar cut through the polycrystalline unit cube is low compared to obtaining some smaller portion of the crystals within the planar section, or thin section (Lorenz, 1989; Russ, 1986). This fact was illustrated by Krumbein (1935) in his size distribution comparison between a thin section and disaggregated grains of the St. Peter sandstone. There is, however, no accurate way to theoretically determine the relationship between true and apparent sizes for irregular objects of unknown size distribution.

The probability of obtaining a particular circle diameter is related to the vertical thickness of a slice of the sphere with that size (Russ, 1986). Cashman and Marsh (1988) showed that the CSD, or density distribution curve for the apparent size of uniformly-sized spheres in thin section, could be calculated. The attempt to determine or calculate the true sizes and distributions becomes problematic when dealing with spheres of different sizes. The apparent size distribution is affected not only by the probability that the apparent diameter of any one sphere will be smaller than its true diameter due to the effect of sectioning, but also because there exists a greater chance of intersecting a large sphere than a small one (Cashman and Marsh, 1988). Russ (1986) gave an example where the smaller grain sizes observed in thin section may be contributed to from the smaller portions of larger grains as well as grains with that true diameter. The frequency distribution of each size will add, giving rise to a complex histogram such as that shown in Figure 7.

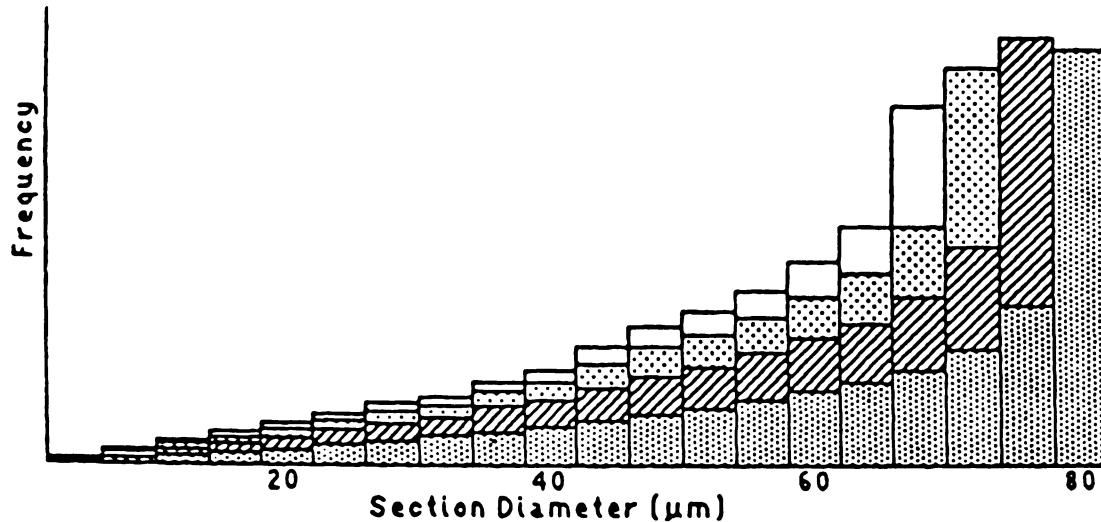


**FIGURE 7** Size histogram of circles measured from intersections on several sphere sizes is the sum of the individual distributions shown by the differently shaded bars (after Russ, 1986).

The problem of true and apparent grain sizes was investigated in this study by conducting an empirical check of size distributions of dolomite in both two and three dimensions. A CSD was determined on a friable dolomite sample from Aruba, Netherlands Antilles (BD6TS). A second CSD was determined from a grain mount of disaggregated grains from the same sample (BD6GM). The diameters measured in the grain mounts are true diameters. Figure 8 shows the frequency histograms and cumulative frequency distribution curves of the CSD's resulting from the grain mount and thin section line point counts. As in the St. Peter sandstone example conducted by Krumbein, the histograms and cumulative frequency distribution curves show that the CSDs between the two and three dimension have changed, and not merely shifted. However, these graphs indicate that the bias due to thin sectioning of dolomites is generally minor because the dolomite crystals tend to maintain an equant form.

In the line point count, it is apparent that a line placed randomly across a polycrystalline microstructure may intersect more of the larger grains than the smaller ones, resulting in

## Frequency Histogram

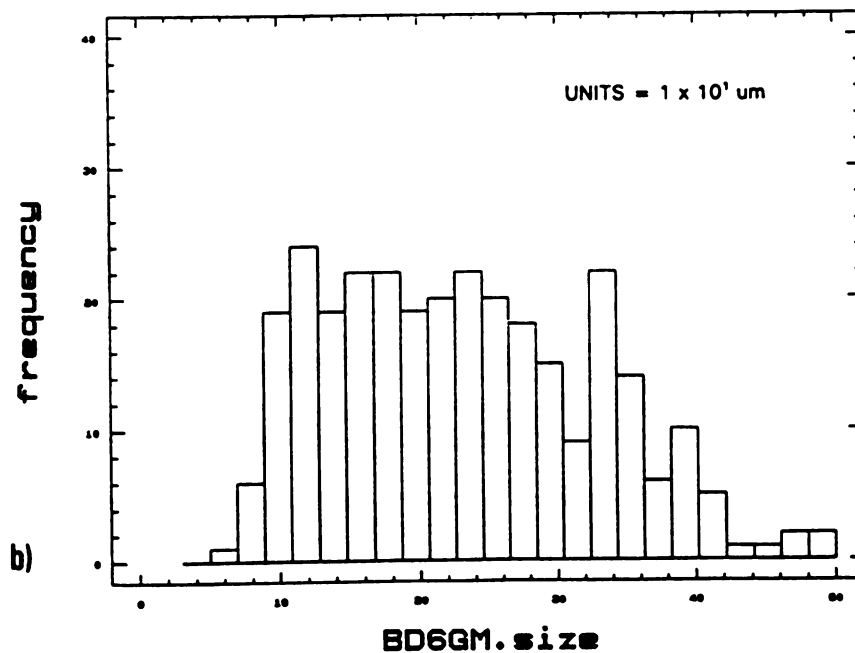
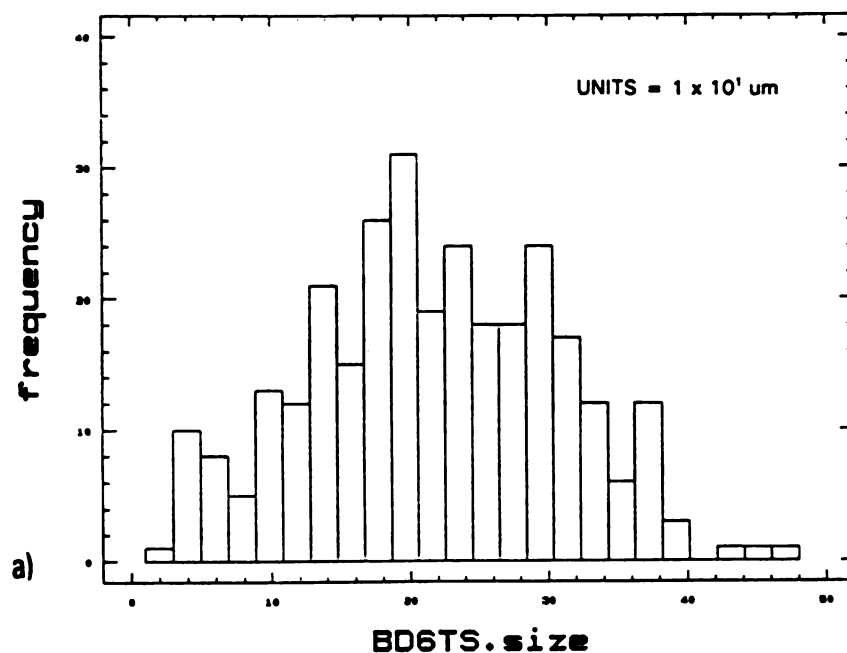


**Figure 8** CSD frequency histograms of Boi Doi dolomite from Aruba, Netherlands Antilles. Histograms are from a) thin-section, and b) disaggregated grain-mount.

the distribution being slightly more finely skewed than a CSD including all grains.

Figure 9 shows the microstructure of a site saturation model on which the grains measured in the line point count have been shaded. It is apparent that more of the smaller-grained areas are excluded from the line point count than if all of the grains were measured. However, it is also apparent that more of the smaller grains are included than if a grid-based point count were completed. For the purposes of this study it is assumed that if the same method of measuring grain sizes and determining CSDs is applied to all experimental samples and computer-generated models, the resulting CSDs will represent the nucleation and growth processes of the sample. The problem of the difference in the true and apparent CSDs is diminished in this study because both the experimental and theoretical CSDs are determined using the same method of measurement from a two-dimensional view of the microstructures.

Saetre, Hunderi and Nes (1986) point out the problem of the smaller grains being lost in experimental CSD analyses because of either the sample preparation procedures, or the limiting resolving power of the technique used to image, identify, and measure the grains. They propose using a cut-off effect in the computer-generated microstructures, to eliminate small grains in order to simulate the experimental effect in the computer models. They removed all grains smaller than 0.153 of the mean grain area. The cut-off effect is not very noticeable on the linear or logarithmic scale frequency histograms. It is quite noticeable, however, when it is plotted as a cumulative frequency distribution. This cut-off gives the tendency towards a more lognormal distribution for the Johnson-Mehl model. They note that when comparing experimental distributions to theoretical ones, the cut-off effect is relatively unimportant when comparing probability densities, but is substantial when comparing cumulative distributions, noting that cumulative distributions are more sensitive to variations at the small areas. It might be noted that the line point count method for the experimental CSDs may slightly exaggerate this cut-off

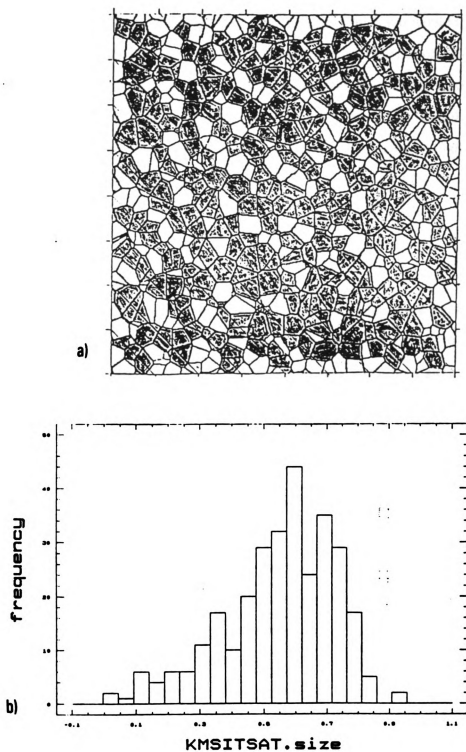


**Figure 9** a) Shaded grains show those measured in a line point count, and b) the corresponding CSD frequency histogram.

effect by eliminating a greater number of the small grains from the count and tending to produce a more normal-like distribution. However, the line point count would most likely simulate this cut-off effect in the computer-generated models. The cut-off effect was applied to the experimental CSDs as well as to the computer-generated microstructure CSDs, and it was found that it made very little difference in the resulting cumulative frequency distribution curves. For this reason a cut-off effect was not applied to the computer-generated model CSDs when comparing them to the empirical CSDs.

### **Statistical Analyses**

Five statistical methods of comparing the CSDs were applied to this study, to characterize the differences in shape of the CSDs. Two of the statistical methods rely on the Kolmogorov-Smirnov goodness-of-fit test. As indicated above, comparing the cumulative distributions is a more sensitive measurement of the variations in small areas than that of the frequency histograms. The Kolmogorov-Smirnov test is a nonparametric statistical procedure which measures the difference between two cumulative distribution functions. The test was originally developed for continuous distributions. However, it can be applied to discrete distributions as well, though the critical values tend to be over-conservative with discrete distributions [i.e. the true may be less than the nominal  $\alpha$  (Neave and Worthington, 1988, p.90)]. The Kolmogorov-Smirnov test determines the differences between two distributions by measuring the maximum vertical distance (Maximum D) between each cumulative distribution function at any point in the two distributions. Using the STATGRAPHICS Statistical Program, version 4.2, the two distributions may be a theoretical distribution compared to an experimental distribution (one-sample test) or two experimental distributions (two-sample test). The number of  $n$  values do not have to be the same in each distribution to perform the test. The two-tailed test is sensitive to differences in location (central tendency), in dispersion, in skewness,

etc. (Siegel, 1956, p.127). It is the best known of several distribution-free procedures which compare two (2) cumulative distribution functions in order to test for differences of any kind between the distributions of the populations from which the samples were obtained. The Kolmogorov-Smirnov test is best used in situations where it is perhaps unclear what kind of differences to expect between populations, or where expected differences do not fit into the usual categories of location or spread (Neave and Worthington, 1988, p.149-153). The Kolmogorov-Smirnov test is probably more powerful than the chi-square test in most situations (Conover, 1971, p 295). The most obvious advantage of the Kolmogorov-Smirnov test is that it is not necessary to group observations into arbitrary categories; for this reason it is more sensitive to deviations in the tails of distributions where frequencies are low than is the chi-square test (Davis, 1986).

The first method used a one-sample Kolmogorov-Smirnov test to evaluate the goodness-of-fit of each CSD to a normal (Gaussian) and lognormal distribution calculated from the mean and standard deviation of the CSD at hand. It was also used to evaluate the goodness-of-fit of each CSD to a corresponding gamma distribution. The results of the test were evaluated by examining the significance level at which the null hypothesis (that the experimental and theoretical distributions are from the same population) could be rejected without a type 1 error. The null hypothesis was rejected if the significant level was less than 0.05.

In the second statistical method, the CSDs for each sample were normalized by dividing each measurement by the corresponding CSD mean value. This placed each distribution at a central location equal to 1. The resulting difference in the cumulative frequency distributions of the CSDs would then only be characterized by the differences in shape or spread, and not in location. The CSDs were run through the two-sample Kolmogorov-Smirnov goodness-of-fit test provided by the STATGRAPHICS statistical



program. Again, an arbitrary limit of 0.05 significance value has been selected, and the test data yield a general relationship of the CSDs.

The third, fourth and fifth statistical methods yield numerical values which characterize the CSD shape. T-tests were conducted with these values to establish their similarity or difference as CSD shape characterizing values.

The third statistical method calculated the normalized standard deviation (NSD) following work of Tweed, Hansen, and Ralph (1983). Tweed, Hansen and Ralph (1983) compared grain size distributions before and after recrystallization grain growth and noted that variances of distributions can be directly compared only if the distributions have the same mean. Since the data in their study approximated a lognormal distribution, the distributions were normalized after scaling geometrically (Tweed, Hansen and Ralph, 1983, p.2237). The change in the normalized geometric standard deviation before and after grain growth could then be compared quantitatively. They followed the method described by Moore (1969). The CSDs in this study were not all close to lognormal and, thus, scaling them geometrically would not be appropriate. Therefore, the standard deviations of the normalized CSDs were compared in this study, and are termed the normalized standard deviations.

The fourth statistical method used to characterize the CSD shape was skewness. Both the inclusive graphic skewness, as described by Folk (1980), and skewness calculated by the STATGRAPHICS statistical program are included in this study.

The fifth statistical value characterizing the CSD shape is the gamma distribution shape factor  $\alpha$  ( $\alpha$ ) derived from each CSD using the STATGRAPHICS program. The general shape of the dolomite CSDs shows relatively low probabilities for intervals

close to zero, with the probability increasing for a period as the interval moves to the right (positive direction) and then decreasing at a more gradual rate as the interval moves further to the extreme positive region of the distribution. A class of functions that serve as good models for this type of distribution behavior is the gamma class. The gamma probability density function used in the STATGRAPHICS program is given by the equation:

$$f(x) = \frac{\beta^\alpha x^{\alpha-1} e^{-\beta x}}{\Gamma(\alpha)}$$

where  $\alpha$  is termed the gamma distribution “shape parameter” and  $\beta$  is termed the gamma distribution “scale parameter”, (Bury, 1975, p.299). The *gamma*  $\Gamma(\alpha)$  function is defined by:

$$\Gamma = \int_0^{\infty} x^{\alpha-1} e^{-x} dx$$

The tails of the exponential, gamma, and lognormal distributions all decrease rapidly. For  $x$  large, the tail of the gamma distribution is dominated by the term  $e^{-x/\beta}$ . Figure 10 (after Breiman, 1973) demonstrated the differences between the lognormal and gamma distributions where in each distribution the maximum of each occurs at  $x = 1$ .

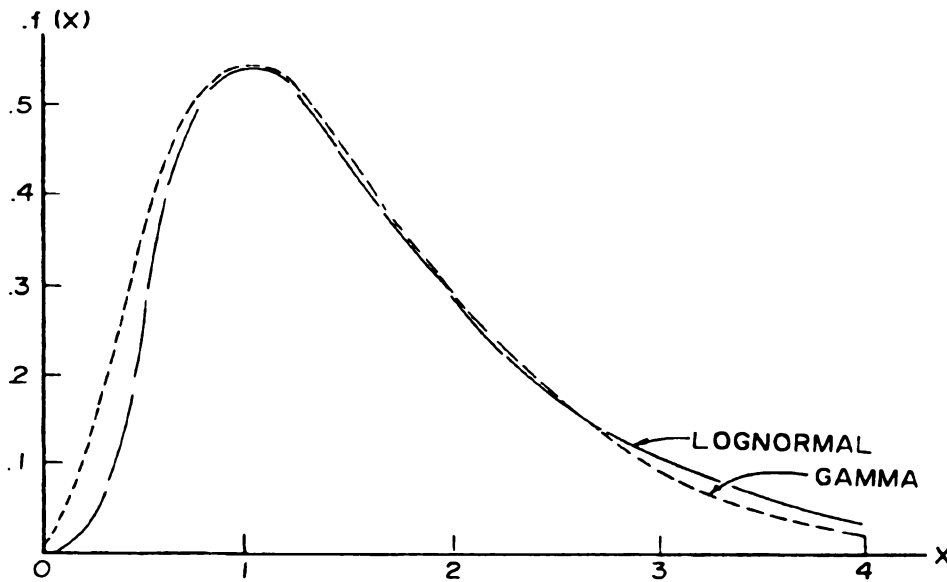


**FIGURE 10** Densities of the gamma and lognormal distribution with parameters selected to give maximum value .54 at  $x=1$  (after Breiman, 1973).

A series of gamma distributions is shown in Figures 11, 12, and 13, to illustrate the characteristics of gamma distributions with different alpha and beta values. Figure 11a illustrates the shape of several gamma distributions which have varying alpha values and a beta value of 1, and 11b shows the corresponding cumulative frequency distributions of 11a. Figure 12a shows the shape of several gamma distributions which have a constant alpha and varying beta values, and 12b shows the corresponding cumulative frequency distributions from the gamma distributions in 12a. Figures 13a and 13b show the shape of the density distribution and the corresponding cumulative frequency distribution for several gamma distributions which have equal alpha and beta values. When CSD data is normalized, the value of the gamma distribution scale factor, beta, will become equal to the value of the gamma distribution shape factor, alpha.. The alpha value does not change between the normalized (NormSize) and directly measured (Size) CSD data. The alpha value defines the shape of the CSD in terms of the gamma distribution that best represents the CSD data, either as the directly measured data or the normalized data.

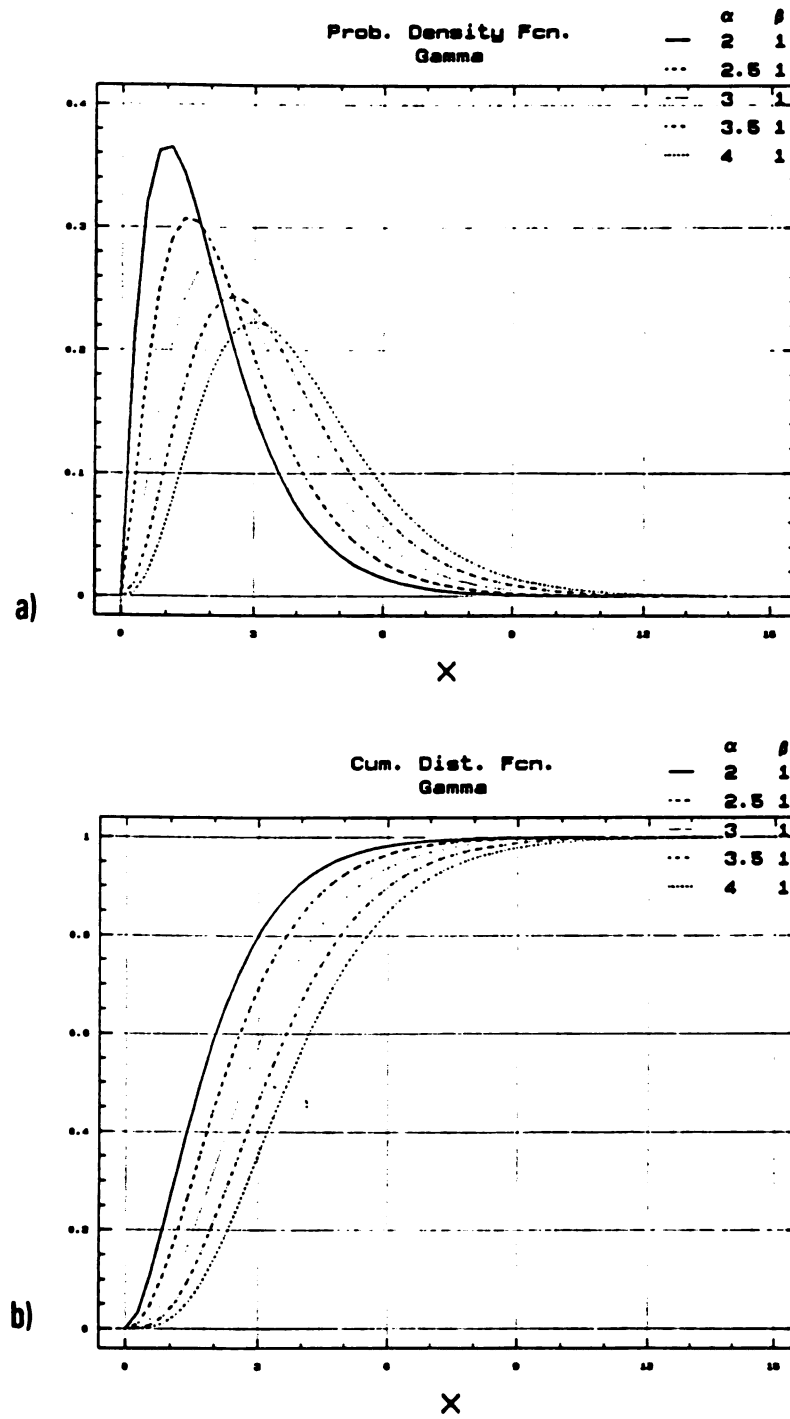


**Figure 11** a) frequency histograms, and b) cumulative relative frequency distributions of Gamma distributions using a constant  $\beta$  (scale) value and different  $\alpha$  (shape) values.

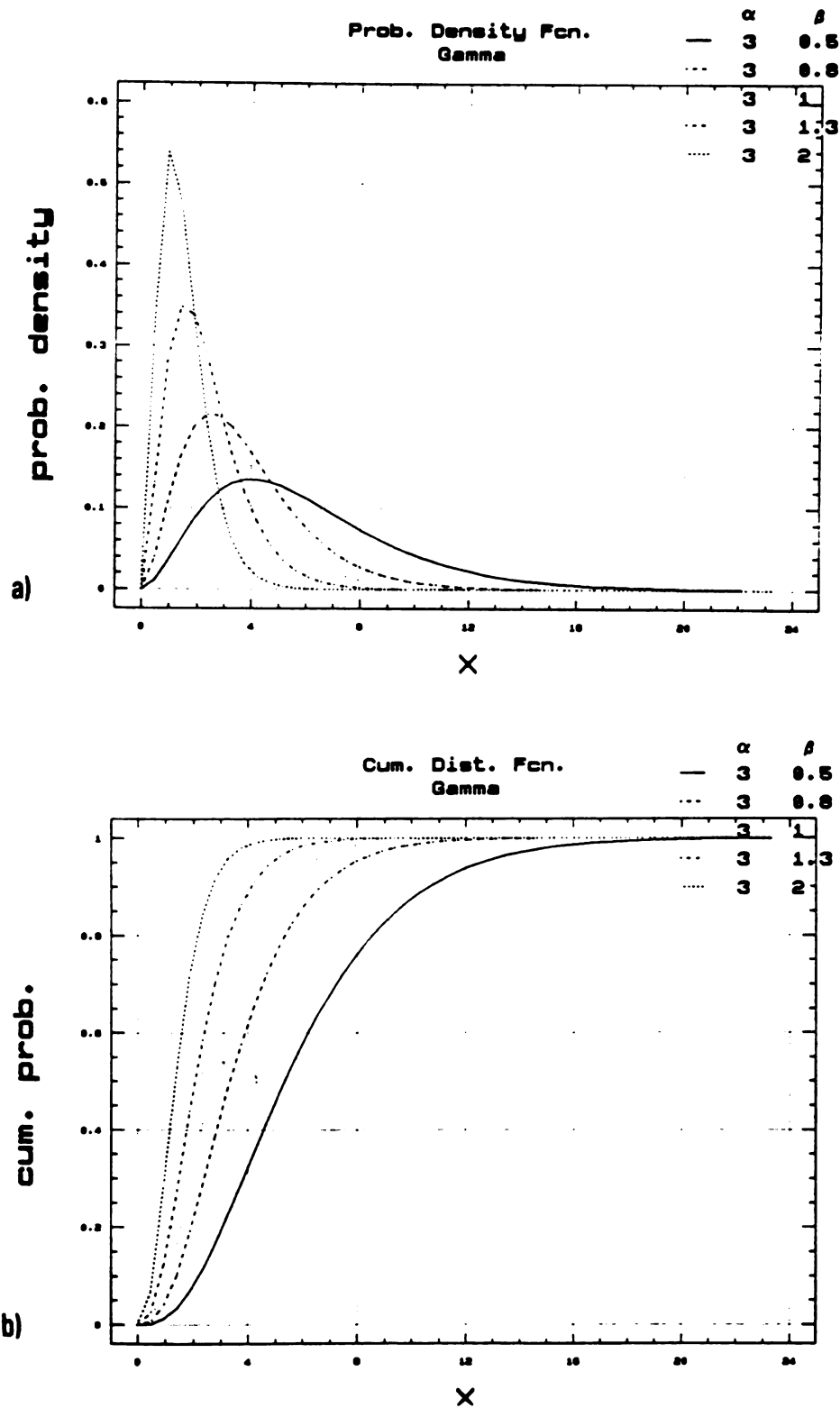


**Figure 12** a) frequency histograms, and b) cumulative relative frequency distributions of Gamma distributions using a constant  $\alpha$  (shape) value and different  $\beta$  (scale) values.

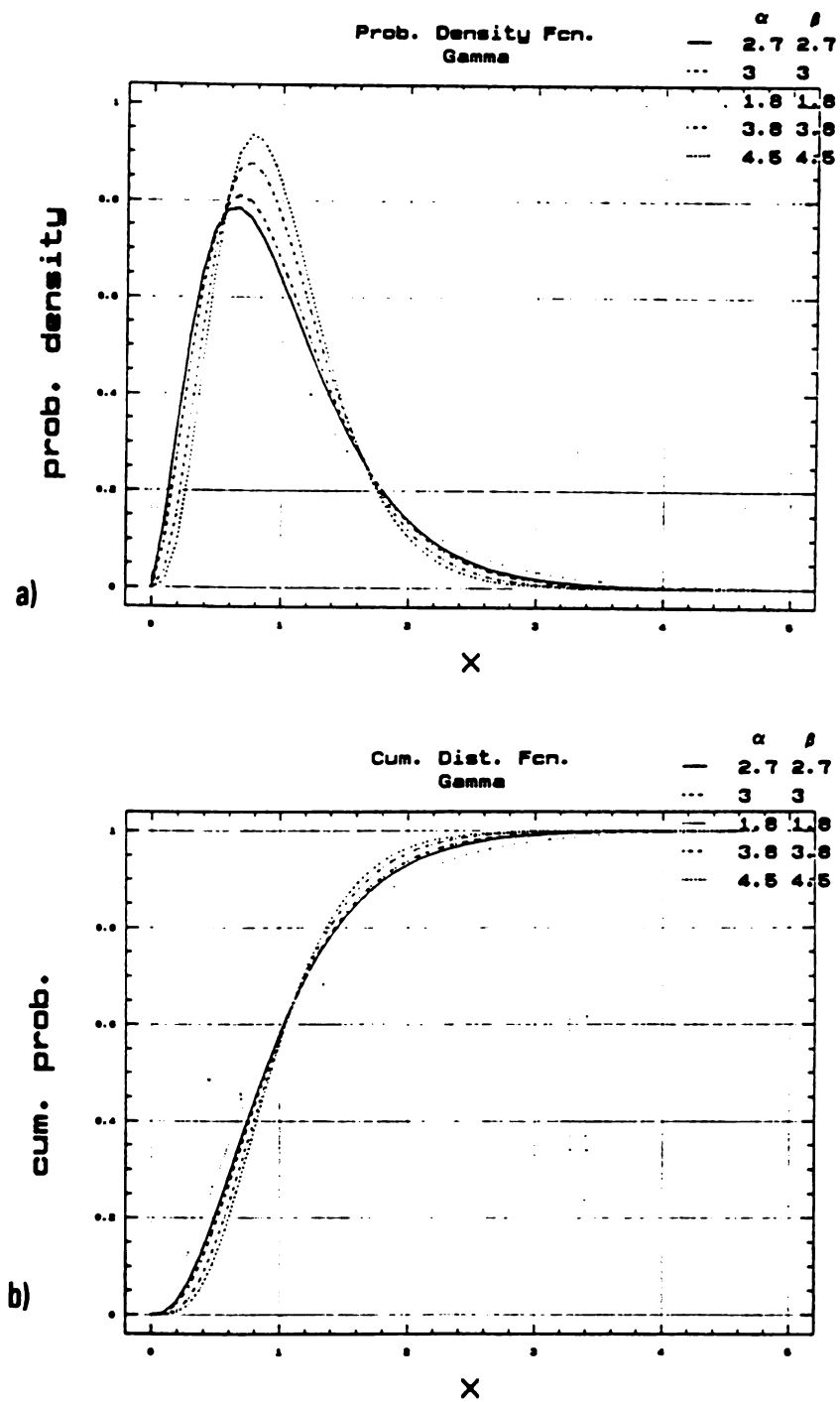


**Figure 13** a) frequency histograms, and b) cumulative relative frequency distributions of Gamma distributions using equal  $\alpha$  (shape) and  $\beta$  (scale) values.

It is evident from Figures 11b, 12b, and 13b that relatively minor variation exists between the cumulative frequency distributions which have equal alpha and beta values compared to the variations observed between cumulative frequency distributions where one gamma distribution variable (alpha or beta) is held constant and the other changes. The Kolmogorov-Smirnov goodness-of-fit tests were completed between normalized CSDs, each of which have a beta value equal to its corresponding alpha value.

### **Method Reproducibility**

For evidence of reproducibility in the line point count method, three CSD counts on each of two clasts within the Trenton formation core were conducted. Two CSD counts were also conducted on the Netherlands Antilles sample (BD6TS). Figure 14 shows two of the three frequency histograms, and Figure 15 shows the respective cumulative frequency curves from the TL1A clast of the Trenton Formation. Figure 16 shows two of the three frequency histograms, and Figure 17 shows the respective cumulative frequency curves from the TL1B clast of the Trenton Formation. Figure 18 shows the frequency histograms and Figure 19 shows the respective cumulative frequency curves from the Netherlands Antillies sample. The histograms and relative cumulative frequency distributions are comparing the direct measurements taken (size) and are not the normalized distributions (NormSize). It is evident from all of the histograms and cumulative frequency curves that relatively good reproducibility is obtained for the method. Similarly, a duplicate thin section sample of the same clast was made, and the grain sizes were measured as described above (clast/count TL4B and TL13B). The resulting frequency histograms are shown on Figure 20, and the respective cumulative frequency distribution curves are shown in Figure 21. Table 1 shows the two-sample Kolmogorov-Smirnov goodness-of-fit test significance levels for the respective clasts and counts. The significance levels indicate that the distributions are not significantly different.

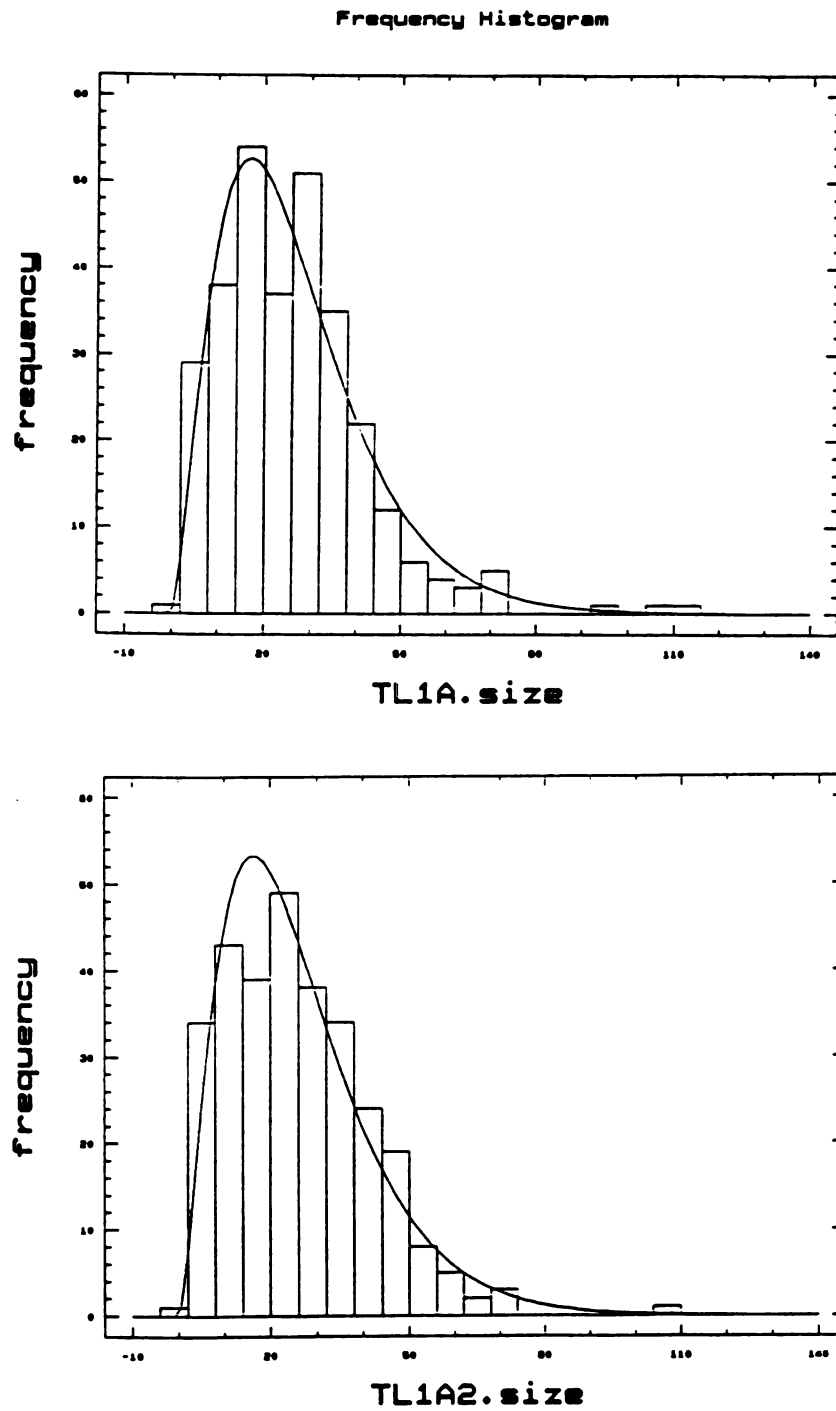


**Figure 14** Two of the three frequency histograms of line point counts of Trenton clast TL1A. (Note: size data is measured data and not normalized.)



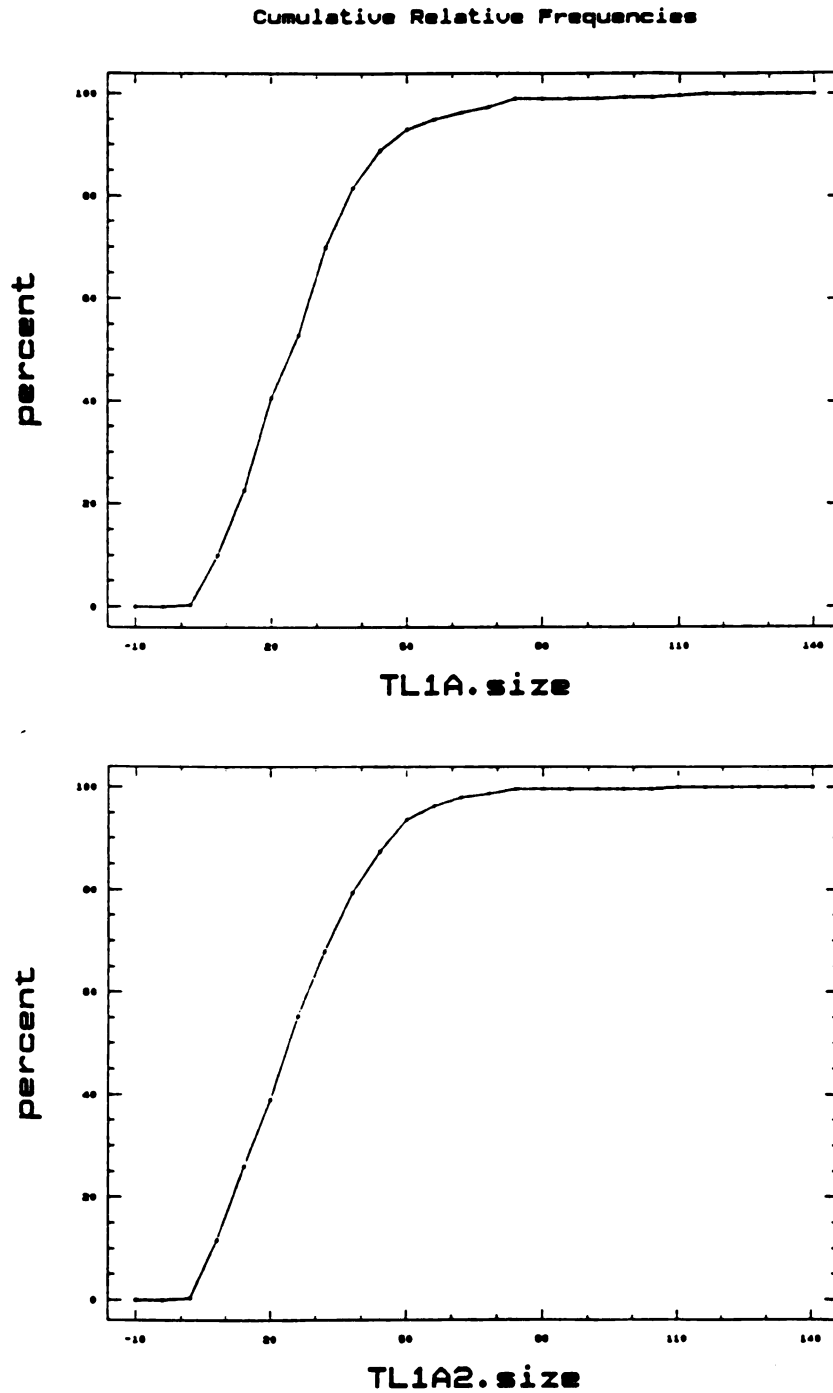


**Figure 15** Respective cumulative relative frequency distributions of the frequency histograms of Trenton clast TL1A shown in Figure 14.

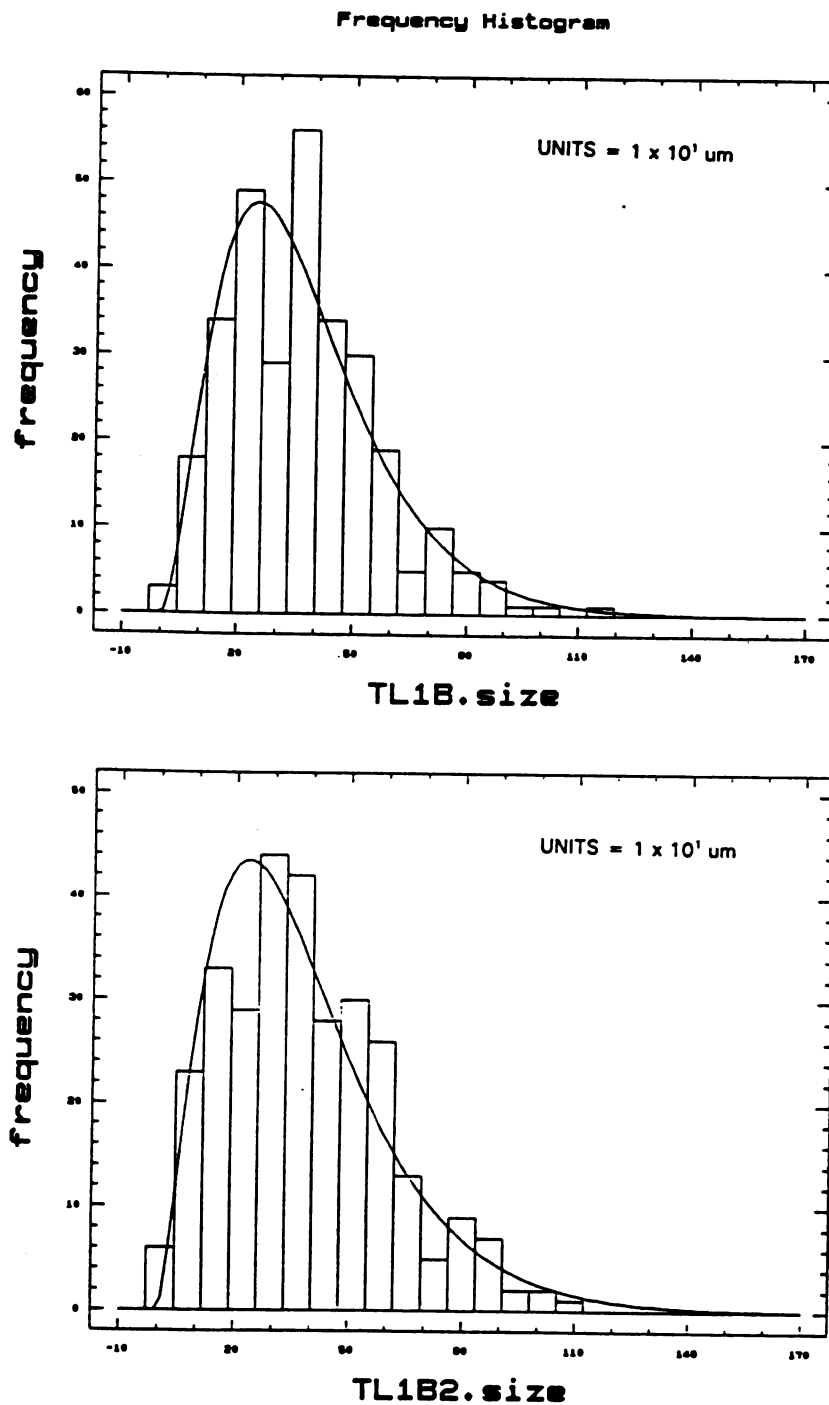


**Figure 16** Two of the three frequency histograms of line point counts of Trenton clast TL1B. The solid line is a fitted gamma distribution. (Note: size data is measured data and not normalized.)

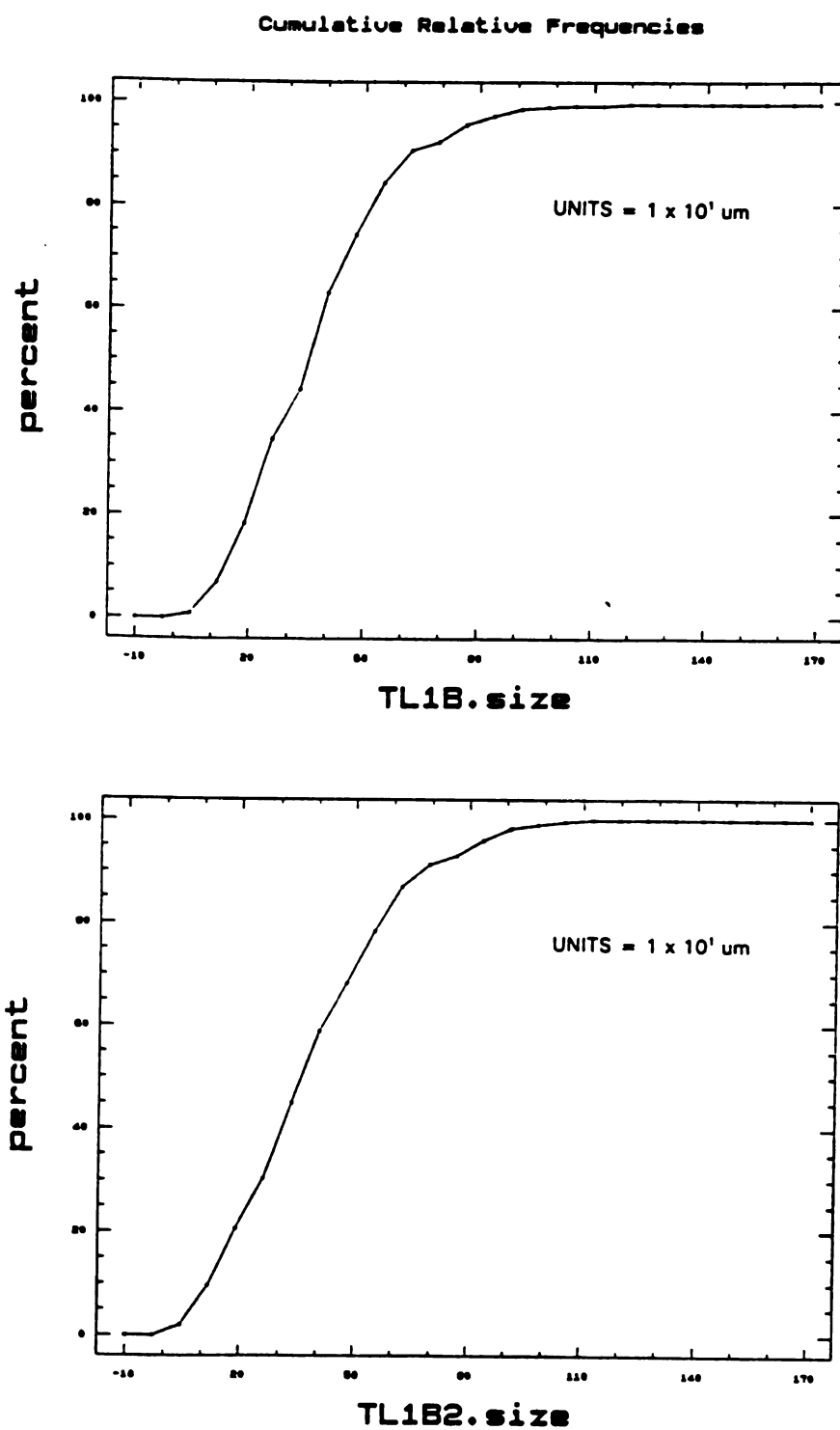


**Figure 17** Respective cumulative relative frequency distributions of frequency histograms of Trenton clast TL1B shown in Figure 16.

## Frequency Histogram

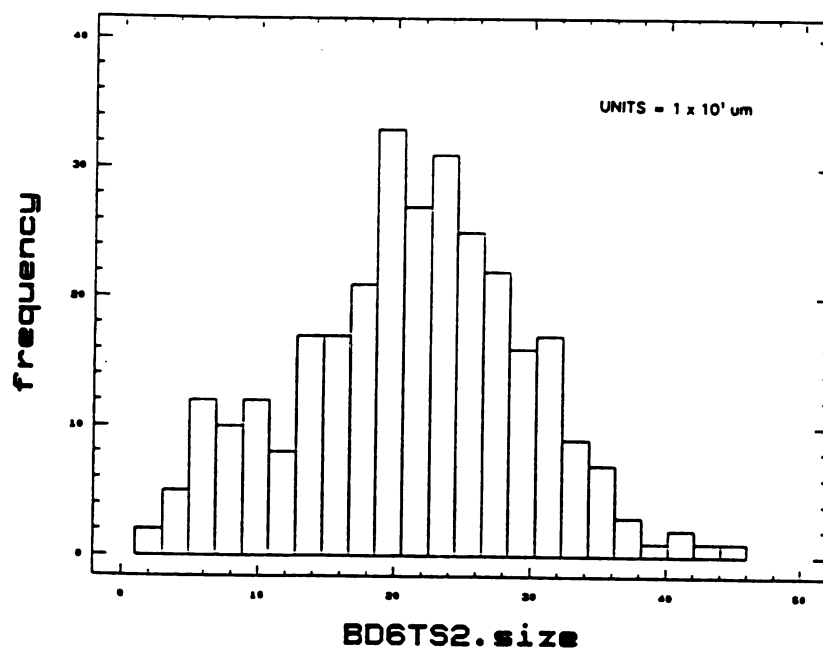
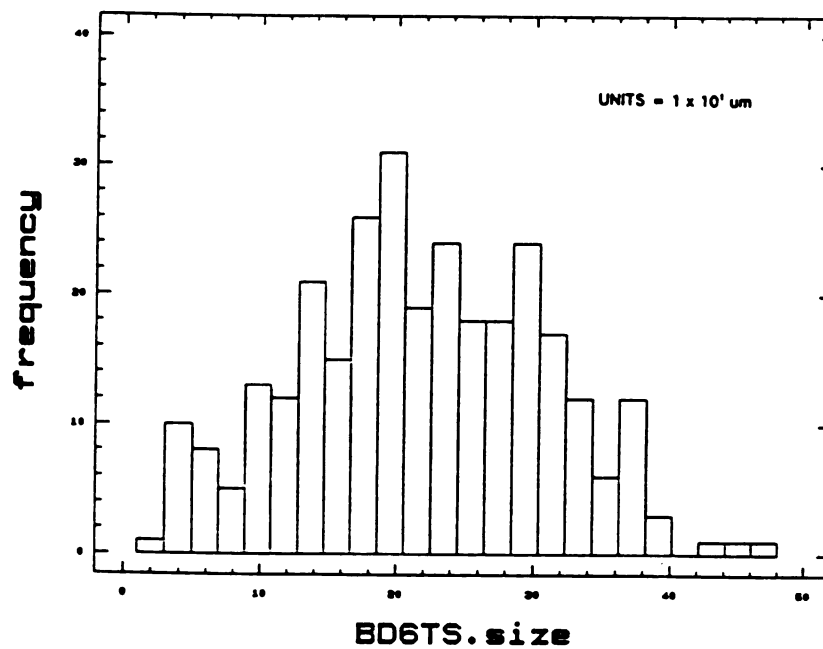


**Figure 18** Frequency histograms of duplicate line point counts of Boi Doi dolomite from Aruba, Netherlands Antilles. The solid line is a fitted gamma distribution. (Note: size data is measured data and not normalized.)

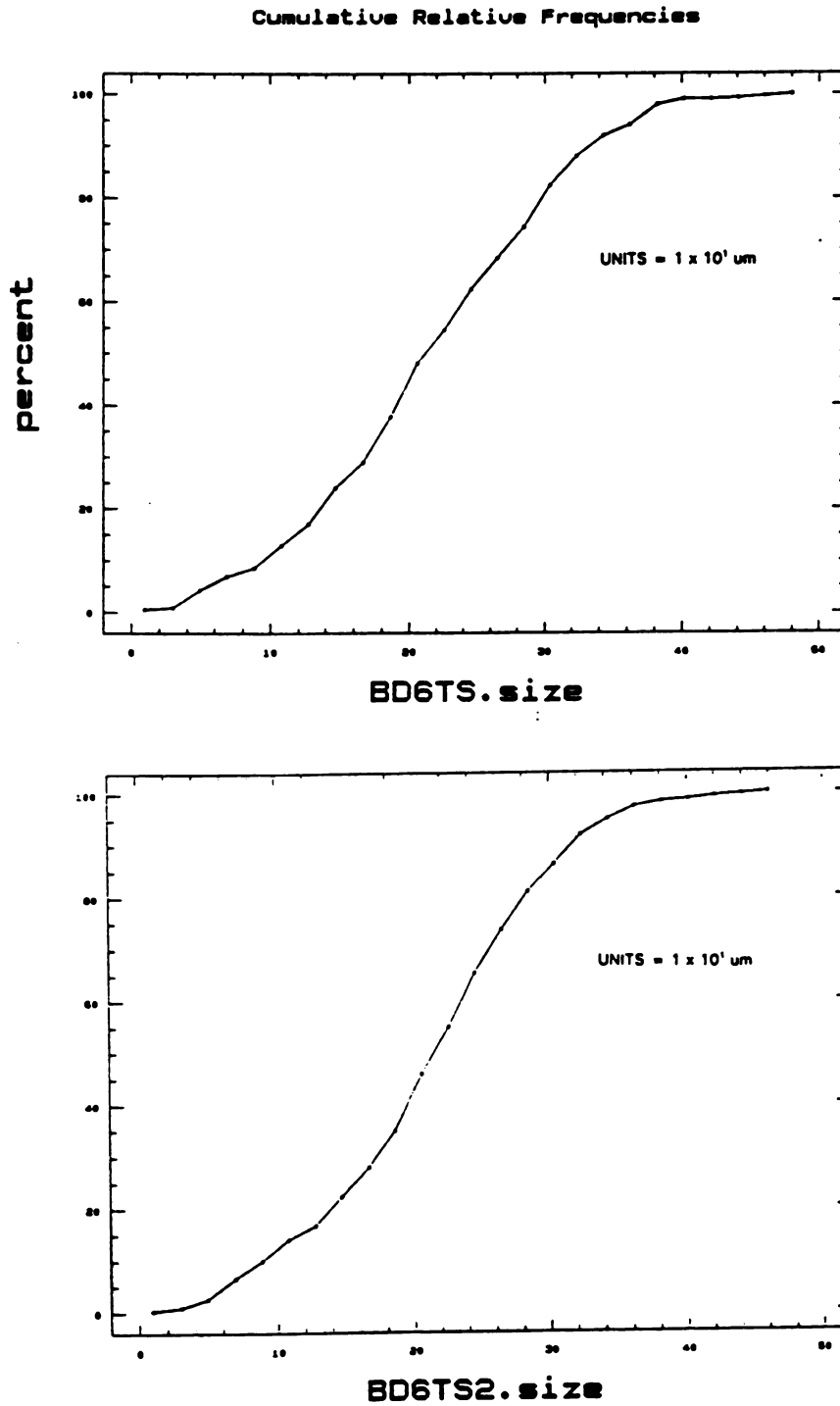


**Figure 19** Respective cumulative relative frequency distributions of the frequency histograms of the Boi Doi dolomite shown in Figure 18.

## Frequency Histogram

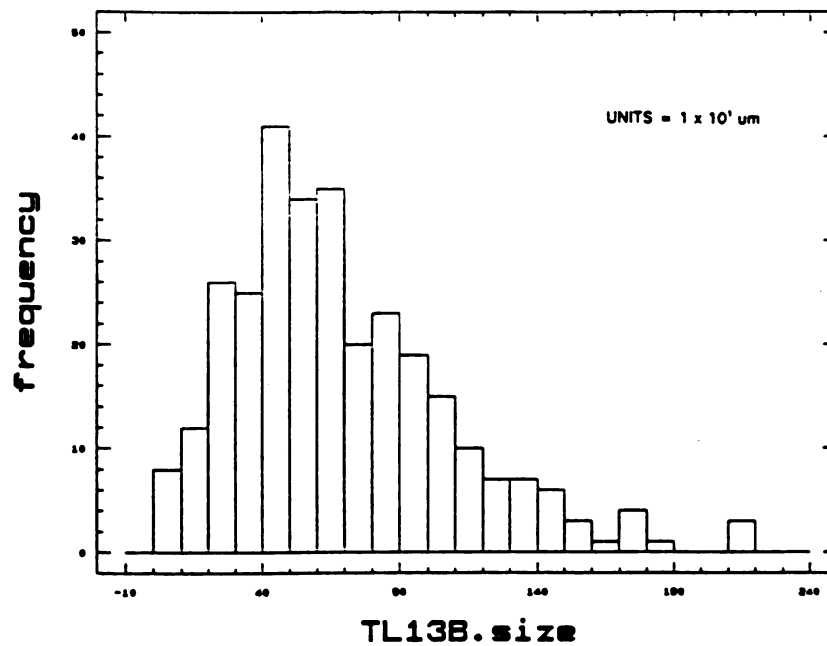
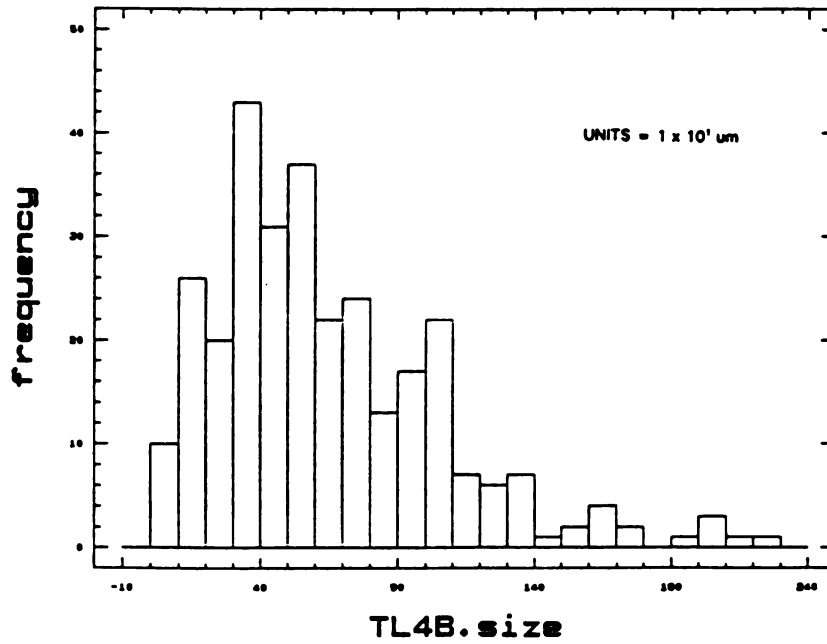


**Figure 20** Frequency histograms of line point counts of duplicate thin-section samples of the same clast from the Trenton Formation. (Note: size data is measured data and not normalized.)

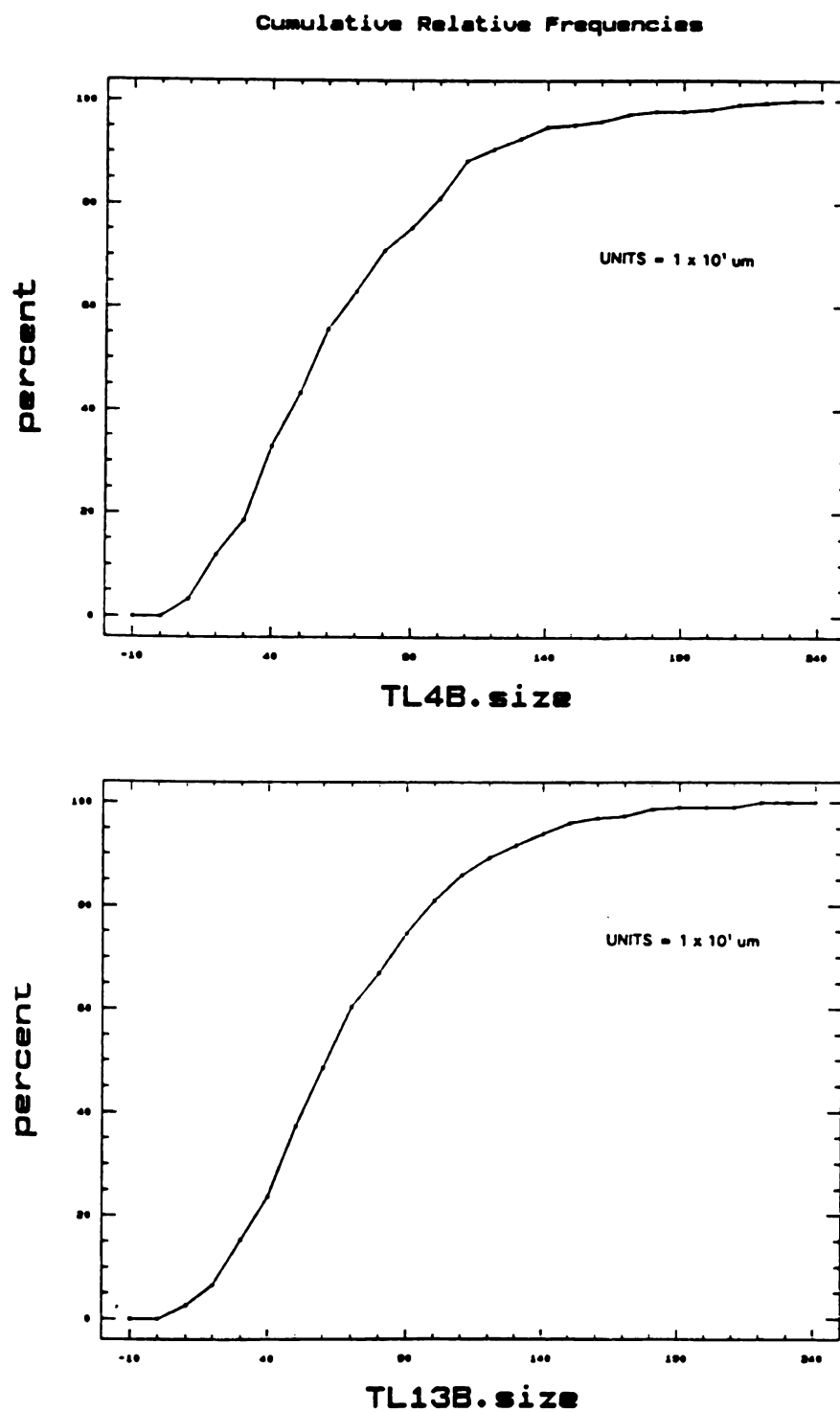


**Figure 21** Respective cumulative relative frequency distributions of the frequency histograms shown in Figure 20.

**TABLE 1**  
**Two-Sample Kolmogorov-Smirnov Test Evidence of**  
**Reproducibility On Measured Crystal Size Distribution Data**

Clast/Count	K-S Significance Level of CSD Data		K-S Significance Level of Normalized CSD Data	
	TL1A2	TL1A3	TL1A2	TL1A3
TL1A	.7870	.2098	.7870	.5175
TL1A2		.6527		.5842
	TL1B2	TL1B3	TL1B2	TL1B3
TL1B	.2098	.3412	.7212	.7870
TL1B2		.6527		.3953
	BD6TS2		BD6TS2	
BD6TS	.2923		.2923	
	TL13B		TL13B	
TL4B	.0659		.5175	

Table 2 shows the comparative mean, the standard deviation, the normalized standard deviation, the skewness (as calculated by STATGRAPHICS), the inclusive graphic skewness (Folk, 1980), the value of the gamma distribution shape factor  $\alpha$  (alpha), and the one-sample K-S significance value to the normal, lognormal, and gamma theoretical distributions.



**TABLE 2**  
**Comparison of Statistical Values of Duplicate CSD Counts and Thin-Section Samples**

Clast	Mean	SD	NSD	SK	IGSK	N	L	G	Alpha
TL1A	26.88	16.49	.6134	1.537	.145	.051	.011	.3265	2.700
TL1A2	26.32	15.56	.5914	1.004	.169	.0634	.007	.3302	2.613
TL1A3	27.34	16.98	.6208	1.231	.323	.0012	.158	.5011	2.581
TL1B	36.94	20.94	.5669	1.639	.065	.0300	.0001	.0569	3.038
TL1B2	38.43	21.82	.5678	1.627	.157	.1900	.001	.0524	2.544
TL1B3	38.51	23.01	.5974	1.301	.175	.0024	.0088	.3566	2.764
BD6TS	21.46	9.31	.4341	.0050	.0262	.3921	3.5E-6	.0019	3.768
BD6TS2	21.04	8.61	.4093	-.0808	-.0340	.2934	1.9E-7	.0005	4.258
TL4B	65.21	41.91	.6427	1.199	.278	.0023	.1727	.9191	2.382
TL13B	69.05	40.26	.5831	1.056	.205	.0005	.0987	.7293	2.824

SD = Standard Deviation

alpha = Gamma Distribution Shape Factor

N = Kolmogorov-Smirnov Test Significance Level to a Normal Distribution

L = Kolmogorov-Smirnov Test Significance Level to a Lognormal Distribution

G = Kolmogorov-Smirnov Test Significance Level to a Gamma Distribution

NSD = Normalized Standard Deviation

IGSK = Inclusive Graphic Skewness

SK = STATGRAPHICS Skewness

The values presented in Table 2 show that relatively good correlation exists for the STATGRAPHICS skewness, the normalized standard deviation, and the gamma distribution shape factor (alpha) as CSD shape descriptors. The mean and standard deviation values also indicate relatively good reproducibility of the line point count method.

The size distributions obtained for the Trenton and Saluda Dolomites were compared to each other, and to the three computer-generated models. CSD measurements on the computer-generated microstructures of the Johnson-Mehl and site saturation nucleation and growth models, obtained from Dr. Knut Marthinsen, were also conducted by the line point count method.

## **CSD DATA**

### **Trenton Formation**

In the Trenton Formation samples, CSDs of fifty-seven clasts in twelve thin-sections of core were measured. The CSDs within the Trenton Formation contained a range of mean grain sizes from approximately 103  $\mu\text{m}$  (microns) to 690  $\mu\text{m}$ . Table 3 lists the mean, normalized standard deviation (NSD), STATGRAPHICS skewness (SK), inclusive graphic skewness (IGSK), and gamma distribution shape factor alpha ( $\alpha$ ) of the gamma distributions fitted to the CSDs by the STATGRAPHICS program. The table also shows the significance values for the one-sample Kolmogorov-Smirnov goodness-of-fit test of the normal (N), lognormal (L), and gamma (G) distributions, fitted to the Trenton CSDs by the STATGRAPHICS program..

Almost all of the CSDs are coarsely skewed, and, as can be seen by Table 3, the skewness varies considerably between clasts within the same thin-section. There is no correlation between mean grain size and skewness. X-Y plots of the skewness, normalized standard deviation, and alpha values to the mean grain size values yield shotgun patterns. The mean significance level for goodness-of-fit to a normal distribution for the Trenton samples is 0.046. Nine of the fifty-seven samples (approx. 15.8%) have a significance level greater than 0.05 for the Kolmogorov-Smirnov goodness-of-fit test to a normal distribution. The mean significance level for the Kolmogorov-Smirnov goodness-of-fit test to a lognormal distribution is 0.080. Twenty-six of the fifty-seven samples (approx. 45.6%) have a significance level greater than 0.05 for the Kolmogorov-Smirnov goodness-of-fit

**TABLE 3**  
**Trenton Formation CSD Statistical Values**

Clast	Mean	NSD	SK	IGSK	Normal	Lognormal	Gamma	Alpha
TL1A	26.88	0.6134	1.537	0.145	0.051	0.011	0.3265	2.69989
TL1A2	26.32	0.5914	1.004	0.169	0.0634	0.007	0.3301	2.61313
TL1A3	27.34	0.6208	1.231	0.323	0.0012	0.158	0.5012	2.58154
TL1B	36.94	0.5669	1.639	0.065	0.03	0.0001	0.0569	3.03783
TL1B2	38.43	0.5678	0.627	0.157	0.19	0.001	0.0524	2.54382
TL1B3	38.51	0.5974	1.301	0.175	0.0024	0.0088	0.3566	2.76443
TL1C	22.92	0.6131	1.066	0.179	0.0157	0.027	0.5166	2.55078
TL1D	18.3	1.0823	5.014	0.299	0	0.017	0.0025	1.8009
TL1E	46.04	0.6607	2.033	0.254	0.0089	0.064	0.8578	2.42403
TL1F	31.88	0.5942	0.986	0.196	0.0653	0.0073	0.3555	2.61838
TL1G	45.06	0.7171	0.87	0.092	0.0403	0.0056	0.0312	2.53753
TL1H	31.3	0.7306	4.786	0.171	0.0005	0.05	0.5381	2.51445
TL1I	32.4	0.7009	1.575	0.3	0.0008	0.247	0.9046	2.21197
TL2A	46.92	0.8608	2.888	0.299	0.00008	0.068	0.9548	1.61387
TL2B	15.18	0.6029	1.287	0.163	0.0019	0.008	0.3097	2.66052
TL2C	27.75	0.5599	0.836	0.217	0.037	0.0605	0.7608	2.93696
TL2D	32.59	0.5854	1.025	0.261	0.007	0.266	0.8198	2.83783
TL3A	28.42	0.3903	1.117	0.24	0.0111	0.0416	0.5021	2.37905
TL3B	26.32	0.5565	1.008	0.202	0.0205	0.083	0.8628	3.08421
TL3C	21.7	0.6438	1.3	0.224	0.0063	0.0041	0.1948	2.36045
TL3F	10.33	0.5541	0.6681	0.319	0.00018	0.02467	0.0735	3.01835
TL3G	23.15	0.8531	2.002	0.41	0.00001	0.314	0.555	1.66236
TL3H	42.92	0.5978	0.716	0.222	0.0275	0.0473	0.1229	2.50443
TL3I	20.31	0.5596	0.505	0.166	0.0438	0.0093	0.2565	2.70771
TL3J	32.71	0.5867	0.806	0.261	0.0108	0.0945	0.3716	2.66447
TL3K	35.25	0.5628	0.551	0.144	0.0714	0.0266	0.3466	2.7283
TL3L	19.45	0.7009	1.395	0.41	0.00002	0.213	0.3496	2.20524
TL3M	31.52	0.6363	1.126	0.248	0.0713	0.0153	0.3532	2.34964
TL4A	47.09	0.5834	0.688	0.256	0.0103	0.0541	0.2398	2.57261
TL4B	65.21	0.6427	1.199	0.278	0.0023	0.1727	0.919	2.38188
TL5K	39.14	0.6571	2.217	0.093	0.046	0.0008	0.0842	2.30262
TL5L	42.17	0.7128	3.042	0.181	0.0006	0.0068	0.3428	2.51035

TABLE 3 (cont'd)

Clast	Mean	NSD	SK	IGSK	Normal	Lognormal	Gamma	Alpha
TL5W	23.76	0.5643	0.736	0.262	0.0038	0.088	0.6169	2.88956
TL6H	25.88	0.5560	1.084	0.258	0.0026	0.0839	0.8383	3.24926
TL7A	25.7	0.6273	1.017	0.423	0.000034	0.5184	0.122	2.64872
TL7B	30.81	0.6894	3.398	0.32	0.000015	0.22255	0.2922	2.68066
TL7C	35.68	0.6145	0.666	0.205	0.02145	0.001766	0.1573	2.18132
TL7D	41.79	0.5938	0.867	0.184	0.02776	0.03202	0.6349	2.51771
TL7E	26.45	0.4796	0.739	0.017	0.2395	0.004146	0.0733	3.87437
TL8A	29.11	0.6512	1.28	0.281	0.00147	0.09016	0.6839	2.42907
TL8B	22.91	0.5055	0.774	0.226	0.01174	0.2059	0.8156	3.78985
TL8C	22.64	0.6125	1.201	0.261	0.00377	0.19866	0.5798	2.71994
TL8D	44.79	0.4901	0.508	0.175	0.12023	0.07603	0.3081	3.63656
TL8E	18.65	0.5100	0.876	0.169	0.08047	0.04682	0.4353	3.62261
TL8F	27.07	0.4986	0.537	0.207	0.0126	0.028736	0.1945	3.66526
TL8G	19.26	0.5614	1.217	0.322	0.00263	0.32612	0.4358	3.36934
TL9A	25.93	0.5589	0.913	0.205	0.013305	0.05073	0.6351	3.1558
TL9B	11.91	0.5282	1.327	0.205	0.006545	0.060908	0.3966	3.79039
TL9C	42.53	0.4281	0.112	-0.053	0.43555	0.000493	0.0124	4.55155
TL9D	30.54	0.6058	0.986	0.243	0.005413	0.042485	0.7139	2.50886
TL10A	61.43	0.5751	0.432	0.129	0.60593	0.009861	0.1509	2.37001
TL10B	40.63	0.5879	1.007	0.205	0.032994	0.01646	0.2365	2.7784
TL10C	57.76	0.6190	1.686	0.138	0.05275	0.01817	0.3987	2.68302
TL11A	43.96	0.5607	1.001	0.262	0.01774	0.09693	0.907	3.13785
TL11B	23.45	0.6944	1.156	0.289	0.0013	0.01803	0.4758	1.95518
TL11C	27.75	0.5503	0.974	0.171	0.099663	0.02201	0.3406	3.0576
TL11D	46.78	0.5489	0.744	0.201	0.026245	0.0068453	0.3212	2.82855
TL11E	33.76	0.6788	1.186	0.337	0.00063	0.117445	0.9593	2.13452
TL11F	34.51	0.5916	0.91	0.244	0.006776	0.004342	0.2773	2.58217
TL11G	33.79	0.8715	5.862	0.366	0.000087	0.37035	0.3932	2.0578
TL12A	33.38	0.6844	3.196	0.205	0.002226	0.017637	0.5091	2.56273
TL13B	69.05	0.5831	1.056	0.205	0.004825	0.098746	0.7293	2.82419

NSD = Normalized Standard Deviation

Alpha = Gamma Distribution Shape Factor

Normal = Kolmogorov-Smirnov Test Significance Level to a Normal Distribution

IGSK = Inclusive Graphic Skewness

Lognormal = Kolmogorov-Smirnov Test Significance Level to a Lognormal Distribution

SK = STATGRAPHICS Skewness

Gamma = Kolmogorov-Smirnov Test Significance Level to a Gamma Distribution

&lt; 0.05

test to a lognormal distribution. The mean goodness-of-fit significance level to a gamma distribution is 0.440. Fifty-four out of the fifty-seven samples (approx. 94.7%) have a significance level greater than 0.05 to a gamma distribution.

Table 3 shows that the gamma distribution has very few Kolmogorov-Smirnov goodness-of-fit values less than 0.05, and can probably best describe most of the CSD shapes relative to the other distribution types. It is apparent that the gamma distribution shape factor may be a good value to represent the shape of each CSD, and can be quantitatively compared to determine CSD shape variability.

The Trenton core sample CSDs were divided into two groups based on mean grain size to determine if trends in the shape of the CSDs were present in the alpha, skewness, and normalized standard deviation values of the two groups. A large mean grain size group and a small mean grain size group were evaluated. The small mean group contained those CSDs with a mean grain size between 113 and 313  $\mu\text{m}$ . The large mean group contained those CSDs with a mean grain size between 315 and 652  $\mu\text{m}$ . A two-sample t-test was performed between the mean, alpha, normalized standard deviation, and skewness values in each group. A significance level less than 0.05 was used to reject the null hypothesis. The two-sample t-test between the alpha values resulted in a significance value of 0.15. The two-sample t-test between the normalized standard deviation values of the two groups resulted in a significance value of 0.56. A two-sample t-test significance value of 0.096 was obtained for the inclusive graphic skewness values of the two groups. The significance value for the two-sample t-test between the STATGRAPHICS skewness values was 0.98. The significance value for the two-sample t-test between the mean grain sizes was  $5.3 \times 10^{-13}$ . Thus, the null hypothesis that there is a difference in the shape of the Trenton CSDs based on mean grain size is rejected.

Tables 4 through 10 show significance level results of the normalized CSD two-sample Kolmogorov-Smirnov goodness-of-fit test between clasts from the same thin-section. The significance levels less than 0.05 are shaded.

**TABLE 4**  
**Two Sample K-S Tests Between Thin-Section TL1 Clasts**

	TL1A2	TL1A3	TL1B	TL1B2	TL1B3	TL1C	TL1D	TL1E	TL1F	TL1G	TL1H	TL1I
TL1A	0.7870	0.5175	0.5842	0.5175	0.7212	0.7870	0.0000	0.5842	0.8475	0.1759	0.6527	0.2923
TL1A2		0.5842	0.3953	0.6527	0.4543	0.7870	0.0031	0.6527	0.8996	0.7212	0.7870	0.2098
TL1A3			0.1465	0.0996	0.4543	0.7870	0.0056	0.5842	0.6524	0.3412	0.8996	0.4543
TL1B				0.7212	0.7870	0.2098	0.0002	0.1465	0.4543	0.1212	0.3412	0.0266
TL1B2					0.3953	0.2098	0.0013	0.5175	0.8475	0.3953	0.2098	0.0659
TL1B3						0.3412	0.0042	0.5842	0.8996	0.0337	0.5175	0.1759
TL1C							0.0136	0.8475	0.4543	0.3412	0.9408	0.6427
TL1D								0.0266	0.0006	0.0003	0.0040	0.1465
TL1E									0.7870	0.1759	0.7212	0.6527
TL1F										0.2485	0.7870	0.2485
TL1G											0.7212	0.0812
TL1H												0.4543

**TABLE 5**  
**Two Sample K-S Tests Between Thin-Section TL2 Clasts**

	TL2B	TL2C	TL2D
TL2A	0.0031	0.0031	0.0056
TL2B		0.8475	0.6527
TL2C			0.8475

**TABLE 6**  
**Two Sample K-S Tests Between Thin-Section TL3 Clasts**

Clast	TL3B	TL3C	TL3F	TL3G	TL3H	TL3I	TL3J	TL3K	TL3L	TL3M
TL3A	0.3953	0.5175	0.1212	0.0096	0.4543	0.6527	0.8996	0.7870	0.2485	0.7212
TL3B		0.5842	0.1465	0.0007	0.1759	0.5175	0.2923	0.5842	0.0337	0.1759
TL3C			0.1759	0.0208	0.6527	0.3412	0.5842	0.7212	0.2098	0.6527
TL3F				0.0001	0.2485	0.3412	0.3953	0.3953	0.1212	0.0424
TL3G					0.0530	0.0031	0.0056	0.0162	0.0424	0.0812
TL3H						0.4543	0.7870	0.9700	0.2485	0.4543
TL3I							0.7212	0.9408	0.0337	0.4543
TL3J								0.7870	0.2485	0.4543
TL3K									0.0530	0.5842
TL3L										0.1465

**TABLE 7**  
**Two Sample K-S Tests Between Thin-Section TL7 Clasts**

	TL7B	TL7C	TL7D	TL7E
TL7A	0.2485	0.1465	0.1759	0.0013
TL7B		0.0659	0.3412	0.0208
TL7C			0.8475	0.0424
TL7D				0.0659

**TABLE 8**  
Two Sample K-S Tests Between Thin-Section TL8 Clasts

	TL8B	TL8C	TL8D	TL8E	TL8F	TL8G
TL8A	0.0337	0.6527	0.0659	0.0266	0.0659	0.0208
TL8B		0.3953	0.7212	0.9700	0.7212	0.3953
TL8C			0.0812	0.1465	0.0996	0.4543
TL8D				0.6527	0.8475	0.5842
TL8E					0.4543	0.4543
TL8F						0.5175

**TABLE 9**  
Two Sample K-S Tests Between Thin-Section TL9 Clasts

	TL9B	TL9C	TL9D
TL9A	0.2098	0.0424	0.7212
TL9B		0.0162	0.0812
TL9C			0.0056

**TABLE 10**  
Two Sample K-S Tests Between Thin-Section TL11 Clasts

Clast	TL11B	TL11C	TL11D	TL11E	TL11F	TL11G
TL11A	0.0056	0.5842	0.8475	0.1759	0.6527	0.0659
TL11B		0.0074	0.0074	0.7212	0.1212	0.3412
TL11C			0.7212	0.2098	0.6527	0.0337
TL11D				0.0996	0.6527	0.0162
TL11E					0.2098	0.7212
TL11F						0.0530



From Tables 4 through 10 it appears that about one CSD (clast) is significantly different in shape from most of the other CSDs (clasts) in the same thin-section.

The normalized CSD two-sample Kolmogorov-Smirnov goodness-of-fit tests between all normalized Trenton samples are presented as a table in Appendix B. All two-sample Kolmogorov-Smirnov goodness-of-fit significance levels less than 0.05 are shaded in the table of Appendix B. Of the 1,596 comparisons between the Trenton clast CSDs, 1,290 (81%) show goodness-of-fit values  $>0.05$ , indicating that they are from the same population. Of the 306 comparisons (19%) with goodness-of-fit values  $<0.05$ , 174 (57%) of those are from 4 of the 57 clasts. The clasts include TL1D, TL2A, TL3G, and TL9C. The majority of the Trenton CSDs are not significantly different in shape from each other, though the mean grain sizes do vary significantly.

### **Saluda Formation**

Eight CSDs from seven thin-sections of hand samples from the Saluda Formation were measured by the line point count method. The mean grain size of the CSDs of the mudstones measured decreased down section, and ranged from  $31\mu\text{m}$  to  $69\mu\text{m}$ . Figure 22 shows two of the eight normalized CSD frequency histograms. The normalized frequency histograms of the CSDs are also included in Appendix C. Table 11 lists the mean, the normalized standard deviation (NSD), the STATGRAPHICS skewness (SK), the inclusive graphic skewness (IGSK), and the gamma distribution shape factor alpha ( $\alpha$ ) for the Saluda sample CSDs. It also lists the significance values for the one-sample Kolmogorov-Smirnov goodness-of-fit tests of the normal, lognormal, and gamma distribution fitting to the Saluda Formation CSDs.

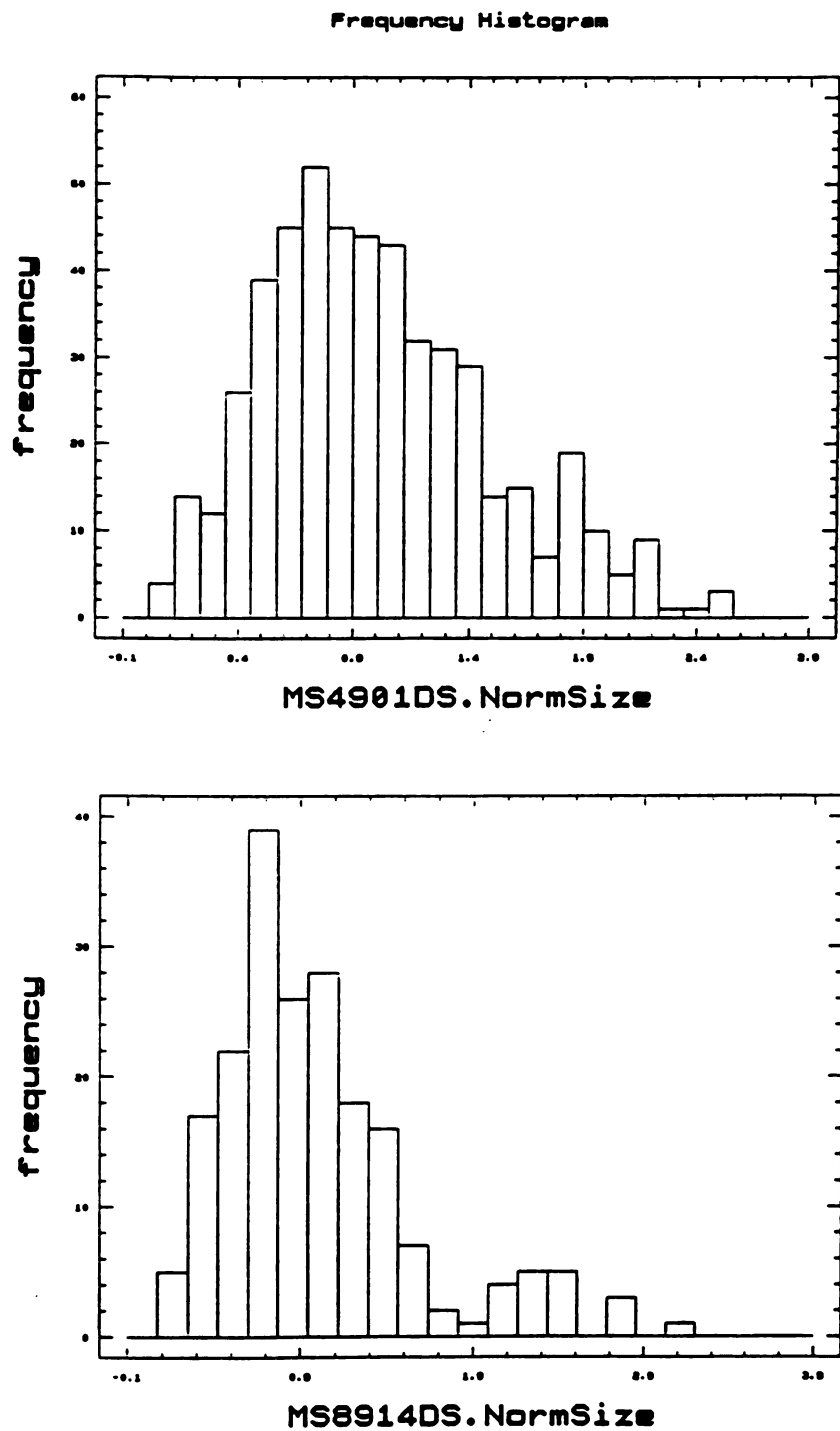


**Figure 22** Two of the eight frequency histograms of the Saluda dolomite samples.

**TABLE 11**  
**Saluda Formation CSD Statistical Values**

Sample	Mean	NSD	SK	IGSK	Normal	Lognormal	Gamma	Alpha
MS4901DS.SZ	68.905	0.4963	0.6592	0.2679	0.00004	0.0041	0.2932	3.7044
MS4901DS.SH	67.253	0.4012	0.5258	0.125	0.0001	0.0217	0.0501	6.1786
MS4904DS	57.512	0.4530	0.7654	0.1145	0.0873	0.0267	0.2579	4.5784
MS8903DS	55.675	0.4978	1.055	0.1472	0.1551	0.0576	0.2013	3.8924
MS8904DS	53.801	0.4668	1.1053	0.1515	0.0294	0.4254	0.5647	4.9075
MS8907DS	37.023	0.4990	0.7085	0.319	0.0049	0.1053	0.1373	3.9175
MS8912DS	49.711	0.5217	0.6341	0.2661	0.0279	0.122	0.5755	3.4214
MS8914DS	30.741	0.5662	1.4115	0.4500	0.0001	0.1005	0.0243	3.5505

**NSD** = Normalized Standard Deviation

**Alpha** = Gamma Distribution Shape Factor

**Normal** = Kolmogorov-Smirnov Test Significance Level to a Normal Distribution

**IGSK** = Inclusive Graphic Skewness

**Lognormal** = Kolmogorov-Smirnov Test Significance Level to a Lognormal Distribution

**SK** = STATGRAPHICS Skewness

**Gamma** = Kolmogorov-Smirnov Test Significance Level to a Gamma Distribution

< 0.05

All of the Saluda Formation sample normalized CSDs are coarsely skewed. Table 11 shows that skewness also varies moderately between the Saluda Formation samples. As with the Trenton samples, there appears to be very little correlation between mean grain size and skewness in the Saluda dolomite samples.

The mean significance level for goodness-of-fit to a normal distribution is 0.035. Two of the eight samples have a significance level greater than 0.05 for Kolmogorov-Smirnov goodness-of-fit test to a normal distribution. The mean significance level for goodness-of-fit to a lognormal distribution is 0.108. Five of the eight samples have a significance level greater than 0.05 for Kolmogorov-Smirnov goodness-of-fit test to a lognormal distribution. The mean goodness-of-fit significance level to a gamma distribution is 0.263, and seven out of the eight samples have a significance level greater than 0.05.

Tables 12 shows the results of the normalized CSD two-sample Kolmogorov-Smirnov goodness-of-fit test between the Saluda Formation samples.

**TABLE 12**  
**Two-Sample Kolmogorov-Smirnov Goodness-Of-Fit Tests**  
**Between Saluda Formation Samples**

Sample	MS4901DS.SH	MS4904DS	MS8912DS	MS8914DS	MS8903DS	MS8904DS	MS8907DS
MS4901DS.SZ	0.0377	0.2533	0.4440	0.0940	0.4145	0.3644	0.2965
MS4901DS.SH		0.3231	0.0073	0.0023	0.0468	0.6578	0.0315
MS4904DS			0.1605	0.0141	0.4653	0.5637	0.1053
MS8912DS				0.1401	0.7005	0.2497	0.6240
MS8914DS					0.0968	0.0306	0.3896
MS8903DS						0.5934	0.2080
MS8904DS							0.2382
< 0.05							

Of the 28 Saluda CSD comparisons, 7 (25%) show goodness-of-fit values  $< 0.05$ . Of those 7, 5 (71%) of them are from the sample MS4901DS.SH. However, the majority are not significantly different from each other.

### **Theoretical Computer - Generated Microstructures**

It is expected that the CSDs for the computer-generated models will vary according to the differing nucleation and growth parameters used to generate them. Those differences should be reflected in the differences in the appearance of the CSDs, and in the statistical values characterizing the CSD shape, as well as in the normalized CSD two-sample

Kolmogorov-Smirnov goodness-of-fit tests. The normalized frequency histograms are also shown in Appendix C. The CSD for the site saturation model is finely skewed, the Johnson-Mehl model is more normally distributed, and the site saturation model with weakly clustered nuclei is quite normally distributed. Table 13 lists the statistical values for the theoretical models, as was done for the Trenton and Saluda Formations.

**TABLE 13**  
**Theoretical Computer-Generated Microstructure CSD Statistical Values**

Model	Mean	NSD	SK	IGSK	Normal	Lognormal	Gamma	Alpha
KMSITSAT	0.5532	0.3135	-0.6830	-0.2494	0.0017	4.89E-8	0.00001	6.7425
KMJNSMEL	0.8015	0.4124	-0.2642	-0.1185	0.2896	0.0008	0.0101	3.8401
KMSSWKCL	0.5363	0.3797	-0.2059	-0.0085	0.9386	0.000065	0.0087	5.2698

KMSITSAT = Site Saturation (Cellular) Nucleation and Growth Model

KMJNSMEL = Johnson-Mehl Nucleation and Growth Model

KMSSWKCL = Site Saturation Model With Weakly Clustered Nuclei

NSD = Normalized Standard Deviation

Alpha = Gamma Distribution Shape Factor

Normal = Kolmogorov-Smirnov Test Significance Level to a Normal Distribution

IGSK = Inclusive Graphic Skewness

Lognormal = Kolmogorov-Smirnov Test Significance Level to a Lognormal Distribution

SK = STATGRAPHICS Skewness

Gamma = Kolmogorov-Smirnov Test Significance Level to a Gamma Distribution

< 0.05

The gamma distribution shape factor does not adequately describe these distributions. The weakly clustered site saturation model is quite normally distributed. The Johnson-Mehl model is somewhat normally distributed, but is slightly finely skewed, as can be seen on Figure 6. The site saturation model is quite finely skewed and does not compare to a normal, lognormal, or gamma distribution.

Table 14 shows the results of the two-sample Kolmogorov-Smirnov goodness-of-fit test between the normalized CSDs of the three theoretical nucleation and growth models used in this study.

**TABLE 14**  
**Two-Sample Kolmogorov-Smirnov Goodness-Of-Fit Tests**  
**Between Normalized Theoretical Computer-Generated Microstructure CSDs**

Model	KMJNSMEL	KMSSWKCL
KMSITSAT	0.0452	0.0337
KMJNSMEL		0.3512
< 0.05		

The results of the statistical analyses of the theoretical models shows that the site saturation and Johnson-Mehl models differ according to the nucleation and growth kinetics used to generate them. As would be expected, the Johnson-Mehl model has an increase in the frequency of smaller grains over the site saturation model (Figure 6). The effect of weakly clustered nuclei in a site saturation model appears to broaden the distribution, and to increase the number of small grains, thereby making the CSD less finely skewed than the site saturation model with random nucleation sites. The resulting weakly clustered model CSD mimics the shape of the Johnson-Mehl model, as can be seen by the Kolmogorov-Smirnov goodness-of-fit test value in Table 14, but it still maintains a lower frequency of the smaller grains than the Johnson-Mehl model. This illustrates the effect of varying the location of nuclei on the resulting CSD.

#### **Analysis and Comparison Between Formation and Theoretical CSDs**

The two-sample Kolmogorov-Smirnov goodness-of-fit values of the Saluda normalized CSDs to the Trenton and computer-generated normalized CSDs are presented in the table

of Appendix B. The goodness-of-fit values in Appendix B show that of the 456 comparisons between the Saluda and the Trenton samples, 243 (53.3%) have values  $<0.05$ , indicating that those samples are not from the same population. Five of the eight Saluda samples account for 204 (84%) of the 243 goodness-of-fit values that are  $<0.05$ . These include MS4901.SZ, MS4901.SH, MS4904, MS894, and MS8914. Thus, a majority of the normalized CSDs for the Saluda Formation samples are significantly different from those of the Trenton Formation samples.

The means and standard deviations of the alpha, normalized standard deviations, STATGRAPHICS skewness, and inclusive graphic skewness values for the Trenton and Saluda CSDs are presented in Table 15

**TABLE 15**  
Comparison of Mean and Standard Deviations of the Means and Standard Deviations of the Alpha, Normalized Standard Deviation, Skewness, and Inclusive Graphic Skewness Values for the Saluda and Trenton Formations

	SALUDA FM.		TRENTON FM.	
CSD Shape Descriptor	Mean	Standard Dev.	Mean	Standard Dev.
Alpha	4.269	0.923	2.720	0.542
Normalized Standard Dev.	0.488	0.049	0.615	0.107
STATGRAPHICS skewness	0.858	0.302	1.379	1.089
Inclusive Graphic skewness	0.222	0.087	0.230	0.117

This table shows significant differences between the alpha values of the two formations, and between the normalized standard deviation values of the two formations. There is moderate-to-low difference between the STATGRAPHICS skewness values between the

two formations, and very little difference between the inclusive graphic skewness values of each formation. Two-sample t-tests performed between the shape descriptors of the two formations resulted in similar conclusions. Significance levels less than 0.05 result in rejection of the null hypothesis. The two-sample t-tests for the alpha and normalized standard deviation values of the two formations yielded significance levels of  $1.7 \times 10^{-9}$  and 0.0015 respectively. The two-sample t-test for the STATGRAPHICS skewness and inclusive graphic skewness values of the two formations yielded significance levels of 0.1853 and 0.8184 respectively.

The table in Appendix B also shows that the theoretical model CSDs are significantly different from both the Saluda and Trenton Formation samples. There are no goodness-of-fit values greater than 0.05 for the site saturation model. The Kolmogorov-Smirnov goodness-of-fit tests between the weakly clustered site saturation model and the Trenton Formation samples have only two significance values greater than 0.05 out of the 62 comparisons. Kolmogorov-Smirnov goodness-of-fit tests between the weakly clustered site saturation model and the eight Saluda Formation samples resulted in only one significance value greater than 0.05. The Johnson-Mehl model goodness-of-fit to the Trenton Formation samples resulted in nineteen significance values greater than 0.05 out of the 62 tests. Three of the eight goodness-of-fit tests between the Johnson-Mehl and Saluda Formation samples resulted in values greater than 0.05. This indicates that the Johnson-Mehl model is the closest of the three theoretical models to the dolomite CSDs, but all theoretical models have relatively poor representation of the experimental data.



## DISCUSSION

CSD shape comparison between the Saluda and the Trenton samples appear to show the Saluda Formation sample CSDs have slightly lower frequencies of very small grains. Figure 23 is a cumulative frequency graph of Saluda and Trenton Formation samples which illustrates the CSD behavior observed between the two formations.

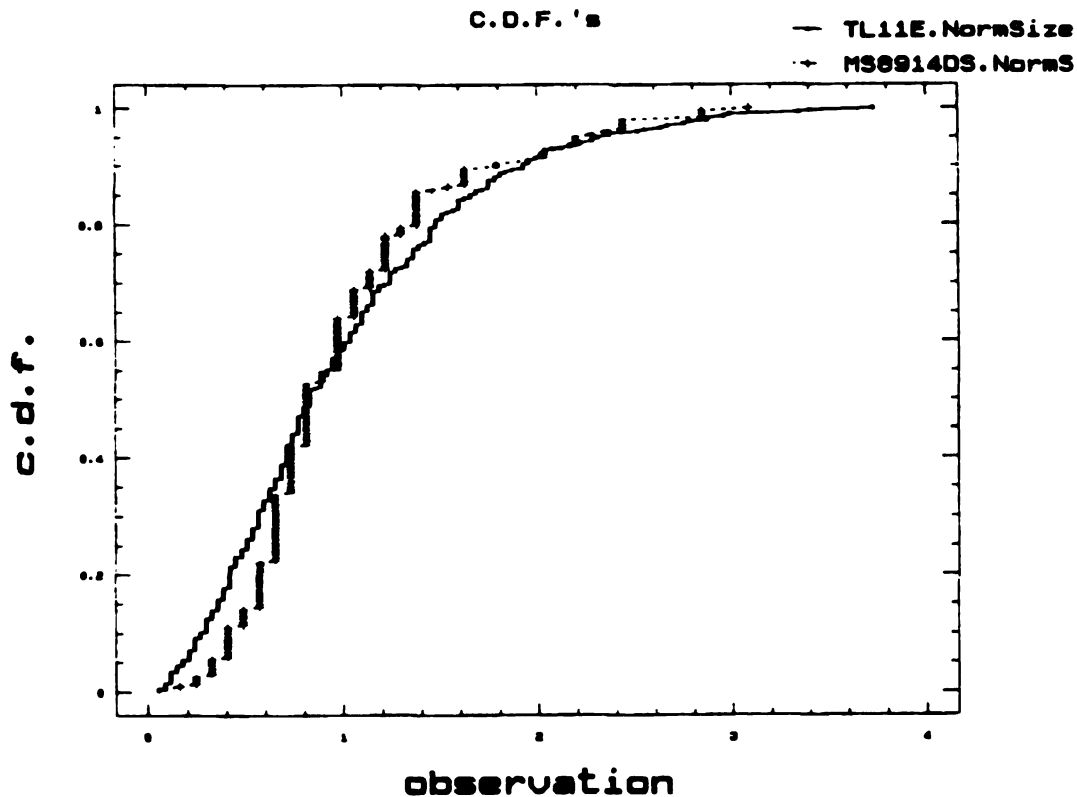


**FIGURE 23** Kolmogorov-Smirnov goodness-of-fit test cumulative relative frequency distribution showing the consistent differences between the Saluda and Trenton Formation CSDs.

The lower number of small grains in the normalized Saluda sample CSDs, relative to the

number observed in the Trenton, implies a lower nucleation to growth ratio in the Saluda Formation than that of the higher temperature Trenton Formation samples. It cannot be determined if the lower ratio in the Saluda is due to a decreasing nucleation rate, an increasing growth rate, or both, relative to those of the Trenton samples. Occasionally, much larger grain growth, also termed “run-away growth”, is also evident in the higher temperature Trenton samples, and can be associated with elevated temperatures. Run-away growth was not observed in the Saluda Formation samples.

The values of skewness did not show significant differences between the Trenton and Saluda samples, as is evident by the two-sample t-test results shown previously, as opposed to the gamma distribution shape factor alpha. It may be that the skewness factors do not detect significant differences between the CSDs due to the nature of the skewness statistic. Groeneveld (1991) compared several measures of skewness of univariate distributions, and used Hampel’s influence function to clarify the similarities and differences among the measures of skewness. “Skewness, like kurtosis, is a qualitative property of a distribution... A general concept of skewness as a location- scale-free deformation of the probability mass of a symmetric distribution emerges. Positive skewness can be thought of as resulting from movement of mass at the right of the median from the center to the right tail of the distribution together with movement of mass at the left of the median from the left tail to the center of the distribution,” (Groeneveld, 1991, p.97). The steps outlined by Hartmann (1988) indicate that the gamma distribution shape factor (alpha) and the normalized standard deviation values may be better descriptors of the CSDs than skewness values. “Instead of using a goodness-of-fit parameter to something which is only assumed, I propose the following procedure:

- 1) Make a decision about the statistical system, thus, the right descriptive statistics to be used.
- 2) Estimate the parameters of the experimental data.

- 3) Check the goodness-of-fit to the theoretical distributions for the purposes of quality control," (Hartmann, 1988, p.915).

Use of the gamma distribution in describing CSDs is also supported in work by Vaz and Fortes (1988) in which they show the gamma distribution to have the type of asymmetry observed in actual grain size distributions.

The majority of CSDs in this study do not resemble lognormal distributions. It is common to find lognormally shaped CSDs in materials believed to have undergone aggrading neomorphism by Ostwald ripening (recrystallization due to surface free energy differences whereby large crystals grow at the expense of smaller crystals). An aggregate of grains can reduce its total interfacial free energy by forming grains as large as possible, thereby reducing the total interface area (Vernon, 1975). The Trenton and Saluda Formations do not have lognormally shaped CSDs and do not show petrographic evidence of neomorphism. Recent dolomite crystal size distribution studies (Gregg and Howard, 1990; Gregg and Shelton, 1990) have found lognormally shaped distributions in dolomites. Using the line point count method with scanning electron microscopy, Gregg and Howard (1990) determined CSDs on Recent dolomites forming in peritidal savannahs on the Caribbean island of Ambergris Cay, Belize. The Belize samples had an average Kolmogorov-Smirnov goodness-of-fit test significance level of 0.17 to a normal distribution, and 0.58 to a gamma distribution, whereas the average for a lognormal distribution was 0.69. Only two of the normal distribution tests had significance levels less than 0.05, and none of the lognormal or gamma distribution tests had significance levels less than 0.05. The submicron to micron sizes of the Belize dolomites are within the range in which surface free energies can contribute to the stability of a crystal. The lognormal distributions are therefore consistent with the hypothesized Ostwald ripening process. Gregg and Shelton (1990) also determined the CSDs of the back reef facies

dolomite of the Bonneterre Dolomite in southeastern Missouri. The Bonneterre Dolomite forms the lower part of an upper Cambrian platform carbonate sequence which is a primary host to the Mississippi Valley-type sulfide ore deposits of that region. The resulting CSDs were all coarsely skewed and typically lognormally distributed. The Bonneterre samples had a mean Kolmogorov-Smirnov goodness-of-fit test significance level of approximately 0.14 to the normal distribution, and 0.25 to the lognormal distribution. The lognormal distributions observed in the Bonneterre dolomite could be attributed to further dolomitization and neomorphism during the sulfide mineralization. It is assumed, for lack of other evidence, that the neomorphism was driven by surface energy (e.g. Ostwald ripening) during the regional mineralization. The lack of neomorphism in the Saluda dolomite is suggested by the presence of well preserved CL zoning. The dolomite probably did undergo partial re-equilibration of unstable cores. However, that would be a compositionally driven process and not a surface energy driven one.

The thickness of contemporary CL zones can be used to distinguish flux-limited crystal growth from surface-reaction-limited crystal growth (Kretz, 1974; Carlson, 1989). Heterogeneity in the flux of dolomitizing solution is based on Pingitore's (1982) concept of macropore and micropore solute transport. In macropores the solute may be transported under hydraulic gradient whereas in micropores, or in isolated intragranular pores which form culs-de-sac off the flow path, the solute is subject to transported by diffusion. The chemical isolation, and the ability to exchange ions between these two water/solute regimes, determines the openness of the system to dolomitization, the degree of textural preservation, and the resulting trace-element chemistry of the dolomite. Assumptions made for this model are that for most of a given volume of rock solute transport is by diffusion, that a much smaller volume receives solute by advective flux, and that there is a continuum between advective flux and diffusion flux. In flux-limited crystal growth, contemporaneous CL zones in crystals of different sizes will vary with the radius of the

crystal. The larger grains presumably receive a greater flux of solute from which growth occurs, and will grow at a quicker rate than smaller grains, which receive a smaller flux of solute. The larger grains will subsequently grow thicker CL zones than those of the contemporaneous smaller grain CL zones. In surface-reaction-limited crystal growth, the contemporaneous CL zones will have a constant thickness regardless of the crystal diameter. The variation in crystal size results only from the age of the crystal. Nordeng and Sibley (1990) conducted such a study on the Saluda Formation dolomite and found that the contemporaneous CL zone thicknesses were a function of the crystal diameter, and therefore fit a flux-limited model.

The theoretical models indicate that the CSD skewness could be augmented if the preferred nucleation sites were slightly clustered, and not homogeneously or randomly distributed. Qualitatively, only clast TL1D, and possibly TL3G, of the Trenton dolomite clasts had noticeably 'clustered' sizes. Petrographic inspection suggests that these clasts may have initially incorporated two textural sizes within them, because groups of small dolomite crystals were distinct and did not necessarily grade into the surrounding larger crystals, as seen in the theoretical model. The CSDs for these clasts were among those most different from the other Trenton CSDs. Clustering in the Saluda was not apparent.

## **CONCLUSIONS**

Several characteristics of the CSDs observed in this study can be noted.

- 1) The CSDs for almost all samples are coarsely skewed with the exception of the computer-generated microstructures.
- 2) The shape of the majority of CSDs for the Trenton and Saluda Formations are represented more closely by the gamma-type distributions than they are by the lognormal or normal distributions. This is evident by the greater percent of Kolmogorov-Smirnov goodness-of-fit values  $>0.05$  for the gamma distributions than the lognormal or normal distributions.
- 3) The majority of the Trenton CSDs have a similar shape regardless of their mean grain size. This is evident by the 81% of the goodness-of-fit values  $>0.05$  between Trenton samples, and the two-sample t-tests of the mean grain sizes, and the alpha values between the large mean grain size Trenton clasts and those of the small mean grain size Trenton clasts. In addition, the X - Y plots of the alpha and NSD values of all Trenton samples against the corresponding sample mean grain size values showed no linear trends.
- 4) The shapes of the majority of the Trenton CSDs show significantly different distributions than those of the Saluda Formation. This is evident by the mean and standard deviation values of the respective alpha and normalized standard deviation CSD shape descriptors, and a two-sample t-test conducted on those values. It is also evident by the 53.3 % of the goodness-of-fit values  $<0.05$  between the Trenton and Saluda samples

- 5) The mean dolomite crystal size decreases down section in the Saluda Formation. This down section decrease in mean grain size is consistent with the flux-limited growth identified by the Nordeng and Sibley (1990) CL zone thickness study.
- 6) Lognormally shaped CSDs may be supplemental evidence of neomorphism of dolomite. This is evident by the lognormal distributions of the Belize modern dolomite and the Upper Cambrian, Bonnetterre dolomite CSD studies by Gregg et al., and by the lack of evidence of neomorphism in the Saluda samples.
- 7) CSDs of the computer-generated microstructures do not resemble those of the Trenton or Saluda Formations.

Further study of the limestone Trenton clast CSDs would be required to compare the difference between the dolomite and precursor limestone CSDs. A similar relationship between the mean grain size and CSD in the limestone clasts as observed in the dolomite would indicate that the precursor limestone texture exerts significant control of the nucleation and growth of the dolomite. In addition, further studies in similar geologic settings are needed to determine if the differences between the Saluda and Trenton samples are a consistent characteristic of CSD shape between the different settings.

## **APPENDICIES**



## **APPENDIX A**

### **Thin-Section Descriptions, Photographs, and Drawings**

## APPENDIX A

### Thin-Section Description, Photographs, and Drawings

#### TRENTON Formation Samples

##### L1-12 C3 B21 4931: (TL1)

<u>Clast</u>	<u>Description</u>
--------------	--------------------

- |      |  |
|------|--|
| A.   | Fine to medium grained, planar dolomite.   |
| B.   | Fine to medium grained, planar dolomite.   |
| C.   | Very-fine to fine grained, planar dolomite.  |
| D.   | Very-fine to fine grained, planar dolomite with a few large echinoid replaced grains. some clays and minor porosity. |
| E.   | Medium to coarse grained, planar dolomite.   |
| F.   | Fine to medium grained, planar dolomite.   |
| G.   | Fine to medium grained, planar dolomite with a silica replaced brachiopod.   |
| * H. | small amount of anhydrite and some clays which allowed more plucking from minor porosity.                            |

##### TL 1-12 C3 B55 4891: (TL2)

- |    |  |
|----|--|
| A. | Coarse grained planar dolomite with some plucking during sample preparation. |
| B. | Medium to coarse grained, planar dolomite.                                   |
| C. | Fine to medium grained, planar dolomite with some plucking.                  |
| D. | Medium to coarse grained, planar dolomite with some plucking.                |

##### L1-12 C1 B1: (TL3)

- |      |   |
|------|---|
| A.   | Medium to coarse grained, porous, non-planar, with significant clays between crystals. Vug?                           |
| B.   | Fine to medium grained, planar dolomite.  |
| C.   | Fine to medium grained, planar dolomite.  |
| D.   | Fine to coarse grained, porous, non-planar dolomite, with some anhydrite and significant clays between crystals. Vug? |
| E.   | Fine to coarse grained, porous, non-planar dolomite, with some anhydrite and significant clays between crystals. Vug? |
| * F. | Very-fine to fine grained, planar dolomite. Dirty, with pyrite.   |
| G.   | Fine to medium grained, planar dolomite.  |
| H.   | Medium to coarse grained, planar dolomite with minor porosity.  |
| * I. | Fine to medium grained, planar dolomite with some porosity between clasts.  |

- J. Medium to coarse grained, planar dolomite with some porosity between clasts.
  - K. Medium to coarse grained, planar dolomite.
  - L. Fine to medium grained, planar dolomite with some clays between crystals and minor porosity.
  - M. Medium to coarse grained, planar dolomite with an area (vug?) of fine to medium grained, porous dolomite which has more clays.
  - N. Medium to coarse grained, planar dolomite.
- L1-12 C3 B2: (TL4)**
- A. Coarse grained, porous, planar dolomite with a few anhydrite grains and some plucked grains.
  - B. Coarse grained, porous, planar dolomite with some plucked grains. No anhydrite grains.
- L1-12 C1 B5: (TL5)**
- K. Coarse grained, porous, planar dolomite with some pore filling clays, much anhydrite and plucking.
  - L. Medium to very-coarse grained, porous, planar dolomite with some anhydrite, pore filling clays and plucking.
  - \* W. Fine to medium grained, dirty, planar dolomite(?), with minor porosity (in one area), some plucking and a stylolitic boundary.
- Luck 1-12 C1 B5 485?: (TL6)**
- \* H. Medium grained, porous, planar dolomite with some plucked grains. (Same as TL7E) Partial?
- L1-12 C1 B5: (TL7)**
- A. Fine to medium grained, porous, planar dolomite with a moderate amount of clays and silt size quartz grains in the pore spaces and between crystal grains.
  - B. Medium to coarse grained, porous, planar dolomite with a few large, run-away growth dolomite rhombs, and minor amount of clays in the pore spaces.
  - C. Medium to coarse grained, very porous, planar dolomite with an appreciable amount of anhydrite and pore filling clays.
  - D. Medium to coarse grained, very porous, planar dolomite with some anhydrite and pore filling clays.
  - E. Fine to medium grained, porous, planar dolomite with a minor amount of pore filling clays.
- Luck 4864½ (C1 B8?): (TL8)**
- A. Fine to medium grained, moderately porous, planar dolomite filling a fossil mold and non-mimetically replacing it. A moderate amount of pore filling clay and a small amount of anhydrite.
  - B. Fine to medium grained, slightly porous, planar dolomite with a minor amount of pyrite.
  - C. Fine to medium grained, porous, planar dolomite with a minor amount of pyrite.
  - D. Medium to coarse grained, very porous, non-planar dolomite with a moderate amount of anhydrite.

- E. Fine to medium grained, slightly porous, planar dolomite with a moderate amount of clays in the pore spaces, a minor amount of pyrite, and a dingy appearance.
- F. Fine to medium grained, slightly porous, planar dolomite with a minor amount of pyrite and a dingy appearance.
- G. Fine to medium grained, planar dolomite with minor porosity,, a minor amount of pyrite, and a dingy appearance.

Luck 1-12 C1 B5 4852½: (TL9) (same as 6, 7, and 5?)

- A. Fine to medium grained, porous, planar dolomite with a minor amount of pore filling clays.
- B. Very-fine to fine grained, moderately porous, planar dolomite with a significant amount of clays in the pore spaces and between grains. Some anhydrite and a large, replaced echinoid grain.
- C. Medium to coarse grained, porous, planar dolomite with a minor amount of pore filling clays.
- D. Medium to coarse grained, porous, planar dolomite.

Luck 1-12 C3 B5 4891: (TL10) (same as TL2?)

- A. Coarse grained, porous, planar dolomite.
- B. Medium to coarse grained, porous, planar dolomite.
- C. Coarse grained, very porous, planar dolomite with a minor amount of pore filling clays.

Luck 1-12 C2 B1 4867: (TL11)

- A. Medium to coarse grained, very porous, planar dolomite, with a minor amount of pore filling clays.
- B. Fine to coarse grained, very porous, planar dolomite, with an appreciable amount of pore filling clays.
- C. Medium grained, porous, planar dolomite with a minor amount of pore filling clays.
- D. Medium to coarse grained, very porous, planar dolomite with one large calcite crystal, and a minor amount of pore filling clays.
- E. Medium to coarse grained, porous, planar dolomite with a minor amount of pore filling clays.
- F. Medium to coarse grained, moderately porous, planar dolomite.
- G. Medium to coarse grained, porous, planar dolomite with a minor amount of pore filling clays.

Luck 1-12 C3 B21: (TL12)

- A. Fine to coarse grained, very porous, planar dolomite with an appreciable amount of pore filling clays and a few, very large, replaced, echinoid grains.

L1-12 C3 B2 4882: (TL13) (mirror of TL4B)

- A. Same as TL4B, but with an anhydrite grain present and also a heavier amount of pore filling clays.

## **SALUDA Formation Samples**

**3-28-89**

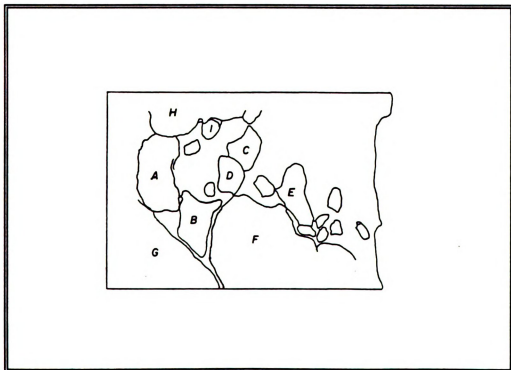
- #4** Very fine to fine grained, non-planar dolomite with minimal porosity.
- #7d** Fine grained, non-planar dolomite with minimal porosity.
- #7** Partially dolomitized section of thinsection. Very fine grained, mudstoned.
- #15** Grainstone with partially dolomitized matrix between, or within some allochems/grains.
- #20** Non-planar dolomite with some echinoid grains replaced.
- #22** Partially dolomitized area, euhedral dolomite, some of which outline former grainstone particles/allochems. Rhombs are cemented within, or growing within, large calcite crystals. Some pyrite and si, especially near contact with the completely dolomitized area. Completely dolomitized area, non-planar, very fine grained with occ. glauconite grain, and laminations.
- #23** Nearly completely dolomitized. In areas where there is some calcite cement, the grains that are completely dolomitized appear to be non-planar. There are a few fossil molds replaced with calcite cement and are partially dolomitized.

## **Grain Mount Method**

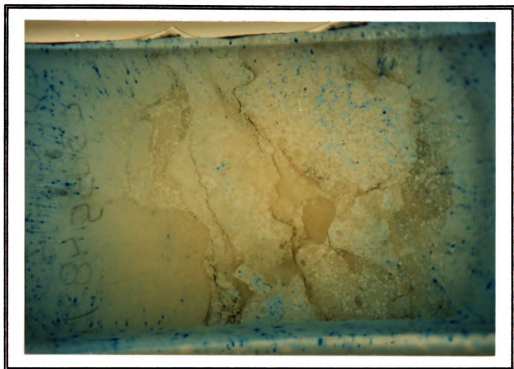
- #22** One large piece of partial dolomite was soaked in a 1% solution of HCl for 4 days. The solution was changed approximately every 12 hours by decanting the old solution without disturbing the sediment. The large sample was removed and the sediment was removed with an eye dropper, placed on a slide and allowed to air dry. This residue was then brushed onto a slide coated with Canada balsam for measurement.



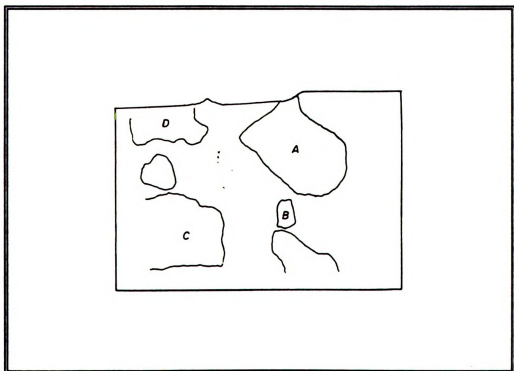
TL - 1 (TL 1 - 12 C3 B21 4931)



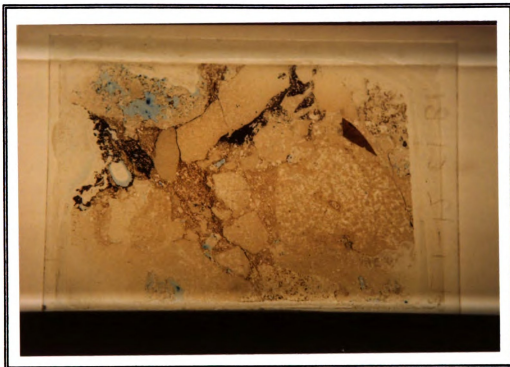
TL - 1 CLAST DRAWING



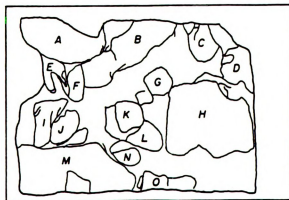
**TL - 2 (TL 1 - 12 C3 B55 4891)**



**TL - 2 CLAST DRAWING**

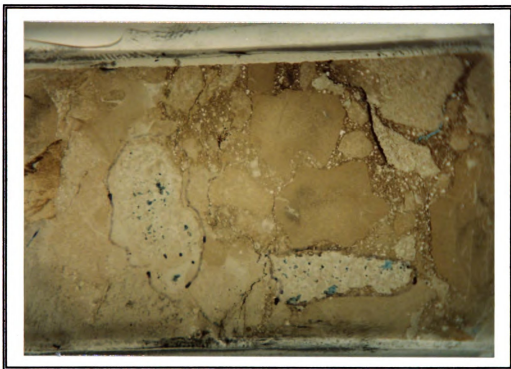


**TL - 3 (L 1 - 12 C1 B1)**

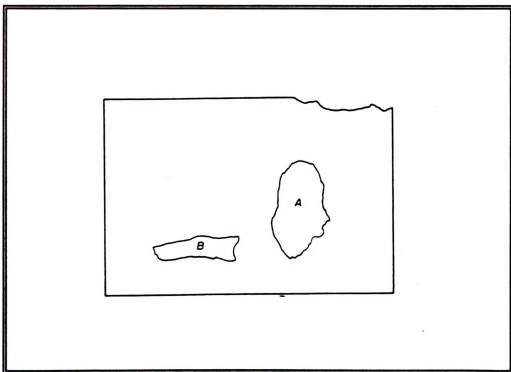


**TL - 3 CLAST DRAWING**





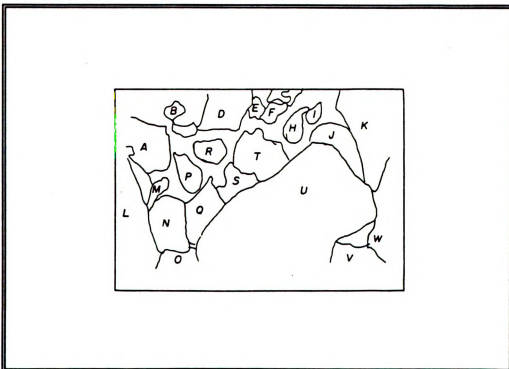
**TL - 4 (L 1 - 12 C3 B2 4882)**



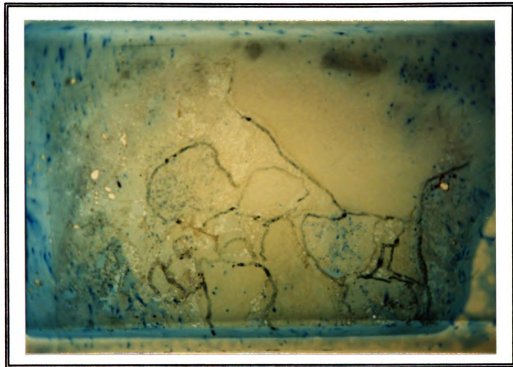
**TL - 4 CLAST DRAWING**



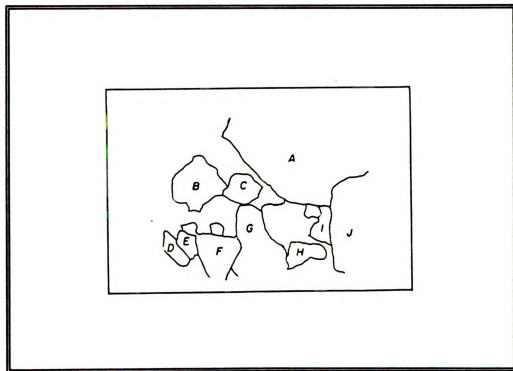
**TL - 5 (L 1 - 12 C1 B5)**



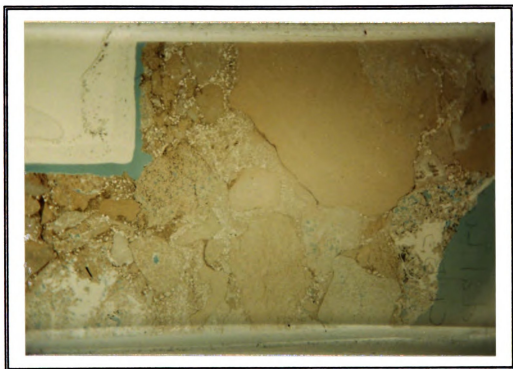
**TL - 5 CLAST DRAWING**



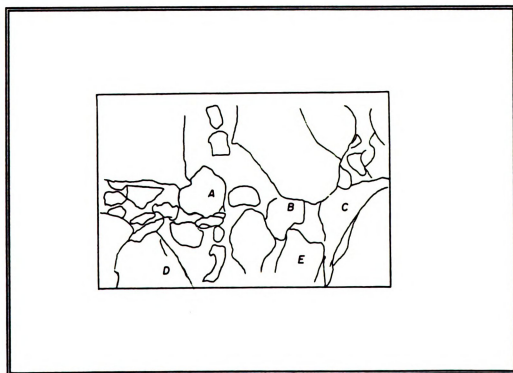
TL - 6 (LUCK 1 - 12 C1 B5 485?)



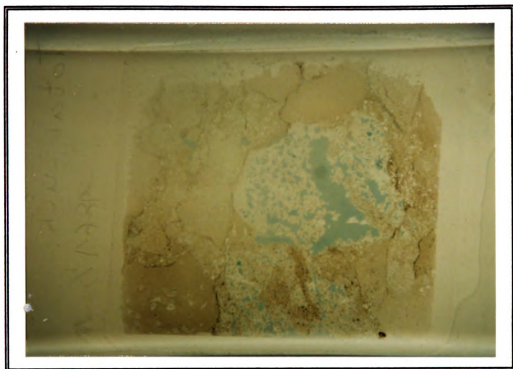
TL - 6 CLAST DRAWING



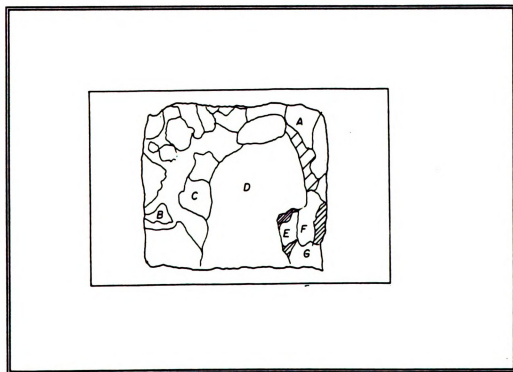
**TL - 7 (L 1 - 12 C1 B5)**



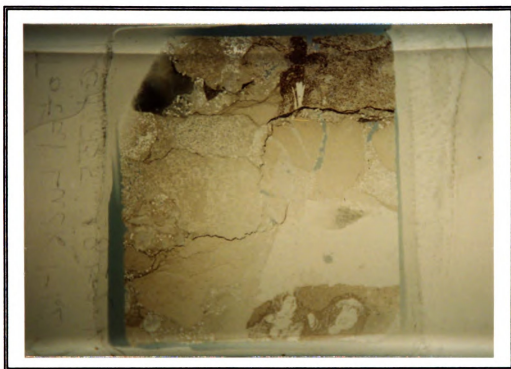
**TL - 7 CLAST DRAWING**



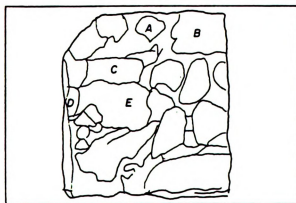
TL - 8 (LUCK 4864½ C1 B8?)



TL - 8 CLAST DRAWING



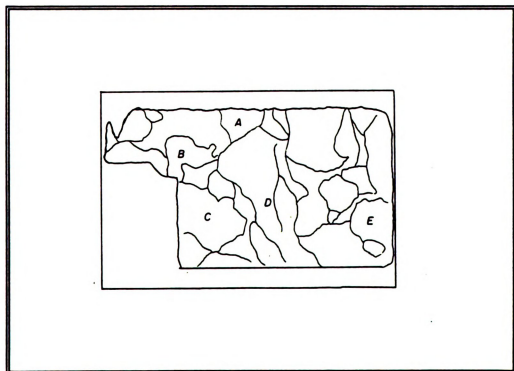
**TL - 9 (LUCK 1 - 12 C1 B5 4852½)**



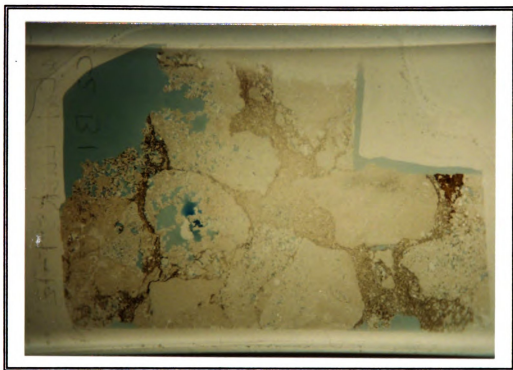
**TL - 9 CLAST DRAWING**



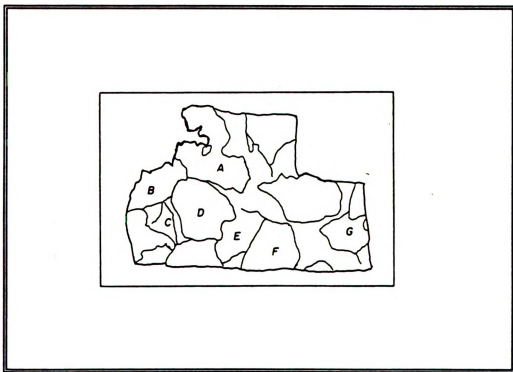
TL - 10 (LUCK 1 - 12 C3 B5 4891)



TL - 10 CLAST DRAWING

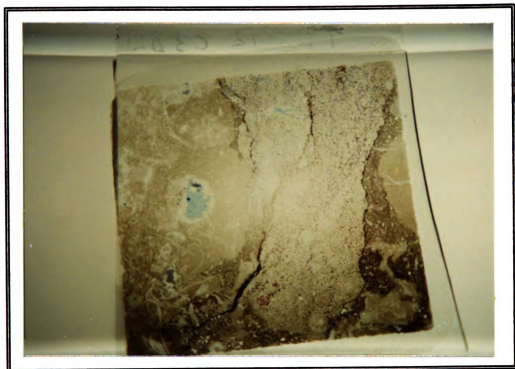


TL - 11 (LUCK 1 - 12 C2 B1 4867)

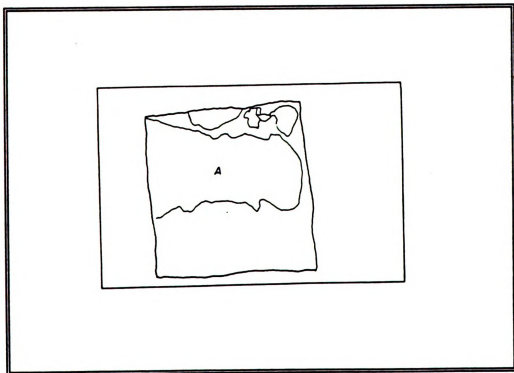


TL - 11 CLAST DRAWING

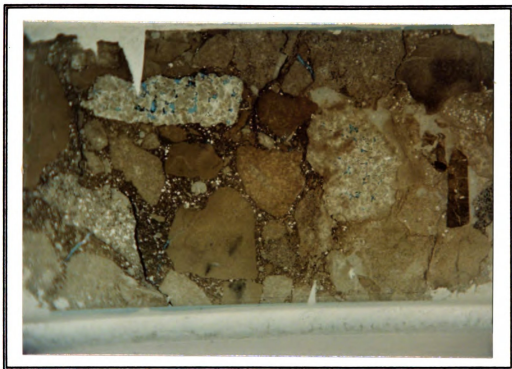




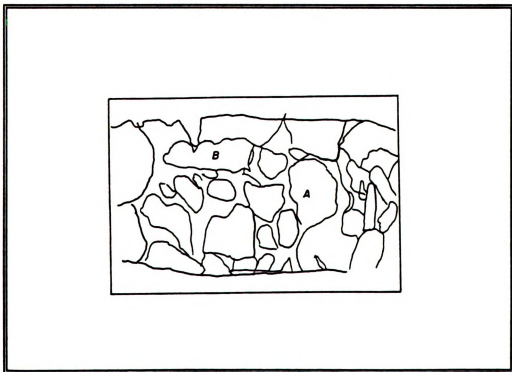
TL - 12 (LUCK 1 - 12 C3 B21)



TL - 12 CLAST DRAWING



**TL - 13 (L 1 - 12 C3 B2 4882) [mirror of TL -4]**



**TL - 13 CLAST DRAWING**

## **APPENDIX B**

### **Two-Sample Kolmogorov-Smirnov Goodness-Of-Fit Tests**

TWO SAMPLE KOLMOGOROV - SMIRNOV TEST FOR NORMALIZED CSD's (size / ave. size) SHADING = <0.05

Class/Count	TL1A	TL1A2	TL1A3	TL1B	TL1B2	TL1B3	TL1C	TL1D	TL1E	TL1F	TL1G	TL1H	TL1I
TL1A													
TL1A2	0.7870												
TL1A3	0.5175	0.5842											
TL1B	0.5175	0.3953	0.1465										
TL1B2	0.5175	0.3953	0.1465	0.7212									
TL1B3	0.7212	0.4543	0.4543	0.7870	0.3953								
TL1C	0.7870	0.7870	0.7870	0.7870	0.7870	0.3412							
TL1D	0.0009	0.0031	0.0056	0.0002	0.0013	0.0042	0.0126						
TL1E	0.5842	0.8527	0.5842	0.1465	0.5175	0.5842	0.8475	0.0256					
TL1F	0.8475	0.8527	0.8475	0.8475	0.8475	0.8527	0.8475	0.8475	0.8475	0.8475	0.8475	0.8475	0.8475
TL1G	0.1360	0.0163	0.0837	0.1196	0.0425	0.0876	0.0063	0.0001	0.0447	0.0252	0.0346	0.0017	0.0017
TL1H	0.0028	0.0003	0.0001	0.0130	0.0001	0.0004	0.0004	0.0000	0.0004	0.0002	0.0002	0.0000	0.0000
TL1I	0.0161	0.0050	0.0202	0.0425	0.0123	0.0222	0.0144	0.0001	0.0071	0.0252	0.0025	0.0001	0.0001
TL1J	0.4939	0.0799	0.3138	0.5511	0.2556	0.4385	0.1864	0.0136	0.2952	0.1864	0.0837	0.0546	0.0546
TL1K	0.0547	0.0664	0.0961	0.0584	0.0603	0.0801	0.0122	0.0021	0.0163	0.0664	0.0061	0.0037	0.0037
TL1L	0.1196	0.0637	0.1384	0.4262	0.0573	0.1418	0.0470	0.0017	0.2289	0.0837	0.0837	0.0102	0.0102
TL1M	0.0891	0.0215	0.0271	0.2414	0.0373	0.0407	0.0411	0.0011	0.0612	0.0457	0.0426	0.0032	0.0032
TL1N	0.1648	0.0538	0.1120	0.2501	0.1120	0.1592	0.0666	0.0149	0.2789	0.0656	0.0533	0.0233	0.0233
TL1O	0.0000	0.0000	0.0000	0.0001	0.0001	0.0000	0.0000	0.0000	0.0000	0.0000	0.0000	0.0000	0.0000
TL1P	0.0730	0.0532	0.0130	0.0963	0.1285	0.0504	0.0240	0.0000	0.0147	0.0561	0.0490	0.0045	0.0045
TL1Q	0.8505	0.0004	0.5707	0.0031	0.0042	0.0002	0.2705	0	0.8305	0.0067	0.8605	0.3507	0.3507

## APPENDIX B

### Kolmogorov-Smirnov Goodness-Of-Fit Tests

Class/Count	TL1A	TL1A2	TL1A3	TL1B	TL1B2	TL1B3	TL1C	TL1D	TL1E	TL1F	TL1G	TL1H	TL1I
TL1A		0.7870	0.5175	0.5842	0.5175	0.7212	0.7870	0.0009	0.5842	0.8475	0.1759	0.6527	0.2923
TL1A2	0.7870		0.5842	0.3953	0.6527	0.4543	0.7870	0.0031	0.6527	0.8996	0.7212	0.7870	0.2098
TL1A3	0.5175	0.5842		0.1465	0.0996	0.4543	0.7870	0.0056	0.5842	0.6524	0.3412	0.8996	0.4543
TL1B	0.5842	0.3953	0.1465		0.7212	0.7870	0.2098	0.0002	0.1465	0.4543	0.1212	0.3412	0.0260
TL1B2	0.5175	0.6527	0.0996	0.7212		0.3953	0.2098	0.0013	0.5175	0.8475	0.3953	0.2098	0.0659
TL1B3	0.7212	0.4543	0.4543	0.7870	0.3953		0.3412	0.0042	0.5842	0.8996	0.0337	0.5175	0.1759
TL1C	0.7870	0.7870	0.7870	0.2098	0.2098	0.3412		0.0126	0.8475	0.4543	0.3412	0.9408	0.6427
TL1D	0.0009	0.0031	0.0056	0.0002	0.0013	0.0042	0.0126		0.0256	0.0096	0.0003	0.0040	0.1465
TL1E	0.5842	0.6527	0.5842	0.1465	0.5175	0.5842	0.8475	0.0256		0.7870	0.1759	0.7212	0.6527
TL1F	0.8475	0.8996	0.6524	0.4543	0.8475	0.8996	0.4543	0.0996	0.7870		0.2485	0.7870	0.2485
TL1G	0.1759	0.7212	0.3412	0.1212	0.3953	0.0337	0.3412	0.0003	0.1759	0.2485		0.7212	0.0912
TL1H	0.6527	0.7870	0.8996	0.3412	0.2098	0.5175	0.9408	0.0040	0.7212	0.7870	0.7212		0.4543
TL1I	0.2923	0.2098	0.4543	0.0260	0.0659	0.1759	0.6427	0.1465	0.6527	0.2485	0.0812	0.4543	
TL2A	0.0260	0.0260	0.0162	0.0013	0.0126	0.0126	0.0530	0.0162	0.0260	0.0162	0.0260	0.1212	0.1212
TL2B	0.4543	0.6527	0.3953	0.2485	0.4543	0.6527	0.3412	0.0056	0.3412	0.6527	0.1212	0.0812	0.0812
TL2C	0.7870	0.5842	0.7870	0.3953	0.5842	0.7870	0.3953	0.0126	0.5842	0.6527	0.3412	0.0530	0.0530
TL2D	0.5842	0.7212	0.8996	0.2098	0.4543	0.7870	0.7212	0.0208	0.7212	0.9408	0.3412	0.6527	0.6527
TL3A	0.6527	0.7870	0.7212	0.4543	0.4543	0.8475	0.1012	0.0126	0.7212	0.7870	0.5842	0.7212	0.7212
TL3B	0.7212	0.3953	0.5175	0.5175	0.5175	0.8485	0.2098	0.0126	0.5175	0.5842	0.1212	0.0996	0.0996
TL3C	0.7870	0.6527	0.8996	0.2098	0.2098	0.3953	0.8475	0.0424	0.6527	0.5175	0.1759	0.2098	0.2098
TL3F	0.2923	0.1465	0.3953	0.0996	0.0530	0.1212	0.2485	0.0007	0.3953	0.2923	0.2923	0.1465	0.1465
TL3D	0.0042	0.0006	0.0126	0.0003	0.0017	0.0056	0.0096	0.1212	0.0074	0.0096	0.0126	0.0659	0.0659
TL3H	0.2923	0.7870	0.7870	0.1465	0.3953	0.1759	0.5175	0.0017	0.1212	0.5842	0.7212	0.2923	0.2923
TL3I	0.6527	0.9408	0.6527	0.4543	0.7212	0.2923	0.7212	0.0009	0.5175	0.7870	0.7870	0.2485	0.2485
TL3J	0.5175	0.7870	0.7870	0.2098	0.3412	0.2098	0.5842	0.0074	0.5842	0.7870	0.6527	0.3953	0.3953
TL3K	0.5842	0.9876	0.4543	0.3412	0.7212	0.3412	0.7870	0.0023	0.4543	0.7870	0.8475	0.3412	0.3412
TL3L	0.0424	0.0659	0.1212	0.0056	0.0096	0.0260	0.1212	0.1759	0.1465	0.0659	0.0530	0.7870	0.7870
TL3M	0.5175	0.7870	0.7870	0.2098	0.2098	0.5175	0.7870	0.0126	0.5175	0.8475	0.3412	0.5842	0.5842
TL4A	0.3412	0.7870	0.6527	0.1759	0.5175	0.1759	0.6527	0.0056	0.5175	0.5842	0.7870	0.3412	0.3412
TL4B	0.3412	0.3412	0.9408	0.0424	0.1759	0.4542	0.6527	0.0659	0.8475	0.6527	0.2098	0.8996	0.8996
TL5K	0.5175	0.7870	0.2423	0.2098	0.5842	0.2485	0.5175	0.0013	0.3412	0.6527	0.7870	0.2098	0.2098
TL5L	0.6527	0.3953	0.4543	0.2098	0.5175	0.9700	0.6527	0.0126	0.7212	0.8475	0.0659	0.3412	0.3412
TL5W	0.4543	0.7212	0.5842	0.2098	0.4543	0.3412	0.3412	0.0056	0.6527	0.9700	0.3953	0.2098	0.2098
TL6H	0.3953	0.4543	0.2098	0.1759	0.5842	0.6527	0.7212	0.0023	0.5842	0.7870	0.1212	0.0812	0.0812
TL7A	0.1759	0.0812	0.3953	0.0126	0.0074	0.0424	0.2485	0.0337	0.2923	0.0812	0.0424	0.4543	0.4543
TL7B	0.1212	0.1212	0.3953	0.0126	0.1465	0.2098	0.2098	0.0337	0.3953	0.3953	0.0126	0.2485	0.2485
TL7C	0.2923	0.6527	0.6527	0.2485	0.3953	0.2923	0.5842	0.0031	0.3412	0.5842	0.8996	0.3412	0.3412
TL7D	0.6527	0.9408	0.7212	0.3953	0.7212	0.3412	0.8996	0.0162	0.5175	0.7870	0.6527	0.5175	0.5175
TL7E	0.1465	0.0659	0.0424	0.3953	0.1465	0.1465	0.0208	0.0000	0.0530	0.1759	0.0424	0.0126	0.0126
TL8A	0.3953	0.1465	0.3412	0.0659	0.0659	0.0659	0.0208	0.0208	0.7212	0.2098	0.5175	0.7870	0.7870
TL8B	0.3412	0.1759	0.2923	0.4543	0.1759	0.3953	0.0530	0.0017	0.1465	0.2098	0.1212	0.0337	0.0337
TL8C	0.3953	0.5175	0.7870	0.1465	0.1759	0.2923	0.7870	0.0337	0.8475	0.4543	0.1759	0.5175	0.5175
TL8D	0.2485	0.1759	0.0812	0.2923	0.1212	0.3953	0.1212	0.0337	0.3953	0.1759	0.0996	0.0659	0.0659
TL8E	0.3412	0.2485	0.0812	0.7212	0.2485	0.5175	0.1465	0.0424	0.1212	0.2485	0.1759	0.0208	0.0208
TL8F	0.8475	0.3412	0.2923	0.5842	0.3953	0.2923	0.2923	0.0031	0.2485	0.4543	0.3412	0.0530	0.0530
TL8G	0.5175	0.1465	0.2923	0.2923	0.2923	0.7212	0.3412	0.0096	0.5175	0.2923	0.0530	0.0530	0.0530
TL9A	0.5842	0.5175	0.5842	0.3412	0.3953	0.8475	0.4543	0.0558	0.7870	0.7870	0.1759	0.2098	0.2098
TL9B	0.1465	0.0208	0.0659	0.3412	0.0659	0.1212	0.0659	0.0007	0.0182	0.0659	0.0659	0.0017	0.0017
TL9C	0.0658	0.0424	0.0007	0.2098	0.1465	0.0812	0.0182	0.0000	0.0074	0.0337	0.0337	0.0031	0.0031
TL9D	0.5175	0.8996	0.8996	0.1465	0.3953	0.5842	0.8996	0.0206	0.6527	0.8996	0.5842	0.2923	0.2923
TL10A	0.8997	0.8223	0.2743	0.4506	0.9194	0.2229	0.5369	0.0020	0.3837	0.7145	0.7835	0.1694	0.1694
TL10B	0.9408	0.9408	0.7212	0.4543	0.6527	0.7212	0.0962	0.0042	0.7212	0.8996	0.4543	0.2485	0.2485
TL10C	0.7212	0.8996	0.3953	0.5842	0.7870	0.2923	0.6527	0.0042	0.8475	0.8996	0.3412	0.4543	0.4543
TL11A	0.7212	0.3953	0.3412	0.4543	0.5175	0.9408	0.6527	0.0042	0.5842	0.4543	0.0659	0.1759	0.1759
TL11B	0.0659	0.2485	0.0812	0.0126	0.0208	0.0162	0.1212	0.0126	0.0530	0.0996	0.0996	0.2485	0.2485
TL11C	0.7870	0.7212	0.3953	0.8996	0.7212	0.5842	0.5175	0.0017	0.6527	0.7870	0.5175	0.1212	0.1212
TL11D	0.5842	0.3412	0.3412	0.4543	0.6527	0.5175	0.2485	0.0056	0.2923	0.6527	0.2923	0.0337	0.0337
TL11E	0.2485	0.2923	0.7212	0.0530	0.0424	0.1759	0.5842	0.0424	0.5842	0.2485	0.2485	0.2485	0.2485
TL11F	0.6527	0.7870	0.3412	0.3412	0.5842	0.8475	0.5175	0.0996	0.6527	0.9877	0.2923	0.2098	0.2098
TL11G	0.1212	0.1212	0.3412	0.0074	0.0031	0.0337	0.1212	0.0996	0.2485	0.0530	0.0337	0.2098	0.2098
TL12A	0.4543	0.3953	0.3953	0.4543	0.7212	0.9700	0.6527	0.0074	0.8475	0.8475	0.8475	0.8475	0.8475
TL13B	0.5175	0.7212	0.8475	0.1212	0.5175	0.7870	0.5842	0.0206	0.4543	0.8996	0.2098	0.5842	0.5842
4901-52	0.1360	0.0163	0.0637	0.1196	0.0425	0.0676	0.0063	0.0001	0.0047	0.0004	0.0002	0.0000	0.0000
4901-54	0.0029	0.0003	0.0001	0.0130	0.0001	0.0004	0.0001	0.0000	0.0004	0.0002	0.0002	0.0000	0.0000
4904	0.0161	0.0065	0.0020	0.0425	0.0120	0.0027	0.0144	0.0001	0.0071	0.0052	0.0005	0.0001	0.0001
8912	0.4939	0.0799	0.3136	0.5811	0.2556	0.4385	0.1884	0.0139	0.2992	0.1884	0.0637	0.0546	0.0546
8914	0.0547	0.0664	0.0961	0.0564	0.0603	0.0801	0.0122	0.0193	0.0664	0.0801	0.0937	0.0937	0.0937
893	0.1196	0.0837	0.0384	0.4282	0.0573	0.1418	0.9407	0.0017	0.2289	0.0837	0.0837	0.0102	0.0102
894	0.0881	0.0215	0.0221	0.2414	0.0373	0.0497	0.0411	0.0011	0.0612	0.0457	0.0428	0.0032	0.0032
897	0.1848	0.0938	0.1120	0.2501	0.1120	0.1592	0.0699	0.0149	0.2799	0.0656	0.0533	0.0203	0.0203
KMSITSAT	0.0000	0.0000	0.0000	0.0001	0.0001	0.0001	0.0000	0.0000	0.0000	0.0000	0.0000	0.0000	0.0000
KMUNSMEL	0.0730	0.0532	0.0130	0.0993	0.1285	0.0504	0.0240	0.0000	0.0147	0.0961	0.0490	0.0045	0.0045
KMSWVKCL	8E-05	0.00024	5.7E-07	0.0031	0.0042	0.00002	2.7E-05	0	8.8E-05	0.00087	5.8E-05	6.3E-07	6.3E-07

Two-Sample Kolmogorov-Smirnov Goodness-Of-Fit Tests



TWO SAMPLE KOLMOGOROV - SMIRNOV TEST FOR NORMALIZED CSD'S (size / ave. size)

SHADING = &lt;0.05

Class/Count	TL2A	TL2B	TL2C	TL2D	TL3A	TL3B	TL3C	TL3F	TL3G	TL3H	TL3I	TL3J	TL3K
TL1A	0.0099	0.4543	0.7870	0.5842	0.6527	0.7212	0.7870	0.2923	0.0042	0.2923	0.6527	0.5175	0.5842
TL1A2	0.0296	0.6527	0.5842	0.7212	0.7870	0.3953	0.6527	0.1465	0.0066	0.7870	0.9408	0.7870	0.9876
TL1A3	0.0162	0.3953	0.7870	0.8996	0.7212	0.5175	0.8996	0.3953	0.0126	0.7870	0.6527	0.7870	0.4543
TL1B	0.0013	0.2485	0.3953	0.2098	0.2485	0.5175	0.2098	0.0996	0.0005	0.1465	0.4543	0.2098	0.3412
TL1B2	0.0126	0.4543	0.5842	0.4543	0.4543	0.5175	0.2098	0.0530	0.0017	0.3953	0.7212	0.3412	0.7212
TL1B3	0.0126	0.6527	0.7870	0.7870	0.4543	0.8485	0.3953	0.1212	0.0056	0.1759	0.2923	0.2098	0.3412
TL1C	0.0530	0.3412	0.3953	0.7212	0.8475	0.2098	0.8475	0.2485	0.0066	0.5175	0.7212	0.5842	0.7870
TL1D	0.0162	0.0059	0.0126	0.0026	0.0162	0.0126	0.0424	0.0007	0.1212	0.0017	0.0059	0.0074	0.0023
TL1E	0.0296	0.3412	0.5842	0.7212	0.7212	0.5175	0.6527	0.3953	0.0074	0.1212	0.5175	0.5842	0.4543
TL1F	0.0162	0.6527	0.6527	0.9408	0.7870	0.5842	0.5175	0.2923	0.0096	0.5842	0.7870	0.7870	0.7870
TL1G	0.0066	0.1212	0.3412	0.3412	0.5842	0.1212	0.1759	0.2923	0.0126	0.7212	0.7870	0.6527	0.8475
TL1H	0.0337	0.6527	0.6527	0.8996	0.8475	0.5175	0.8475	0.1465	0.0309	0.5175	0.5175	0.9408	0.7212
TL1I	0.1212	0.0812	0.0530	0.6527	0.7212	0.0996	0.2098	0.1465	0.0659	0.2923	0.2485	0.3953	0.3412
TL2A		0.0031	0.0031	0.0058	0.0031	0.0031	0.0074	0.0009	0.8996	0.1465	0.0074	0.0126	0.0337
TL2B	0.0031		0.8475	0.6527	0.5842	0.8475	0.6527						
TL2C	0.0031	0.8475		0.8475	0.5842	0.9408	0.5842	0.1759	0.0005	0.3953	0.7870	0.3412	0.5842
TL2D	0.0058	0.6527	0.8475		0.8475	0.7870	0.9408	0.6527	0.0023	0.3953	0.5842	0.5175	0.7212
TL3A	0.0208	0.5842	0.4543	0.8475		0.3953	0.5175	0.1212	0.0096	0.4543	0.6527	0.8996	0.7870
TL3B	0.0013	0.8475	0.9408	0.7870	0.3953		0.5842		0.1465	0.0007	0.1759	0.5175	0.2923
TL3C	0.0074	0.6527	0.5842	0.9408	0.5175	0.5842		0.1759	0.0208	0.6527	0.3412	0.5842	0.7212
TL3F	0.0009	0.1212	0.1759	0.6527	0.1212	0.1465	0.1759		0.0001	0.2485	0.3412	0.3953	0.3953
TL3G	0.8996	0.0023	0.0005	0.0023	0.0009	0.0007	0.0208	0.0001		0.0530	0.0031	0.0058	0.0162
TL3H	0.1465	0.2485	0.3953	0.3953	0.4543	0.4543	0.6527	0.2485	0.0530		0.4543	0.7870	0.9700
TL3I	0.0074	0.7870	0.7870	0.5842	0.6527	0.5175	0.3412	0.3412	0.0031	0.4543		0.7212	0.9408
TL3J	0.0126	0.3412	0.3412	0.5175	0.8996	0.2923	0.5842	0.3953	0.0066	0.7870	0.7212		0.7870
TL3K	0.0337	0.3953	0.5842	0.7212	0.7870	0.5842	0.7212	0.3953	0.0162	0.9700	0.9408	0.7870	
TL3L	0.0530	0.0424	0.0530	0.1759	0.2485	0.0337	0.2098	0.1212	0.0424	0.2485	0.0337	0.2485	0.0530
TL3M	0.1212	0.3412	0.2098	0.3953	0.7212	0.1759	0.6527	0.0424	0.0812	0.4543	0.4543	0.4543	0.5842
TL4A	0.0530	0.2923	0.5842	0.7870	0.4543	0.5175	0.5842	0.2098	0.0424	0.8996	0.5842	0.8475	0.7870
TL4B	0.0208	0.5175		0.3412	0.7212	0.6527	0.2923	0.6527	0.4543	0.0530	0.5842	0.2923	0.8475
TL5A	0.1212	0.2923	0.1212	0.2923	0.5175	0.0996	0.5842	0.0162	0.0162	0.7212	0.4543	0.2923	0.6527
TL5L	0.0208	0.2923	0.5175	0.7870	0.6527	0.3953	0.5842	0.1465	0.0162	0.1465	0.4543	0.3412	0.3953
TL5W	0.0096	0.7870	0.7870	0.9700	0.8475	0.7870	0.6527	0.2923	0.5074	0.6527	0.4543	0.6527	0.6527
TL6H	0.0007	0.7212	0.9408	0.7212	0.4543	0.9408	0.3953	0.2923	0.0017	0.2098	0.3953	0.3412	0.4543
TL7A	0.0162	0.0812	0.0812	0.2485	0.4543	0.0957	0.2923	0.2923	0.0013	0.3412	0.0424	0.3953	0.0812
TL7B	0.0013	0.2098	0.3412	0.5175	0.2485	0.3412	0.4543	0.2098	0.0034	0.2098	0.0996	0.1759	0.1465
TL7C	0.0659	0.3412	0.1759	0.3412	0.4543	0.2923	0.6527	0.0812	0.0208	0.8475	0.6527	0.3953	0.7212
TL7D	0.0337	0.6527	0.6527	0.8475	0.8475	0.4543	0.7212	0.1759	0.0074	0.8996	0.7870	0.8996	0.9408
TL7E	0.0000	0.0996	0.1212	0.0812	0.0337	0.3953	0.0126	0.0208	0.0000	0.0006	0.1759	0.0208	0.0812
TL8A	0.0659	0.0996	0.1465	0.3412	0.7212	0.1212	0.2485	0.1759	0.0208	0.5824	0.2485	0.6527	0.3412
TL8B	0.0001	0.5175	0.6527	0.4543	0.1465	0.7870	0.2098	0.0659	0.0000	0.0659	0.2485	0.1212	0.2485
TL8C	0.0208	0.3953	0.3412	0.7212	0.9408	0.2923	0.1870	0.7212	0.0055	0.6527	0.3953	0.6527	0.3953
TL8D	0.0001	0.2098	0.5842	0.3953	0.1465	0.8475	0.1759	0.1465	0.0004	0.0659	0.2098	0.0996	0.1759
TL8E	0.0001	0.2923	0.6527	0.3412	0.1212	0.5842	0.1754	0.0337	0.0000	0.0996	0.3412	0.1212	0.2485
TL8F	0.0003	0.3953	0.4543	0.5175	0.3953	0.3953	0.2098	0.0812	0.0002	0.1465	0.3412	0.1465	0.4543
TL8G	0.0001	0.4543	0.7212	0.5842	0.4543	0.7870	0.2923	0.0996	0.0001	0.0530	0.2923	0.4543	0.2098
TL9A	0.0013	0.8996	0.9408	0.7212	0.7212	0.9700	0.4543	0.3953	0.0017	0.3412	0.6527	0.5842	0.5842
TL9B	0.0000	0.2485	0.4543	0.0996	0.0659	0.4543	0.0812	0.0031	0.0000	0.0162	0.0812	0.0162	0.1212
TL9C	0.0001	0.0208	0.0424	0.0074	0.0074	0.0812	0.0031	0.0023	0.0000	0.0162	0.0530	0.0096	0.0812
TL9D	0.0337	0.5175	0.4543	0.8475	0.7870	0.3953	0.8996	0.3412	0.0126	0.7870	0.5175	0.7870	0.8475
TL10A	0.0629	0.3182	0.5438	0.3837	0.4317	0.3554	0.4623	0.1121	0.0261	0.5930	0.9194	0.4317	0.9503
TL10B	0.0296	0.2923	0.6527	0.4543	0.9700	0.5175	0.6527	0.4543	0.0126	0.2923	0.7212	0.8996	0.5842
TL10C	0.0530	0.4543	0.5842	0.7212	0.7870	0.3953	0.5842	0.3953	0.0208	0.4543	0.8475	0.8996	0.5842
TL11A	0.0042	0.7870	0.7212	0.7212	0.5842	0.9700	0.5175	0.1759	0.0005	0.2098	0.3953	0.3412	0.3953
TL11B	0.5842	0.0424	0.0942	0.0009	0.2098	0.0162	0.0996	0.0942	0.4543	0.2923	0.0812	0.0162	0.1759
TL11C	0.0056	0.5175	0.7212	0.5842	0.6527	0.8475	0.3953	0.1759	0.0000	0.2923	0.5842	0.4543	0.7212
TL11D	0.0003	0.6527	0.9408	0.4543	0.2098	0.8996	0.2923	0.0996	0.0005	0.1465	0.5842	0.1212	0.4543
TL11E	0.1212	0.1212	0.1465	0.3953	0.6527	0.1212	0.2923	0.0659	0.1759	0.6527	0.0996	0.3412	0.3412
TL11F	0.0162	0.8475	0.7870	0.8996	0.5175	0.5175	0.5842	0.1465	0.0023	0.5175	0.6527	0.7212	0.7870
TL11G	0.1759	0.0208	0.0337	0.2485	0.1212	0.0208	0.0812	0.0424	0.0530	0.2923	0.0337	0.3953	0.1212
TL12A	0.0208	0.8475	0.6527	0.5842	0.6527	0.5175	0.5842	0.2098	0.0042	0.2098	0.5175	0.5542	0.4543
TL13B	0.0017	0.8475	0.9700	0.8475	0.4543	0.8475	0.6527	0.1759	0.0017	0.2098	0.5175	0.3412	0.7212
4901.S2	0.0000	0.0637	0.1418	0.1248	0.0222	0.3395	0.0546	0.0162	0.0000	0.0000	0.0000	0.0000	0.0000
4901.S4	0.0000	0.0023	0.0054	0.0001	0.0004	0.0262	0.0004	0.0000	0.0000	0.0000	0.0000	0.0000	0.0000
4904	0.0000	0.0573	0.0519	0.0144	0.0033	0.0631	0.0055	0.0090	0.0000	0.0022	0.0144	0.0003	0.0129
8912	0.0005	0.4707	0.7351	0.4165	0.2952	0.8757	0.4940	0.1604	0.0002	0.9962	0.2200	0.1955	0.2952
8914	0.0000	0.1020	0.2041	0.0446	0.0122	0.2377	0.0819	0.0460	0.0000	0.0000	0.0460	0.0007	0.0096
893	0.0000	0.2854	0.3953	0.2259	0.0837	0.4909	0.1418	0.0384	0.0000	0.0126	0.9573	0.0837	0.0837
894	0.0000	0.0503	0.1753	0.0541	0.0373	0.2414	0.0271	0.0255	0.0000	0.0007	0.0732	0.0095	0.0033
897	0.0001	0.1120	0.7539	0.2902	0.0781	0.6969	0.1120	0.1072	0.0000	0.0342	0.1120	0.1893	0.9038
H0M1S4T	0.0000	0.0000	0.0000	0.0000	0.0000	0.0000	0.0000	0.0000	0.0000	0.0000	0.0000	0.0000	0.0000
H0M5MEL	0.0000	0.0395	0.0439	0.0100	0.0189	0.0768	0.0195	0.0118	0.0001	0.0255	0.0518	0.0240	0.0518
H0M5SWKCL	0	0.00034	0.0013	0.00024	2.7E-05	0.00002	3.9E-05	8.2E-04	0	2.7E-05	0.00048	3.9E-05	0.00048



TWO SAMPLE KOLMOGOROV - SMIRNOV TEST FOR NORMALIZED CSD'S (size / ave. size)

SHADING = &lt;0.05

Client/Count	TL3L	TL3M	TL4A	TL4B	TL5K	TL5L	TL5W	TL6H	TL7A	TL7B	TL7C	TL7D	TL7E
TL1A	0.0424	0.5175	0.3412	0.3412	0.5175	0.5842	0.4543	0.3953	0.1759	0.1212	0.2923	0.6527	0.1465
TL1A2	0.0659	0.7870	0.7870	0.3412	0.7870	0.3953	0.7212	0.4543	0.0812	0.1212	0.6527	0.9408	0.0659
TL1A3	0.1212	0.7870	0.6527	0.9408	0.2423	0.4543	0.5842	0.2098	0.3953	0.3953	0.6527	0.7212	0.0424
TL1B	0.0096	0.2098	0.1759	0.0424	0.2098	0.2098	0.2098	0.1759	0.0126	0.0162	0.2485	0.3953	0.3953
TL1B2	0.0096	0.2098	0.5175	0.1759	0.5842	0.5175	0.4543	0.5842	0.0074	0.1465	0.3953	0.7212	0.1465
TL1B3	0.0208	0.5175	0.1759	0.4542	0.2485	0.9700	0.3412	0.6527	0.0424	0.2098	0.2098	0.2923	0.3412
TL1C	0.1212	0.7870	0.6527	0.6527	0.5175	0.6527	0.7212	0.3412	0.2485	0.2098	0.5842	0.8996	0.0008
TL1D	0.1759	0.9126	0.0096	0.0659	0.0013	0.0126	0.0096	0.0037	0.0337	0.0031	0.0162	0.0000	
TL1E	0.1465	0.5175	0.5175	0.8475	0.3412	0.7212	0.6527	0.5842	0.2923	0.3953	0.3412	0.5175	0.0530
TL1F	0.0659	0.8475	0.5842	0.6527	0.6527	0.8475	0.9700	0.7870	0.0812	0.3953	0.5842	0.7870	0.1759
TL1G	0.0530	0.3412	0.7870	0.2098	0.7870	0.0659	0.3953	0.1212	0.0424	0.0162	0.8996	0.6527	0.0424
TL1H	0.0996	0.7212	0.5175	0.7870	0.7212	0.4543	0.7212	0.3953	0.1465	0.2485	0.4543	0.7212	0.0208
TL1I	0.7870	0.5842	0.3412	0.8996	0.2098	0.3412	0.2098	0.0812	0.4543	0.2485	0.3412	0.5175	0.0126
TL2A	0.0530	0.1212	0.0530	0.0208	0.1212	0.0208	0.0096	0.0097	0.0162	0.0013	0.0659	0.0337	0.0000
TL2B	0.0424	0.3412	0.2923	0.5175	0.2923	0.2923	0.7870	0.7212	0.0812	0.2098	0.3412	0.6527	0.0996
TL2C	0.0530	0.2098	0.5842	0.3412	0.1212	0.5175	0.7870	0.9408	0.0812	0.3412	0.1759	0.6527	0.1212
TL2D	0.1759	0.3953	0.7870	0.7212	0.2923	0.7870	0.9700	0.7212	0.2485	0.5175	0.3412	0.8475	0.0812
TL3A	0.2485	0.5175	0.4543	0.6527	0.5175	0.6527	0.8475	0.4543	0.4543	0.2485	0.4543	0.8475	0.0337
TL3B	0.0337	0.1759	0.5175	0.2923	0.0996	0.3953	0.7870	0.9408	0.0657	0.3412	0.2923	0.4543	0.3953
TL3C	0.2098	0.6527	0.5842	0.6527	0.5842	0.5842	0.6527	0.3953	0.2923	0.4543	0.6527	0.7212	0.0126
TL3F	0.1212	0.0424	0.2098	0.4543	0.0162	0.1465	0.2923	0.2923	0.2923	0.2098	0.0812	0.1759	0.0208
TL3G	0.0424	0.0812	0.0424	0.0056	0.0162	0.0162	0.0024	0.0017	0.0013	0.0034	0.0208	0.0074	0.0000
TL3H	0.2485	0.4543	0.8996	0.5842	0.7212	0.1465	0.6527	0.2098	0.3412	0.2098	0.8475	0.8996	0.0096
TL3I	0.0337	0.4543	0.5842	0.2923	0.4543	0.4543	0.4543	0.3953	0.0424	0.0996	0.6527	0.7870	0.1759
TL3J	0.2485	0.4543	0.8475	0.8475	0.2923	0.3412	0.6527	0.3412	0.3953	0.1759	0.3953	0.8996	0.0208
TL3K	0.0530	0.5842	0.7870	0.4543	0.6527	0.3953	0.6527	0.4543	0.0812	0.1465	0.7212	0.9408	0.0812
TL3L		0.1465	0.1759	0.5175	0.0337	0.0659	0.0530	0.0126	0.6527	0.2485	0.1465	0.1212	0.0003
TL3M		0.1465		0.6527	0.5842	0.7870	0.6527	0.1759	0.1465	0.1465	0.6527	0.6527	0.0659
TL4A	0.1759	0.6527			0.5842	0.4543	0.2923	0.9408	0.3953	0.2485	0.0530	0.7870	0.9700
TL4B	0.5175	0.5842	0.5842		0.3412	0.6527	0.4543	0.3412	0.6527	0.7870	0.5842	0.7212	0.0208
TL5K	0.0337	0.7870	0.4543	0.3412		0.3953	0.4543	0.3412	0.1212	0.0812	0.0812	0.7870	0.0162
TL5L	0.0659	0.6527	0.2923	0.6527	0.3953		0.5842	0.4543	0.9530	0.5175	0.2923	0.5175	0.0659
TL5W	0.0530	0.6527	0.9408	0.4543	0.3412	0.5842		0.7870	0.9996	0.2098	0.3412	0.8475	0.1759
TL6H	0.0126	0.1759	0.3953	0.3412	0.1212	0.4543	0.7870		0.1212	0.4543	0.2485	0.5842	0.1465
TL7A	0.6527	0.1465	0.3485	0.6527	0.0812	0.0530	0.9996	0.1212		0.2485	0.1465	0.1759	0.0013
TL7B	0.2485	0.1465	0.0530	0.7870	0.0812	0.5175	0.2098	0.4543	0.2485		0.0659	0.3412	0.0208
TL7C	0.1465	0.6527	0.7870	0.5842	0.7870	0.2923	0.3412	0.2485	0.1465	0.9530		0.8475	0.0424
TL7D	0.1212	0.6527	0.9700	0.7212	0.7212	0.5175	0.8475	0.5842	0.1759	0.3412	0.8475		0.0659
TL7E	0.0003	0.0208	0.0208	0.0208	0.0162	0.0659	0.1759	0.1465	0.0013	0.0208	0.0424	0.0659	
TL8A	0.5175	0.5175	0.3412	0.6527	0.3412	0.2485	0.1465	0.0812	0.5175	0.1465	0.4543	0.3953	0.0023
TL8B	0.0162	0.0337	0.2485	0.2098	0.0126	0.1759	0.3953	0.7870	0.0208	0.2923	0.2098	0.2098	0.3412
TL8C	0.1465	0.6527	0.7212	0.7212	0.3412	0.7870	0.4543	0.3412	0.5175	0.2923	0.3412	0.7870	0.0337
TL8D	0.0074	0.0208	0.0812	0.1759	0.0126	0.3412	0.2923	0.3953	0.0126	0.0996	0.0208	0.2098	0.0996
TL8E	0.0074	0.0424	0.2485	0.1212	0.0337	0.1465	0.3412	0.3953	0.0162	0.0812	0.0530	0.2923	0.4543
TL8F	0.0126	0.0996	0.3953	0.2098	0.0530	0.3953	0.7212	0.4543	0.0162	0.0337	0.1212	0.3412	0.0812
TL8G	0.0424	0.0659	0.1965	0.2485	0.0337	0.4543	0.4543	0.6527	0.0424	0.4543	0.0812	0.3412	0.0208
TL9A	0.0337	0.2923	0.5175	0.4543	0.0176	0.7212	0.8996	0.5175	0.2098	0.4543	0.2485	0.6527	0.2485
TL9B	0.0023	0.0126	0.0812	0.0337	0.0096	0.0659	0.3953	0.3953	0.0031	0.1212	0.0337	0.0996	0.2485
TL9C	0.0000	0.0096	0.0074	0.0042	0.0424	0.0530	0.0162	0.0096	0.0001	0.0031	0.0074	0.0126	0.5842
TL9D	0.0657	0.8996	0.9877	0.7870	0.3953	0.5175	0.8996	0.5842	0.2485	0.2485	0.7212	0.9962	0.0530
TL10A	0.0303	0.5577	0.3837	0.2981	0.9104	0.3391	0.4962	0.2981	0.0854	0.0801	0.6001	0.5930	0.1631
TL10B	0.1465	0.8475	0.6527	0.5175	0.5175	0.7212	0.8475	0.3412	0.1759	0.1212	0.5842	0.8475	0.0530
TL10C	0.0812	0.8475	0.4543	0.6527	0.6527	0.3953	0.7870	0.3953	0.1212	0.1212	0.5175	0.8996	0.0424
TL11A	0.0530	0.1759	0.2485	0.5842	0.0659	0.8996	0.5842	0.8996	0.1212	0.5175	0.2098	0.5842	0.2485
TL11B	0.3412	0.4543	0.2923	0.0530	0.3412	0.0337	0.1759	0.0208	0.0337	0.0126	0.2098	0.1759	0.0007
TL11C	0.0337	0.2923	0.5175	0.3412	0.1465	0.4543	0.4543	0.5175	0.0424	0.0812	0.2485	0.5175	0.1759
TL11D	0.0042	0.1465	0.5175	0.1754	0.0996	0.2485	0.6527	0.8996	0.0208	0.2485	0.3412	0.2923	0.1759
TL11E	0.7212	0.6523	0.6527	0.5842	0.1759	0.2098	0.3953	0.0659	0.4543	0.1212	0.5175	0.2923	0.0017
TL11F	0.0337	0.4543	0.7870	0.4543	0.6527	0.7870	0.7870	0.5842	0.0530	0.4543	0.7212	0.8996	0.0424
TL11G	0.7212	0.2485	0.2098	0.3953	0.6527	0.0337	0.0337	0.0013	0.3412	0.0812	0.1759	0.0812	0.2093
TL12A	0.0812	0.5175	0.2098	0.3953	0.3953	0.9993	0.7212	0.3953	0.0812	0.5842	0.4543	0.7212	0.0659
TL13B	0.0208	0.2485	0.5175	0.5175	0.2485	0.3953	0.9408	0.7870	0.0530	0.7212	0.3953	0.6527	0.0812
4901.SH	0.0003	0.0052	0.0329	0.0129	0.0005	0.0226	0.0876	0.3063	0.0029	0.0312	0.0043	0.0208	0.0763
4901.SH	0.0000	0.0000	0.0001	0.0001	0.0000	0.0002	0.0013	0.0130	0.0000	0.0018	0.0000	0.0000	0.2790
4904	0.0001	0.0025	0.0114	0.0025	0.0013	0.0043	0.0348	0.0836	0.0002	0.0025	0.0000	0.0114	0.2854
8912	0.1036	0.0662	0.2200	0.4806	0.0662	0.3389	0.7895	0.2707	0.0521	0.2783	0.1884	0.2556	0.1521
8914	0.0007	0.0191	0.0560	0.0240	0.0059	0.0122	0.0819	0.4757	0.0078	0.0460	0.0209	0.0240	0.0639
893	0.0071	0.0102	0.0384	0.1196	0.0063	0.1673	0.1962	0.2121	0.0114	0.0631	0.0162	0.1196	0.4809
894	0.0041	0.0068	0.0271	0.0579	0.0024	0.0659	0.0612	0.1270	0.0025	0.0702	0.0060	0.0244	0.0639
897	0.0114	0.0289	0.0437	0.0908	0.0116	0.2160	0.2160	0.4871	0.0160	0.3687	0.0140	0.1120	0.1116
KMSITSAT	0.0000	0.0000	0.0000	0.0000	0.0000	0.0000	0.0000	0.0000	0.0000	0.0000	0.0000	0.0000	0.0017
KMUNSMEL	0.0003	0.0247	0.0147	0.0030	0.0434	0.0196	0.0084	0.0075	0.0003	0.0026	0.0189	0.0278	0.4266
KMSWVKCL	6.2E-08	3.6E-05	0.0034	2.7E-05	0.00012	5.7E-05	0.00024	0.00007	1.6E-07	5.8E-05	0.00017	0.00048	0.053



Cast/Count	TL8A	TL8B	TL8C	TL8D	TL8E	TL8F	TL8G	TL8A	TL8B	TL8C	TL8D	TL8A	TL8B
TL1A	0.3953	0.3412	0.3953	0.2485	0.3412	0.8475	0.5175	0.5842	0.1465	0.0658	0.5175	0.8097	0.9408
TL1A2	0.1465	0.1759	0.5175	0.1759	0.2485	0.3412	0.1465	0.5175	0.0209	0.0424	0.8996	0.8223	0.9408
TL1A3	0.3412	0.2923	0.7870	0.0812	0.0812	0.2923	0.2923	0.5842	0.0659	0.0077	0.8996	0.2743	0.7212
TL1B	0.0659	0.4543	0.1465	0.2923	0.7212	0.5842	0.2923	0.3412	0.3412	0.2098	0.1465	0.4506	0.4543
TL1B2	0.0659	0.1759	0.1759	0.1212	0.2485	0.3953	0.2923	0.3953	0.0659	0.2098	0.3953	0.9194	0.6527
TL1B3	0.0659	0.3953	0.2923	0.3953	0.5175	0.2923	0.7212	0.8475	0.1212	0.0812	0.5842	0.2229	0.7212
TL1C	0.7212	0.0530	0.7870	0.1212	0.1465	0.2923	0.3412	0.4543	0.0659	0.0162	0.8996	0.3569	0.9962
TL1D	0.0208	0.0017	0.0337	0.0017	0.0042	0.0031	0.0056	0.0056	0.0007	0.0000	0.0209	0.0020	0.0042
TL1E	0.7212	0.1465	0.8475	0.3953	0.1212	0.2485	0.5175	0.7870	0.0162	0.0074	0.6527	0.3837	0.7212
TL1F	0.2098	0.2098	0.4543	0.1759	0.2485	0.4543	0.2923	0.7870	0.0659	0.0337	0.8996	0.7145	0.8996
TL1G	0.5175	0.1212	0.1759	0.0996	0.1759	0.3412	0.0530	0.1759	0.0206	0.0337	0.5842	0.7835	0.4543
TL1H	0.5175	0.1759	0.5175	0.1759	0.1465	0.3412	0.2098	0.7212	0.0530	0.0074	0.8996	0.3569	0.8996
TL1I	0.7870	0.0337	0.5175	0.0659	0.0208	0.0530	0.0530	0.2098	0.0017	0.0031	0.2923	0.1694	0.2485
TL2A	0.0659	0.0001	0.0208	0.0001	0.0001	0.0003	0.0001	0.0013	0.0000	0.0001	0.0337	0.0629	0.2098
TL2B	0.0996	0.5175	0.3953	0.2098	0.2923	0.3953	0.4543	0.8996	0.2485	0.0208	0.5175	0.3182	0.0530
TL2C	0.1465	0.6527	0.3412	0.5842	0.6527	0.4543	0.7212	0.9408	0.4543	0.0424	0.4543	0.5438	0.6527
TL2D	0.1465	0.4543	0.7212	0.3953	0.3412	0.5175	0.5842	0.7212	0.0996	0.0074	0.8475	0.3837	0.4543
TL3A	0.7212	0.1465	0.9408	0.1465	0.1212	0.3953	0.4543	0.7212	0.0659	0.0074	0.7870	0.4317	0.9700
TL3B	0.1212	0.7870	0.2923	0.8475	0.5842	0.3953	0.7870	0.9700	0.4543	0.0812	0.3953	0.3554	0.5175
TL3C	0.2485	0.2098	0.1870	0.1759	0.1754	0.2098	0.2923	0.4543	0.0812	0.0031	0.8996	0.4623	0.6527
TL3F	0.1759	0.0659	0.7212	0.1465	0.0337	0.0812	0.0996	0.3953	0.0031	0.0023	0.3412	0.1121	0.4543
TL3G	0.0296	0.0000	0.0055	0.0004	0.0000	0.0002	0.0001	0.0017	0.0000	0.0000	0.0126	0.0261	0.0126
TL3H	0.5824	0.0659	0.6527	0.0659	0.0996	0.1465	0.0530	0.3412	0.0162	0.0162	0.7870	0.5930	0.2923
TL3I	0.2485	0.2485	0.3953	0.2098	0.3412	0.3412	0.2923	0.6527	0.0812	0.0530	0.5175	0.7870	0.7212
TL3J	0.6527	0.1212	0.6527	0.0996	0.1212	0.1465	0.4543	0.5842	0.0162	0.0530	0.7870	0.4317	0.8996
TL3K	0.3412	0.2485	0.3953	0.1759	0.2485	0.4543	0.2098	0.5842	0.1212	0.0812	0.8475	0.9623	0.5842
TL3L	0.5175	0.0162	0.1465	0.0074	0.0126	0.0424	0.0337	0.0023	0.0000	0.0000	0.0659	0.3554	0.8475
TL3M	0.5175	0.0337	0.6527	0.0206	0.0424	0.0996	0.0659	0.2923	0.0126	0.0006	0.8996	0.5577	0.8475
TL4A	0.3412	0.2485	0.7212	0.0812	0.2485	0.3953	0.1965	0.5175	0.0812	0.0074	0.9677	0.3837	0.6527
TL4B	0.6527	0.2098	0.7212	0.1759	0.1212	0.2098	0.2485	0.4543	0.0337	0.0042	0.7870	0.2981	0.5175
TL5K	0.3412	0.0126	0.3412	0.0126	0.0337	0.0630	0.0337	0.0178	0.0359	0.0424	0.3953	0.9104	0.5175
TL5L	0.2485	0.1759	0.7870	0.3412	0.1465	0.3953	0.4543	0.7212	0.0659	0.0530	0.5175	0.3391	0.7212
TL5V	0.1465	0.3953	0.4543	0.2923	0.3412	0.7212	0.4543	0.8996	0.3953	0.0162	0.8996	0.4962	0.8475
TL6H	0.0812	0.7870	0.3412	0.3953	0.3953	0.4543	0.6527	0.5175	0.3953	0.0530	0.5842	0.2981	0.4317
TL7A	0.5175	0.0206	0.5175	0.0126	0.0162	0.0162	0.0424	0.2098	0.0337	0.0001	0.2485	0.0654	0.1759
TL7B	0.1465	0.2923	0.2923	0.0996	0.0812	0.0337	0.4543	0.4543	0.1212	0.0337	0.2485	0.0901	0.1212
TL7C	0.4543	0.0206	0.3412	0.0206	0.0530	0.1212	0.0812	0.2485	0.0337	0.0074	0.7212	0.8001	0.5842
TL7D	0.3953	0.2098	0.7870	0.2098	0.2923	0.3412	0.3412	0.6527	0.0996	0.0126	0.9962	0.5930	0.8475
TL7E	0.0203	0.3412	0.0337	0.0996	0.4543	0.0812	0.0206	0.2485	0.2485	0.5842	0.0530	0.1631	0.0530
TL8A	0.0337	0.0337	0.6527	0.0659	0.0206	0.0659	0.0206	0.2485	0.0023	0.0017	0.3412	0.2953	0.6527
TL8B	0.0337		0.3953	0.7212	0.9700	0.7212	0.3953	0.5842	0.8475	0.0530	0.1759	0.1317	0.2098
TL8C	0.6527	0.3953		0.0812	0.1465	0.0996	0.4543	0.6527	0.0337	0.0023	0.5842	0.2981	0.8996
TL8D	0.0659	0.7212	0.0812		0.6527	0.8475	0.5842	0.4543	0.3953	0.1465	0.1465	0.1121	0.2098
TL8E	0.0206	0.9700	0.6527	0.6527		0.4543	0.4543	0.4543	0.4543	0.1465	0.1759	0.1317	0.2098
TL8F	0.0659	0.7212	0.8475	0.8475	0.4543		0.5175	0.7870	0.2485	0.0812	0.4543	0.2426	0.2485
TL8G	0.0206	0.3953	0.5842	0.5842	0.4543	0.5175		0.6527	0.1212	0.0656	0.1759	0.1825	0.1465
TL9A	0.2485	0.5842	0.4543	0.4543	0.4543	0.7870	0.6527		0.2098	0.0424	0.7212	0.3779	0.6527
TL9B	0.0203	0.8475	0.3953	0.3953	0.4543	0.2485	0.1212	0.2098		0.0162	0.0812	0.1144	0.0996
TL9C	0.0017	0.0530	0.1465	0.1465	0.1465	0.0812	0.0056	0.0424	0.0162		0.0056	0.1792	0.0162
TL9D	0.3412	0.1759	0.1465	0.1465	0.1759	0.4543	0.1759	0.7212	0.0812	0.0206		0.3391	0.8996
TL10A	0.2953	0.1317	0.1121	0.1121	0.1317	0.2426	0.1825	0.3779	0.1144	0.1792	0.3391		0.7286
TL10B	0.6527	0.2098	0.2098	0.2098	0.2098	0.2485	0.1465	0.6527	0.0996	0.0162	0.8996	0.7286	
TL10C	0.3412	0.1465	0.1759	0.1759	0.1759	0.2485	0.3412	0.5842	0.0530	0.0812	0.7212	0.7835	0.9677
TL11A	0.2098	0.6527	0.7212	0.7212	0.5842	0.5175	0.7870	0.8475	0.3412	0.0659	0.5175	0.3779	0.5842
TL11B	0.1759	0.0007	0.0007	0.0007	0.0007	0.0056	0.0017	0.0206	0.0017	0.0007	0.2923	0.1032	0.1212
TL11C	0.1759	0.5175	0.5175	0.5175	0.7870	0.7212	0.3953	0.6527	0.3412	0.1759	0.5842	0.3445	0.7870
TL11D	0.0424	0.7870	0.8996	0.8996	0.5175	0.6527	0.5842	0.7212	0.5842	0.0530	0.4543	0.5164	0.2923
TL11E	0.9408	0.0424	0.0126	0.0126	0.0337	0.1465	0.0424	0.2098	0.0074	0.0003	0.5842	0.1694	0.5175
TL11F	0.0812	0.1759	0.1465	0.1465	0.3953	0.5175	0.2098	0.7212	0.1465	0.0042	0.7212	0.4380	0.7870
TL11G	0.7212	0.0126	0.0530	0.0056	0.0017	0.0206	0.0206	0.0659	0.0017	0.0000	0.2098	0.0656	0.1212
TL12A	0.3953	0.1759	0.3412	0.3412	0.3412	0.3953	0.2485	0.5175	0.0996	0.0530	0.6527	0.4194	0.3953
TL13B	0.1465	0.5842	0.5842	0.3953	0.3953	0.7870	0.5842	0.4543	0.0206	0.0009	0.7870	0.3837	0.3953
4901 SZ	0.0015	0.6758	0.6142	0.6142	0.3752	0.4131	0.1145	0.0728	0.4395	0.0067	0.0022	0.0518	0.0053
4901 SH	0.0000	0.0485	0.1081	0.1081	0.0232	0.0115	0.0012	0.0025	0.0251	0.0797	0.0002	0.0019	0.0013
4904	0.0007	0.3262	0.1962	0.1962	0.1303	0.1418	0.0202	0.0763	0.1962	0.1673	0.0280	0.0196	0.0071
8912	0.0889	0.6696	0.5880	0.5880	0.5165	0.6946	0.7010	0.5677	0.5333	0.0858	0.2200	0.3307	0.2952
8914	0.0048	0.0603	0.0480	0.0480	0.0640	0.0575	0.1743	0.1888	0.0330	0.0003	0.0664	0.0466	0.0183
893	0.0312	0.8088	0.4809	0.4809	0.5686	0.5094	0.3063	0.3282	0.2467	0.0673	0.1176	0.0836	
894	0.0024	0.3785	0.1360	0.1360	0.6025	0.1360	0.0467	0.0891	0.3547	0.0745	0.0139	0.0471	0.0215
897	0.0493	0.7706	0.6039	0.6039	0.1841	0.3795	0.2893	0.2964	0.1567	0.0287	0.0781	0.0708	0.1331
KMSITAD	0.0000	0.0000	0.0000	0.0000	0.0001	0.0000	0.0000	0.0000	0.0000	0.0013	0.0000	0.0002	0.0000
KMSIMEL	0.0038	0.0546	0.1062	0.1062	0.1226	0.1011	0.0147	0.0381	0.0183	0.7985	0.0122	0.2101	0.0504
KMSWKL	1.5E-06	0.0042	0.0096	0.0096	0.0126	0.0023	0.00024	0.00048	0.0031	0.1759	0.00024	0.0045	8.3E-05



Class/Count	TL10C	TL11A	TL11B	TL11C	TL11D	TL11E	TL11F	TL11G	TL12A	TL13B	4901.SZ	4901.SH	4904
TL1A	0.7212	0.7212	0.0659	0.7870	0.5842	0.2485	0.6527	0.1212	0.4543	0.5175	0.1360	0.0029	0.0181
TL1A2	0.8996	0.3953	0.2485	0.7212	0.3412	0.2923	0.7870	0.1212	0.3953	0.7212	0.0183	0.0003	0.0050
TL1A3	0.3953	0.3412	0.0812	0.3953	0.3412	0.7212	0.3412	0.1212	0.3953	0.8475	0.0001	0.0001	0.0202
TL1B	0.5842	0.4543	0.0125	0.8996	0.4543	0.0530	0.3412	0.0074	0.4543	0.1212	0.1196	0.2130	0.0245
TL1B2	0.7870	0.5175	0.0208	0.7212	0.6527	0.0424	0.5842	0.0031	0.7212	0.5175	0.0425	0.0001	0.0129
TL1B3	0.2923	0.8408	0.0162	0.5842	0.5175	0.1759	0.8475	0.0337	0.9700	0.7870	0.0076	0.0004	0.0202
TL1C	0.6527	0.6527	0.1212	0.5175	0.2485	0.5842	0.5175	0.1212	0.6527	0.5842	0.0063	0.0001	0.0144
TL1D	0.0042	0.0042	0.0125	0.0017	0.0056	0.0424	0.0036	0.0096	0.0074	0.0208	0.0001	0.0000	0.0001
TL1E	0.8475	0.5842	0.0530	0.6527	0.2923	0.5842	0.6527	0.2485	0.6475	0.4543	0.0447	0.0004	0.0021
TL1F	0.8996	0.4543	0.0996	0.7870	0.6527	0.2485	0.9877	0.0530	0.8475	0.8996	0.0252	0.0002	0.0252
TL1G	0.3412	0.0659	0.0996	0.5175	0.2923	0.2485	0.2923	0.0996	0.0996	0.2098	0.0340	0.0002	0.0025
TL1H	0.7870	0.4543	0.1759	0.5842	0.3412	0.5842	0.7212	0.3412	0.7870	0.5175	0.0085	0.0001	0.0129
TL1I	0.4543	0.1759	0.2485	0.1212	0.0337	0.8996	0.5842	0.4543	0.1212	0.0017	0.0000	0.0000	0.0001
TL2A	0.0530	0.0042	0.5842	0.0056	0.0003	0.1212	0.0162	0.1759	0.0266	0.0077	0.0000	0.0000	0.0000
TL2B	0.4543	0.7870	0.0424	0.5175	0.6527	0.1212	0.8475	0.0208	0.6475	0.8475	0.0337	0.0023	0.0519
TL2C	0.5842	0.7212	0.0042	0.7212	0.8408	0.1465	0.7870	0.0337	0.6527	0.9700	0.1418	0.0054	0.0519
TL2D	0.7212	0.7212	0.0208	0.5842	0.4543	0.3953	0.8996	0.2485	0.5842	0.8475	0.1248	0.0001	0.0144
TL3A	0.7870	0.5842	0.2098	0.6527	0.2098	0.6527	0.5175	0.1212	0.6527	0.4543	0.0202	0.0004	0.0033
TL3B	0.3953	0.9700	0.0162	0.8475	0.8996	0.1212	0.5175	0.0266	0.5175	0.8475	0.3396	0.0262	0.0031
TL3C	0.5842	0.5175	0.0996	0.3953	0.2923	0.2923	0.5842	0.0812	0.5842	0.6527	0.0646	0.0004	0.0055
TL3F	0.3953	0.1759	0.0042	0.1759	0.0996	0.0659	0.1465	0.0424	0.2098	0.1759	0.0182	0.0000	0.0050
TL3G	0.0208	0.0005	0.4543	0.0009	0.0005	0.1759	0.0023	0.0530	0.0042	0.0017	0.0000	0.0000	0.0000
TL3H	0.4543	0.2098	0.2923	0.2923	0.1465	0.6527	0.5175	0.2923	0.2098	0.2098	0.0033	0.0000	0.0022
TL3I	0.8475	0.3953	0.0812	0.5842	0.5842	0.0996	0.6527	0.0337	0.5175	0.5175	0.0346	0.0007	0.0144
TL3J	0.8996	0.3412	0.0162	0.4543	0.1212	0.3412	0.7212	0.3953	0.5842	0.3412	0.0171	0.0000	0.0033
TL3K	0.5842	0.3953	0.1759	0.7212	0.4543	0.3412	0.7870	0.1212	0.4543	0.7212	0.0114	0.0002	0.0129
TL3L	0.0812	0.0530	0.3412	0.0337	0.0042	0.7212	0.0337	0.1212	0.0812	0.0266	0.0000	0.0000	0.0001
TL3M	0.8475	0.1759	0.4543	0.2923	0.1465	0.6523	0.4543	0.2485	0.5175	0.2485	0.0052	0.0000	0.0025
TL4A	0.4543	0.2485	0.2923	0.5175	0.5175	0.6527	0.7870	0.2098	0.2098	0.5175	0.0329	0.0001	0.0114
TL4B	0.6527	0.5842	0.0530	0.3412	0.1759	0.5842	0.4543	0.3953	0.3953	0.5175	0.0129	0.0001	0.0025
TL4C	0.6527	0.0659	0.3412	0.1465	0.1696	0.1759	0.6527	0.0659	0.3953	0.2485	0.0005	0.0000	0.0001
TL4D	0.3953	0.8996	0.0337	0.4543	0.2485	0.2098	0.7870	0.0337	0.9999	0.3953	0.0028	0.0000	0.0046
TL4E	0.7870	0.5842	0.1759	0.4543	0.6527	0.3953	0.7870	0.0337	0.7212	0.9408	0.0878	0.0015	0.0346
TL4F	0.3953	0.8996	0.0208	0.5175	0.8996	0.0659	0.5842	0.0208	0.3953	0.7870	0.3403	0.0030	0.0036
TL4G	0.7870	0.5842	0.1759	0.4543	0.6527	0.3953	0.7870	0.0337	0.7212	0.9408	0.0878	0.0015	0.0346
TL4H	0.3953	0.8996	0.0208	0.5175	0.8996	0.0659	0.5842	0.0208	0.3953	0.7870	0.3403	0.0030	0.0036
TL4I	0.1212	0.1212	0.0337	0.0424	0.0208	0.4543	0.0530	0.3412	0.0812	0.0530	0.0029	0.0000	0.0032
TL4J	0.1212	0.5175	0.0125	0.0125	0.0812	0.2485	0.1212	0.4543	0.0812	0.5842	0.7212	0.0312	0.0018
TL4K	0.5175	0.2098	0.2098	0.2485	0.3412	0.5175	0.7212	0.1759	0.4543	0.3953	0.0040	0.0000	0.0280
TL4L	0.8996	0.5842	0.1759	0.5175	0.2923	0.2923	0.8996	0.0812	0.7212	0.6527	0.0266	0.0003	0.0114
TL4M	0.0424	0.2485	0.0007	0.1759	0.1759	0.0017	0.0424	0.0003	0.0659	0.0812	0.0783	0.2790	0.2854
TL4N	0.3412	0.2098	0.1759	0.1759	0.0424	0.9408	0.0812	0.7212	0.3953	0.1465	0.0001	0.0000	0.0007
TL4O	0.1465	0.6527	0.0007	0.5175	0.7870	0.0424	0.1759	0.0126	0.1759	0.5842	0.6758	0.0485	0.3282
TL4P	0.6527	0.5842	0.0530	0.3412	0.0996	0.6527	0.2485	0.3412	0.5842	0.3412	0.0611	0.0001	0.0043
TL4Q	0.1759	0.7212	0.0007	0.5175	0.8996	0.0126	0.1465	0.0996	0.3412	0.5842	0.6758	0.0485	0.3282
TL4R	0.1759	0.5842	0.0007	0.7870	0.5175	0.0337	0.3953	0.0017	0.3412	0.3953	0.3142	0.0212	0.1303
TL4S	0.2485	0.5175	0.0530	0.7212	0.6527	0.1465	0.5175	0.0208	0.3953	0.3953	0.1411	0.0115	0.1418
TL4T	0.3412	0.7870	0.0017	0.3953	0.5842	0.0424	0.2098	0.0208	0.2485	0.7870	0.1148	0.0012	0.0202
TL4U	0.5842	0.8475	0.0266	0.6527	0.7212	0.2098	0.7212	0.0659	0.5175	0.5842	0.0728	0.0025	0.0763
TL4V	0.0530	0.3412	0.0017	0.3412	0.5842	0.0074	0.1465	0.0017	0.0996	0.4543	0.4395	0.2251	0.1962
TL4W	0.0812	0.0659	0.0007	0.1759	0.0530	0.0003	0.0042	0.0000	0.0530	0.0266	0.0007	0.0797	0.1673
TL4X	0.7212	0.5175	0.2923	0.5842	0.4543	0.5842	0.7212	0.2098	0.6527	0.7870	0.0202	0.0002	0.0036
TL4Y	0.7835	0.3779	0.1032	0.3445	0.5164	0.1694	0.4380	0.0658	0.0494	0.3037	0.0518	0.0019	0.0168
TL4Z	0.9877	0.5842	0.1212	0.7870	0.2923	0.5175	0.7870	0.1212	0.3953	0.3953	0.0153	0.0003	0.0071
TL10C	0.5175	0.1212	0.1212	0.7212	0.2098	0.2098	0.7212	0.0812	0.3953	0.5175	0.0114	0.0000	0.0003
TL11A	0.5175	0.0056	0.5842	0.8475	0.1759	0.6527	0.0659	0.8996	0.9877	0.2540	0.0096	0.0046	0.0000
TL11B	0.1212	0.0530	0.0074	0.0074	0.0074	0.7212	0.1212	0.3412	0.1212	0.0337	0.0000	0.0000	0.0000
TL11C	0.7212	0.5842	0.0074	0.7212	0.2098	0.6527	0.0337	0.5842	0.4543	0.0047	0.0013	0.0012	0.0012
TL11D	0.2098	0.8475	0.0074	0.7212	0.0996	0.6527	0.2162	0.4543	0.8475	0.4809	0.0225	0.0000	0.1418
TL11E	0.2098	0.1759	0.7212	0.2098	0.0996	0.2098	0.2098	0.7212	0.2098	0.1465	0.0074	0.0000	0.0009
TL11F	0.7212	0.6527	0.1212	0.6527	0.6527	0.2098	0.6530	0.7870	0.8475	0.0329	0.0003	0.0003	0.0573
TL11G	0.0812	0.0659	0.3412	0.0337	0.0162	0.7212	0.0530	0.0530	0.0530	0.0424	0.0001	0.0000	0.0001
TL12A	0.1360	0.8996	0.1212	0.5245	0.4543	0.2098	0.7870	0.0530	0.7212	0.0355	0.0001	0.0000	0.0000
TL13B	0.5175	0.9877	0.0337	0.4543	0.8475	0.1465	0.8475	0.0424	0.7212	0.2377	0.0007	0.0028	0.0028
4901.SZ	0.0114	0.2560	0.0000	0.0047	0.4809	0.0024	0.0229	0.0001	0.0085	0.2377	0.0000	0.0377	0.2533
4901.SH	0.0000	0.0000	0.0000	0.0013	0.0025	0.0000	0.0003	0.0000	0.0001	0.0097	0.0377	0.0000	0.3231
4904	0.0003	0.0346	0.0003	0.0312	0.1418	0.0006	0.0573	0.0001	0.0144	0.0226	0.2533	0.3231	0.1605
8912	0.1884	0.6128	0.0122	0.5165	0.8256	0.0958	0.3389	0.0365	0.4165	0.7102	0.4440	0.0073	0.1605
8914	0.0154	0.1480	0.0003	0.1050	0.2293	0.0021	0.0858	0.0007	0.0183	0.3569	0.0940	0.0023	0.0141
893	0.0994	0.4262	0.0004	0.3512	0.5094	0.0003	0.1003	0.0038	0.1418	0.3063	0.4145	0.0488	0.4557
894	0.0172	0.2772	0.0001	0.0732	0.2206	0.0041	0.0174	0.0019	0.0407	0.1503	0.3644	0.6578	0.5637
897	0.0994	0.6042	0.0012	0.2933	0.6289	0.0382	0.0938	0.0059	0.0803	0.3334	0.2965	0.0315	0.1053
KMITSAT	0.0000	0.0000	0.0000	0.0000	0.0000	0.0000	0.0000	0.0000	0.0000	0.0000	0.0000	0.0000	0.0013
KMISMEL	0.0872	0.0278	0.0031	0.1616	0.0477	0.0038	0.0183	0.0003	0.0477	0.0118	0.0073	0.0140	0.0914
KMSWKL	0.00017	0.0013	1E-07	0.0017	0.00067	2.3E-06	0.00034	1.4E-06	0.00024	0.00034	0.0004	0.0008	0.0573



## TWO SAMPLE KOLMOGOROV - SMIRNOV TEST FOR NORMALIZED CSD's (size / ave. size)

SHADING = &lt;0.05

Class/Count	8912	8914	893	894	897	KMSITSAT	KMUNSMEL	KMSSWKCL	Class/Count				
TL1A	0.4039	0.0547	0.1196	0.0891	0.1848	0.0000	0.0730	8E-05	TL1A				
TL1A2	0.0799	0.0664	0.0637	0.0215	0.0938	0.0000	0.0532	0.00024	TL1A2				
TL1A3	0.3138	0.0961	0.0384	0.0271	0.1120	0.0000	0.0130	5.7E-07	TL1A3				
TL1B	0.5511	0.0584	0.4262	0.2414	0.2501	0.0001	0.0963	0.0031	TL1B				
TL1B2	0.2556	0.0603	0.0573	0.0373	0.1120	0.0001	0.1285	0.0042	TL1B2				
TL1B3	0.4385	0.0801	0.1418	0.0497	0.1592	0.0000	0.0504	0.00062	TL1B3				
TL1C	0.1884	0.0122	0.0470	0.0411	0.0666	0.0000	0.0240	2.7E-06	TL1C				
TL1D	0.0130	0.0021	0.0017	0.0011	0.0140	0.0000	0.0000	0	TL1D				
TL1E	0.2952	0.0183	0.2289	0.0612	0.2799	0.0000	0.0147	8.3E-05	TL1E				
TL1F	0.1884	0.0664	0.0637	0.0457	0.0656	0.0000	0.0561	0.00067	TL1F				
TL1G	0.0837	0.0051	0.0637	0.0426	0.0533	0.0000	0.0460	5.5E-05	TL1G				
TL1H	0.2952	0.0449	0.0364	0.0271	0.0938	0.0000	0.0304	3.9E-06	TL1H				
TL1I	0.0546	0.0037	0.0102	0.0032	0.0253	0.0000	0.0045	6.3E-07	TL1I				
TL2A	0.0005	0.0000	0.0000	0.0000	0.0001	0.0000	0.0001	0	TL2A				
TL2B	0.4707	0.1020	0.2854	0.0503	0.1120	0.0000	0.0295	0.00034	TL2B				
TL2C	0.7351	0.2041	0.3063	0.1753	0.2539	0.0000	0.0430	0.0013	TL2C				
TL2D	0.4165	0.0449	0.2289	0.0543	0.2902	0.0000	0.0100	0.00024	TL2D				
TL3A	0.2952	0.0122	0.0637	0.0373	0.0781	0.0000	0.0189	2.7E-05	TL3A				
TL3B	0.8757	0.2377	0.4809	0.2414	0.6969	0.0000	0.0768	0.00002	TL3B				
TL3C	0.4840	0.0819	0.1418	0.0271	0.1120	0.0000	0.0195	3.9E-05	TL3C				
TL3F	0.1904	0.0480	0.0364	0.0295	0.1072	0.0000	0.0118	8.2E-06	TL3F				
TL3G	0.0002	0.0000	0.0000	0.0000	0.0000	0.0000	0.0001	0	TL3G				
TL3H	0.0662	0.0039	0.0129	0.0067	0.0262	0.0000	0.0255	2.7E-05	TL3H				
TL3I	0.2200	0.0480	0.0573	0.0732	0.1120	0.0000	0.0518	0.00048	TL3I				
TL3J	0.1265	0.0070	0.0637	0.0065	0.1893	0.0000	0.0240	3.9E-05	TL3J				
TL3K	0.2952	0.0366	0.0637	0.0331	0.0938	0.0000	0.0518	0.00048	TL3K				
TL3L	0.1036	0.0007	0.0071	0.0041	0.0114	0.0000	0.0003	6.2E-06	TL3L				
TL3M	0.0662	0.0181	0.0102	0.0058	0.0269	0.0000	0.0247	3.9E-05	TL3M				
TL4A	0.2200	0.0560	0.0364	0.0271	0.0437	0.0000	0.0147	0.00034	TL4A				
TL4B	0.4806	0.0240	0.1196	0.0578	0.0908	0.0000	0.0039	2.7E-05	TL4B				
TL5K	0.0662	0.0059	0.0053	0.0024	0.0118	0.0000	0.0404	0.00012	TL5K				
TL5L	0.3389	0.0122	0.1673	0.0659	0.2160	0.0000	0.0195	5.7E-05	TL5L				
TL5W	0.7695	0.0819	0.1962	0.0612	0.2160	0.0000	0.0054	0.00024	TL5W				
TL6H	0.4707	0.2757	0.2121	0.1270	0.487*	0.0000	0.0075	0.00047	TL6H				
TL7A	0.0521	0.0078	0.0114	0.0026	0.0180	0.0000	0.0003	1.8E-07	TL7A				
TL7B	0.2783	0.0480	0.0631	0.0702	0.3687	0.0000	0.0026	5.5E-05	TL7B				
TL7C	0.1884	0.0209	0.0182	0.0069	0.0149	0.0000	0.0189	0.00017	TL7C				
TL7D	0.2556	0.0240	0.1196	0.0294	0.1120	0.0000	0.0278	0.00048	TL7D				
TL7E	0.1521	0.0031	0.4809	0.0923	0.1115	0.0017	0.4266	0.053	TL7E				
TL8A	0.0889	0.0049	0.0312	0.0024	0.0450	0.0000	0.0039	1.5E-05	TL8A				
TL8B	0.6666	0.0603	0.8088	0.3785	0.7706	0.0000	0.0546	0.0042	TL8B				
TL8C	0.3389	0.0679	0.0631	0.0579	0.0908	0.0000	0.0074	5.4E-06	TL8C				
TL8D	0.5880	0.0480	0.4809	0.1360	0.6039	0.0000	0.1062	0.0096	TL8D				
TL8E	0.5165	0.0840	0.5686	0.6025	0.1841	0.0001	0.1226	0.0126	TL8E				
TL8F	0.6946	0.0575	0.5094	0.1360	0.3795	0.0000	0.1011	0.0023	TL8F				
TL8G	0.7010	0.1743	0.3063	0.0497	0.2893	0.0000	0.0147	0.00024	TL8G				
TL9A	0.5877	0.1888	0.3063	0.0891	0.2964	0.0000	0.0391	0.00048	TL9A				
TL9B	0.5333	0.0330	0.3282	0.3547	0.1567	0.0000	0.0183	0.0001	TL9B				
TL9C	0.0658	0.0063	0.2467	0.0745	0.0287	0.0013	0.7965	0.1759	TL9C				
TL9D	0.2200	0.0664	0.0573	0.0139	0.0781	0.0000	0.0122	0.00024	TL9D				
TL9A	0.3307	0.0488	0.1176	0.0471	0.0708	0.0022	0.2101	0.0045	TL9A				
TL9B	0.2952	0.0193	0.0836	0.0215	0.1331	0.0000	0.0504	8.3E-05	TL9B				
TL9C	0.1884	0.0154	0.0694	0.0172	0.0964	0.0000	0.0872	0.00017	TL9C				
TL11A	0.6128	0.1480	0.4262	0.2772	0.5042	0.0000	0.0278	0.0003	TL11A				
TL11B	0.0122	0.0003	0.0064	0.0001	0.0012	0.0000	0.0033	1E-07	TL11B				
TL11C	0.5165	0.1050	0.3512	0.0732	0.2933	0.0000	0.1816	0.00017	TL11C				
TL11D	0.8256	0.2293	0.5094	0.2206	0.6289	0.0000	0.0477	0.00067	TL11D				
TL11E	0.0958	0.0021	0.0063	0.0041	0.0362	0.0000	0.0039	2.3E-06	TL11E				
TL11F	0.3389	0.0858	0.1003	0.0174	0.0938	0.0000	0.0183	0.00024	TL11F				
TL11G	0.0395	0.0007	0.0028	0.0019	0.0069	0.0000	0.0003	1.4E-06	TL11G				
TL12A	0.4185	0.0193	0.1418	0.0407	0.0803	0.0000	0.0477	0.00024	TL12A				
TL13B	0.7102	0.3559	0.3063	0.1503	0.3334	0.0000	0.0118	0.00034	TL13B				
4901.SZ	0.4440	0.0940	0.4145	0.3644	0.2965	0.0000	0.0073	0.0004	4901.SZ				
4901.SH	0.0073	0.0023	0.0465	0.6578	0.0315	0.0000	0.0140	0.0066	4901.SH				
4904	0.1605	0.0141	0.4653	0.5637	0.1053	0.0013	0.0914	0.0573	4904				
8912		0.1401	0.7005	0.2497	0.6240	0.0000	0.0715	0.0033	8912				
8914	0.1401		0.0968	0.0306	0.3896	0.0000	0.0013	2.7E-06	8914				
893	0.7005	0.0968		0.5934	0.2080	0.0006	0.1642	0.0181	893				
894	0.2497	0.0306	0.5934		0.2382	0.0003	0.0332	0.0354	894				
897	0.6240	0.3896	0.2080	0.2382		0.0000	0.0263	0.0011	897				
KMSITSAT	0.0000	0.0000	0.0000	0.0003	0.0000		0.0452	0.0037	KMSITSAT				
KMUNSMEL	0.0715	0.0013	0.1642	0.0332	0.0253	0.0452		0.3512	KMUNSMEL				
KMSSWKCL	0.0003	2.7E-06	0.0181	0.0354	0.0011	0.0037	0.3512		KMSSWKCL				

## **APPENDIX C**

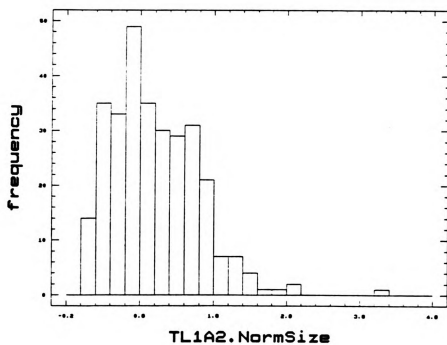
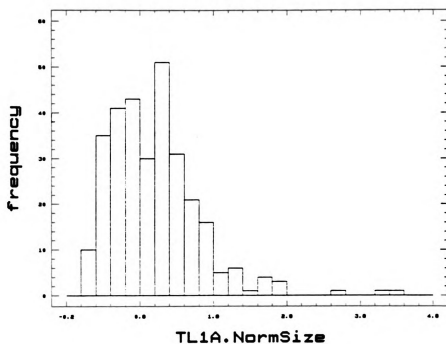
### **Normalized Crystal Size Distribution Frequency Histograms and Crystal Size Distribution to Thin-section/Sample Key**

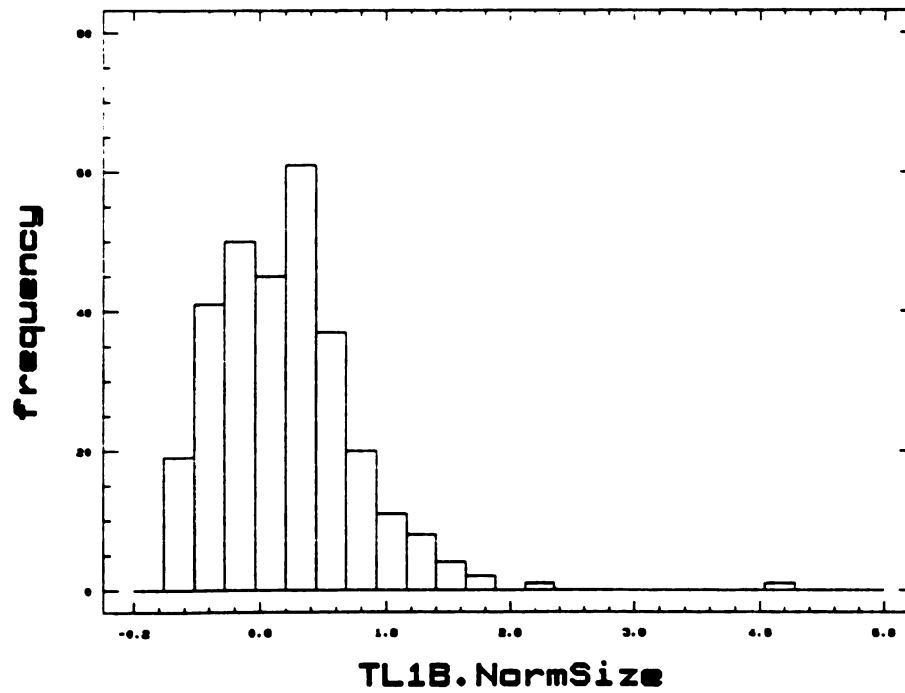
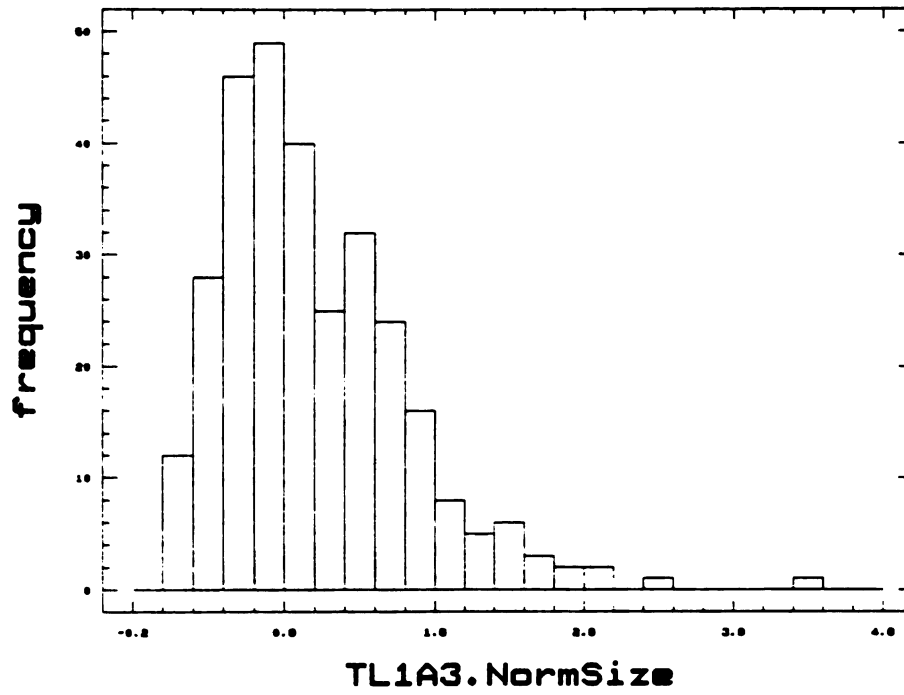
## APPENDIX C

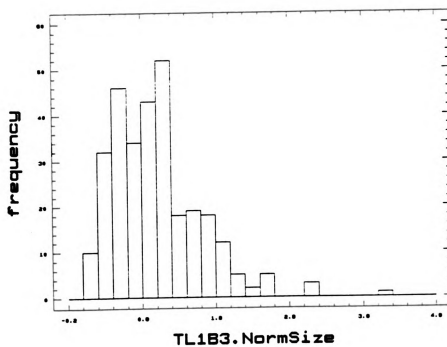
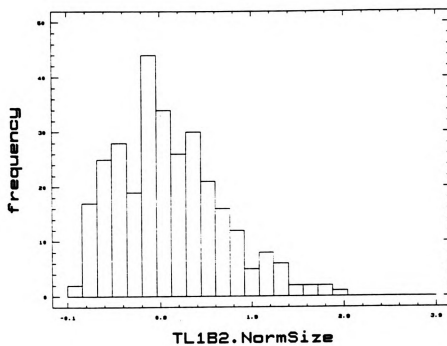
### Normalized Crystal Size Distribution Frequency Histograms And Crystal Size Distribution To Thin-Section Sample Key

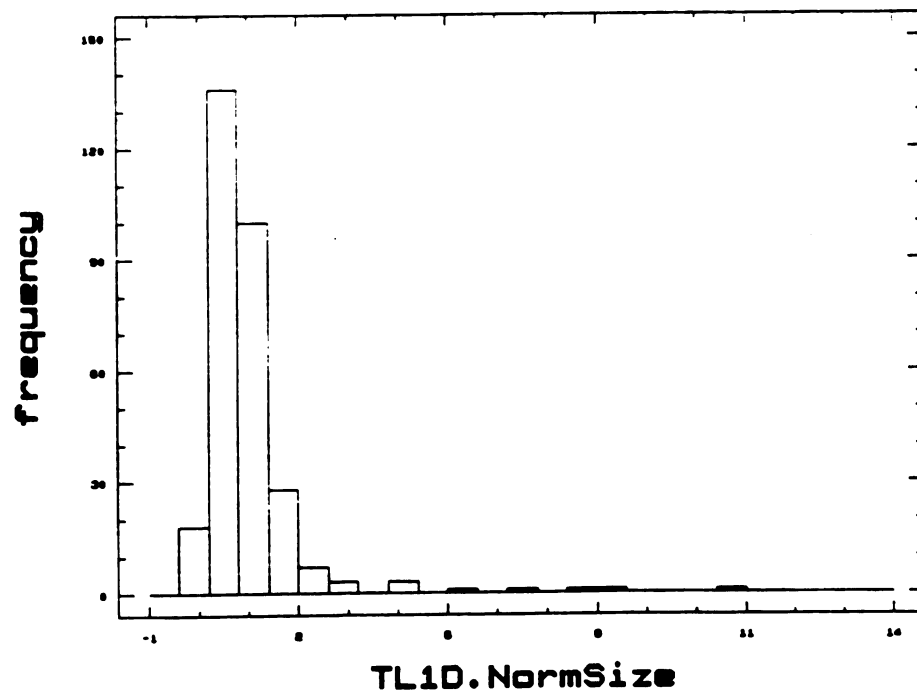
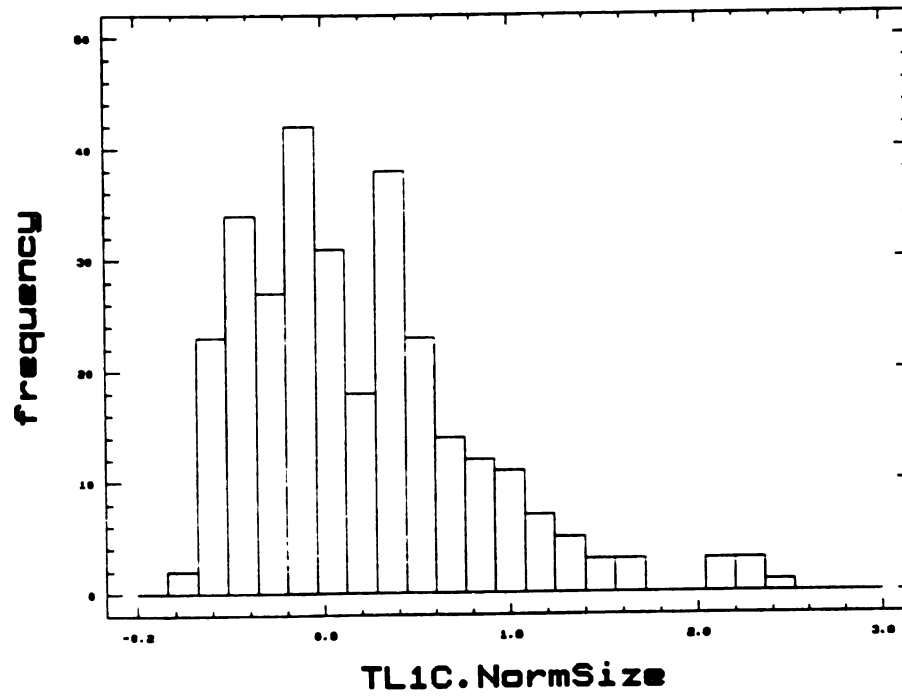
#### THIN SECTION NAMES FOR CSD GRAPH NAMES

<u>CSD Name</u>	<u>Thin Section Name</u>	<u>Clasts</u>
<b>Trenton Formation, Jackson Co., Michigan</b>		
TL-1	TL 1 - 12 C3 B21	A-I 9
TL-2	TL 1 - 12 C3 B55 4891	A-D 4
TL-3	L 1 - 12 C1 B1	A-C,F-M 11
TL-4	L 1 - 12 C3 B2	A,B 2
TL-5	L 1 - 12 C1 B5	K,L,W 3
TL-6	Luck 1 - 12 C1 B5 485?	H 1
TL-7	Total Luck 1 - 12 C1 B5 485?	A-E 5
TL-8	Total Luck (C1 B8 ?) 4864 1/2	A-G 7
TL-9	Total Luck 1 - 12 C1 B5 4852 1/2	A-D 4
TL-10	Total Luck 1 - 12 C3 B5 4891	A-C 3
TL-11	Total Luck 1 - 12 C2 B1 4867	A-G 7
TL-12	Total Luck 1 - 12 C3 B21	A 1
TL-13	Total Luck 1 - 12 C3 B2 4882	B 1
	(Mirror of TL-4B)	
<b>Netherland Antilles, Aruba Dolomite</b>		
BD6TS	BD6 (Boi Doi Thin Section, two CSD counts)	
BD6GM	BD6 (Boi Doi Grain Mount, one CSD count)	
<b>Saluda Formation, Jefferson Co., Indiana</b>		
4901.SZ	MS4901DS (500 grain CSD count)	
4901.SH	MS4901DS (445 grain CSD count)	
4904	MS4904DS	
893	MS893DS	
894	MS894DS	
897	MS897DS	
8912	MS8912DS	
8914	MS8912DS	
<b>Computer Generated Microstructures</b>		
KMSITSAT	Site Saturation (Cellular) Nucleation and Growth	
KMJNSMEL	Johnson-Mehl Nucleation and Growth	
KMSSWKCL	Site Saturation Nucleation and Growth With Weakly Clustered Nuclei	

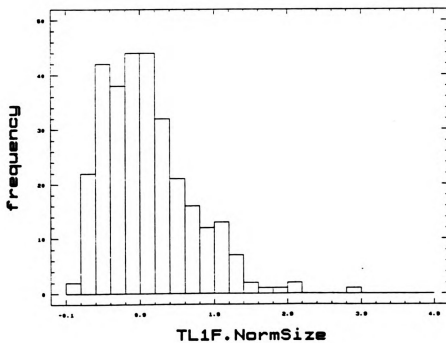
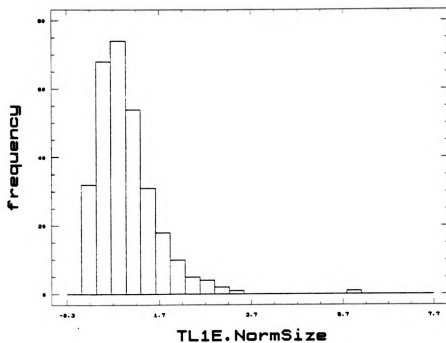


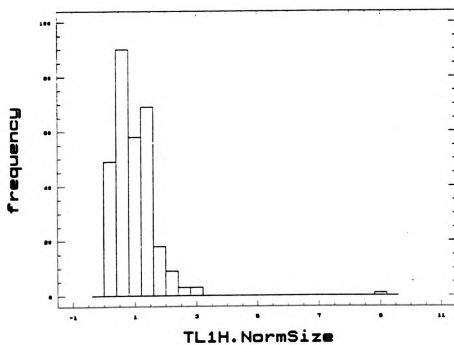
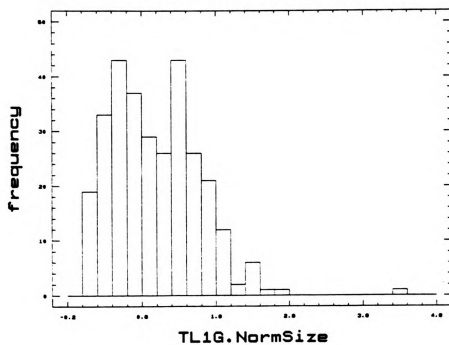


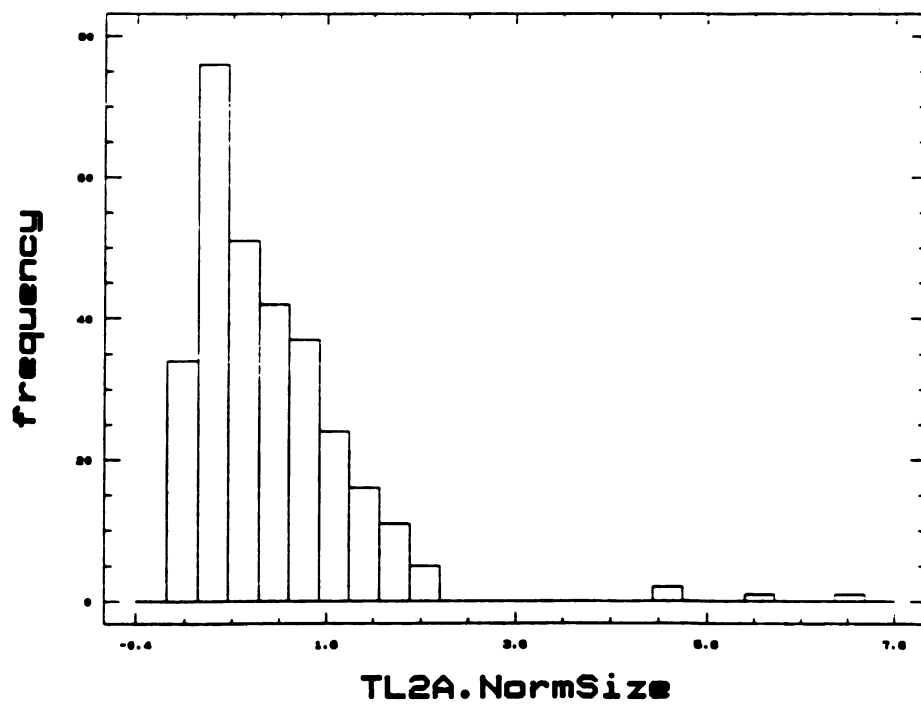
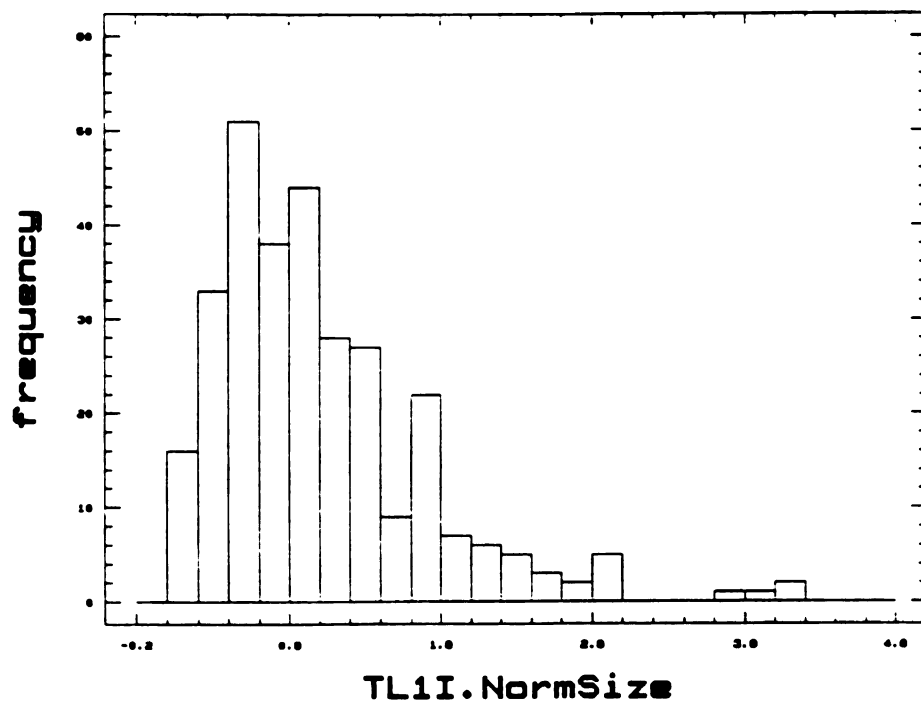


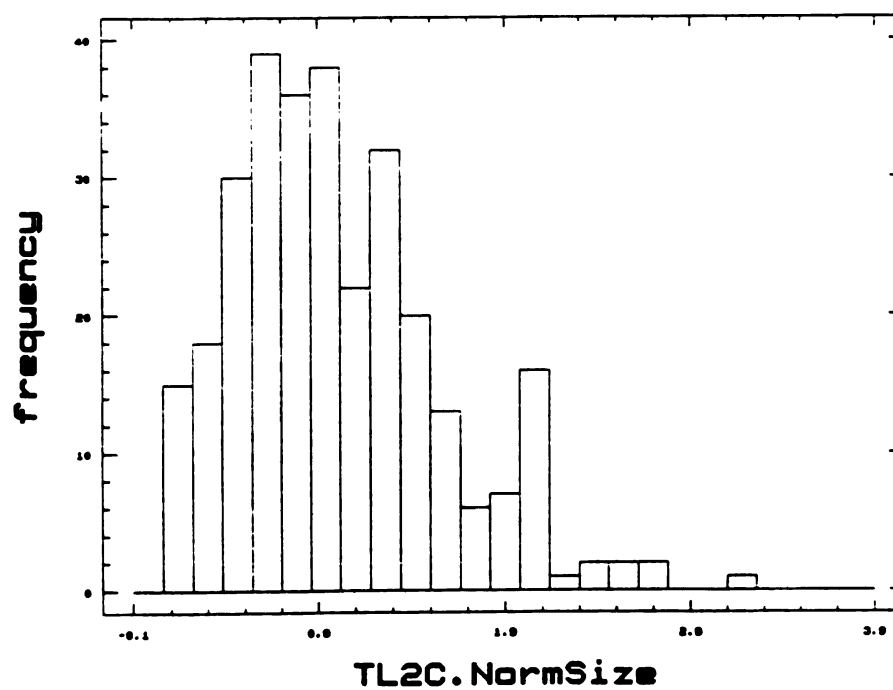
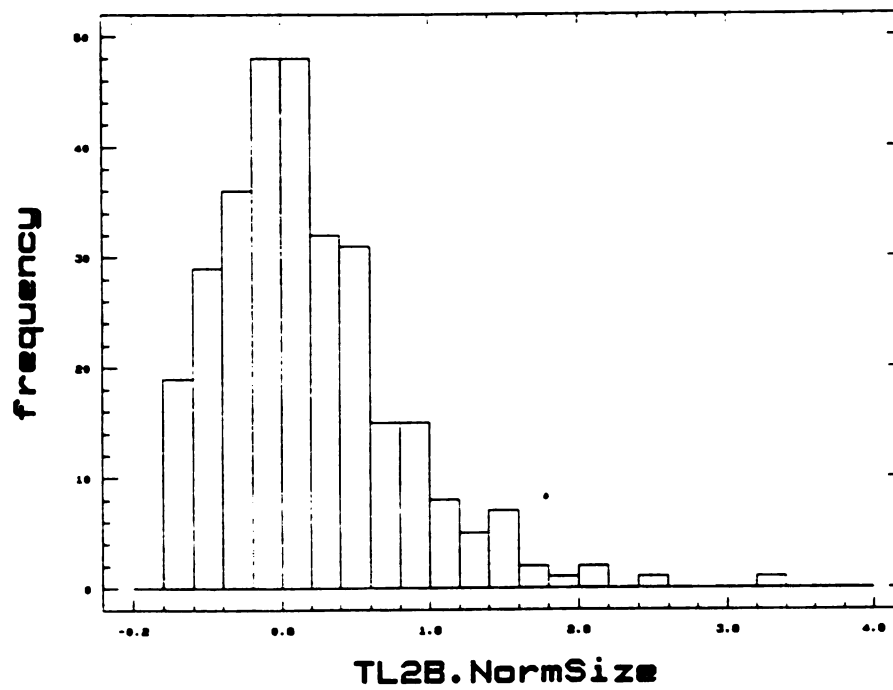


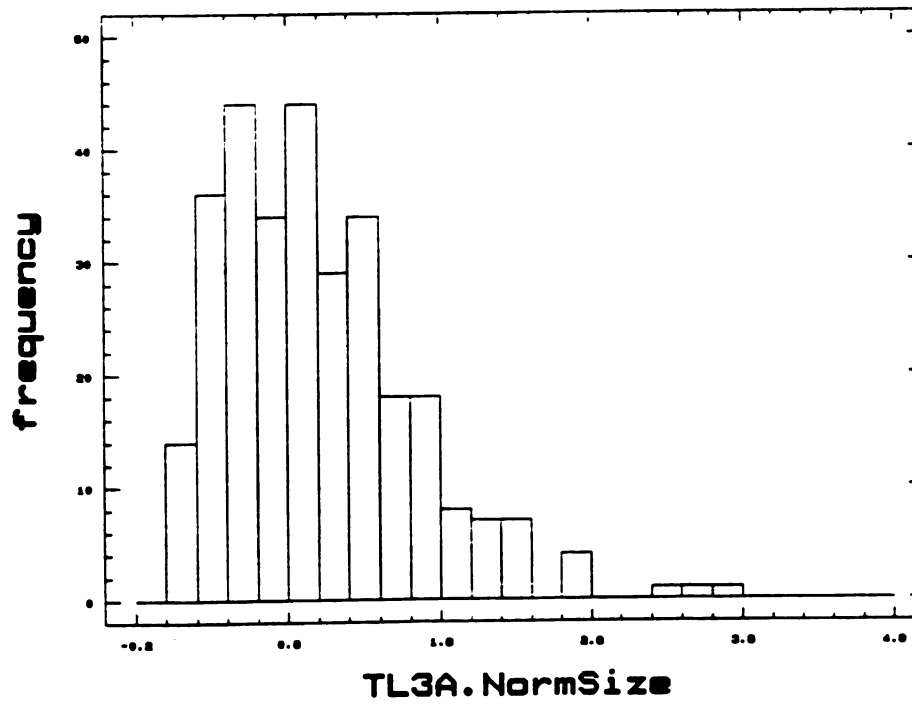
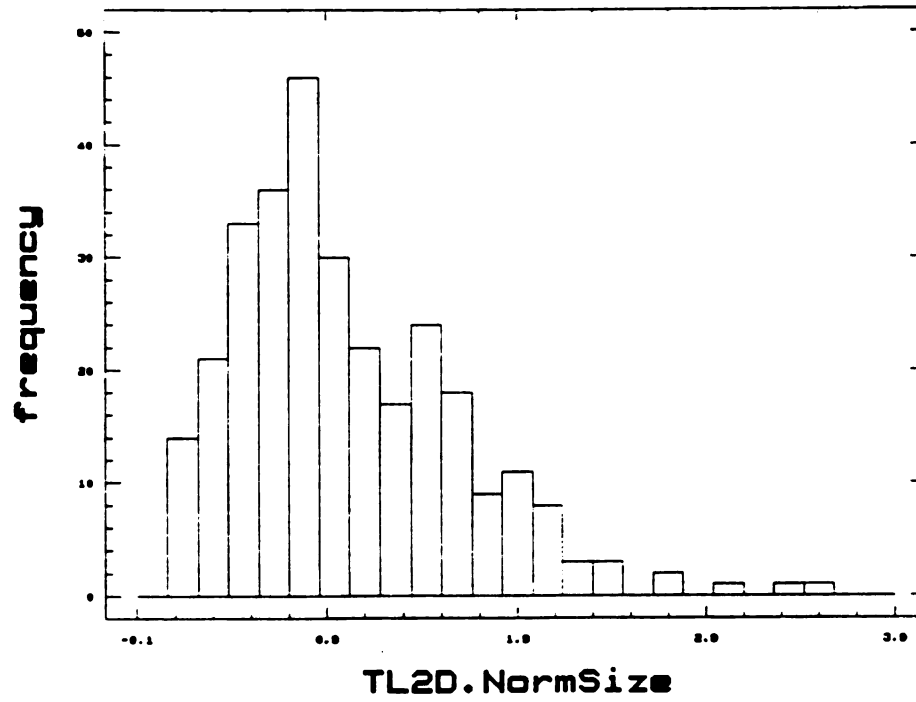


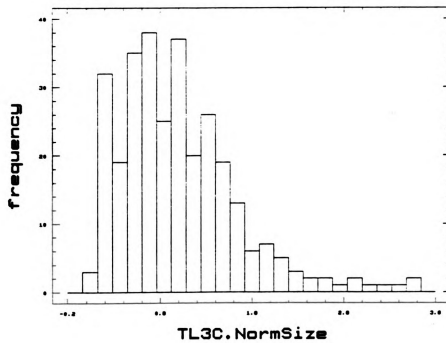
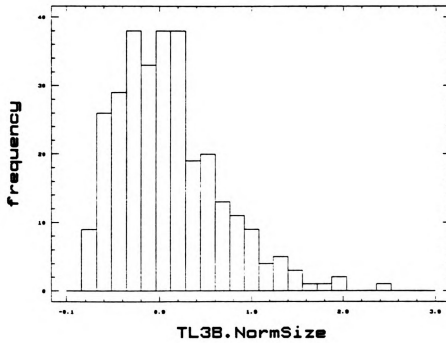


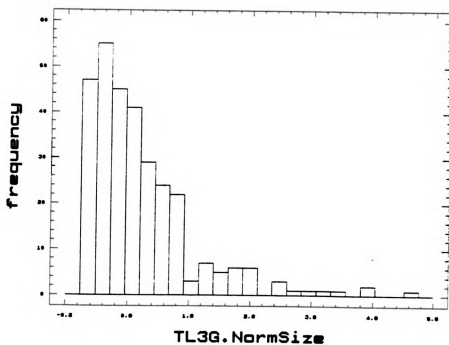
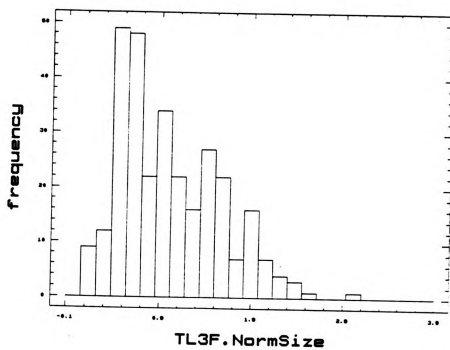


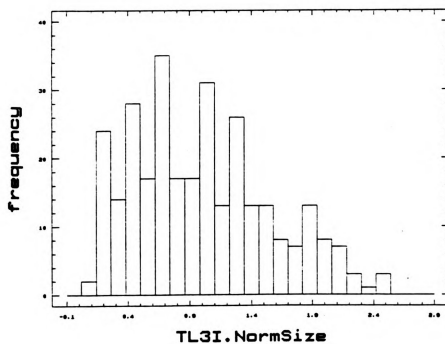
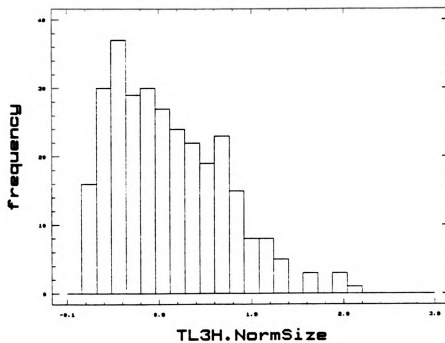




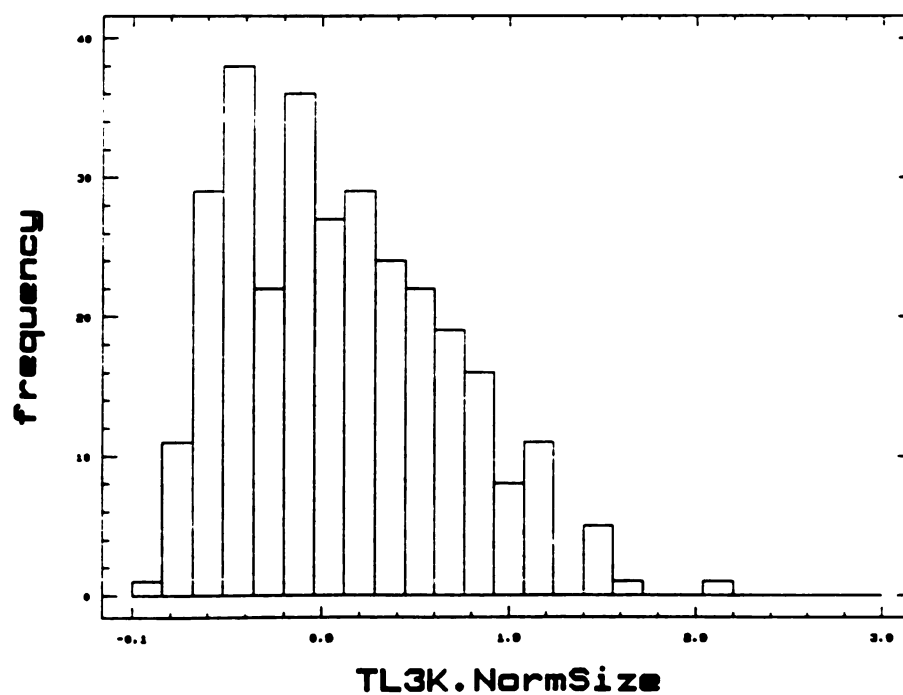
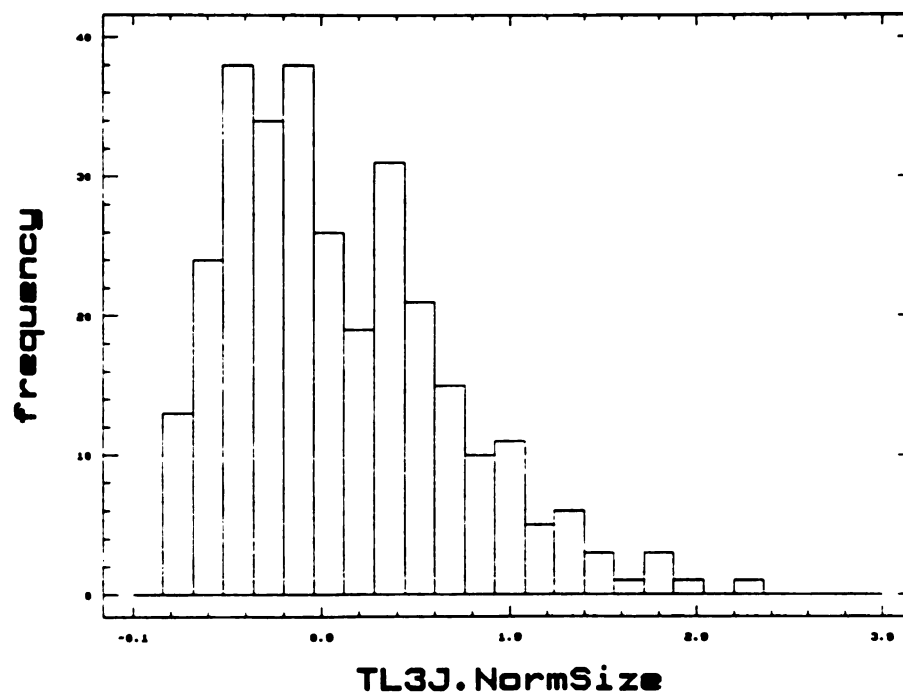


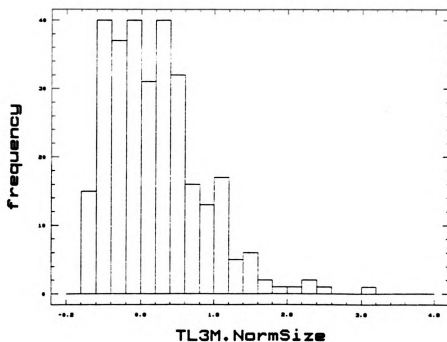
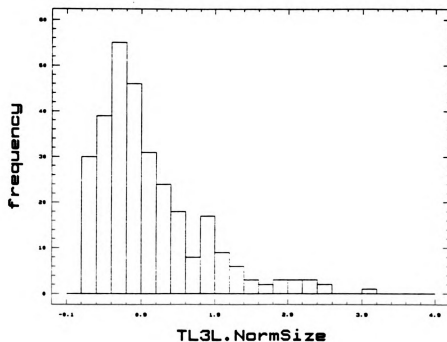


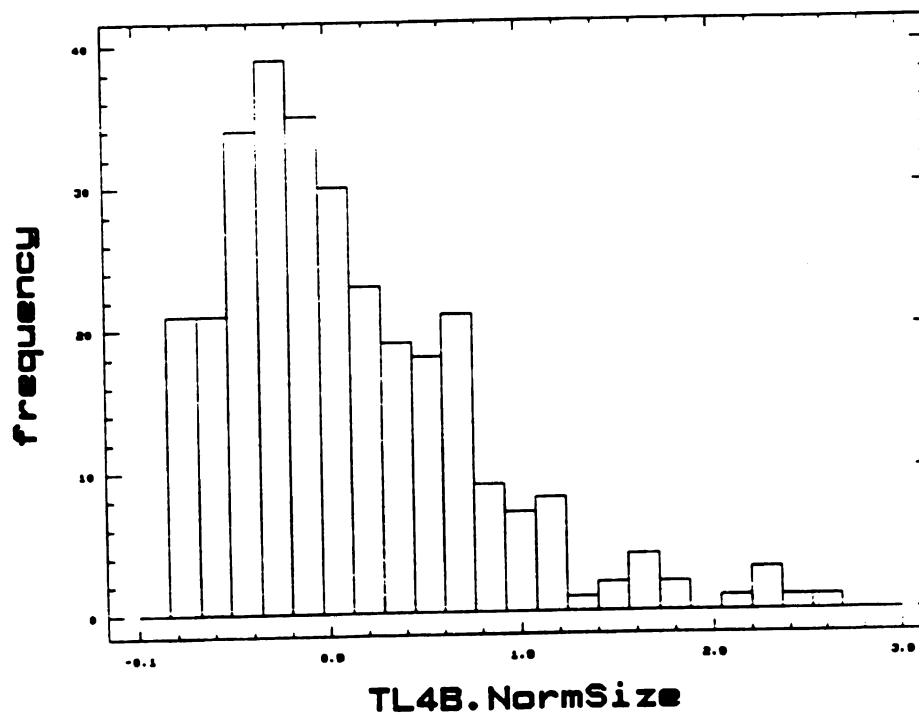
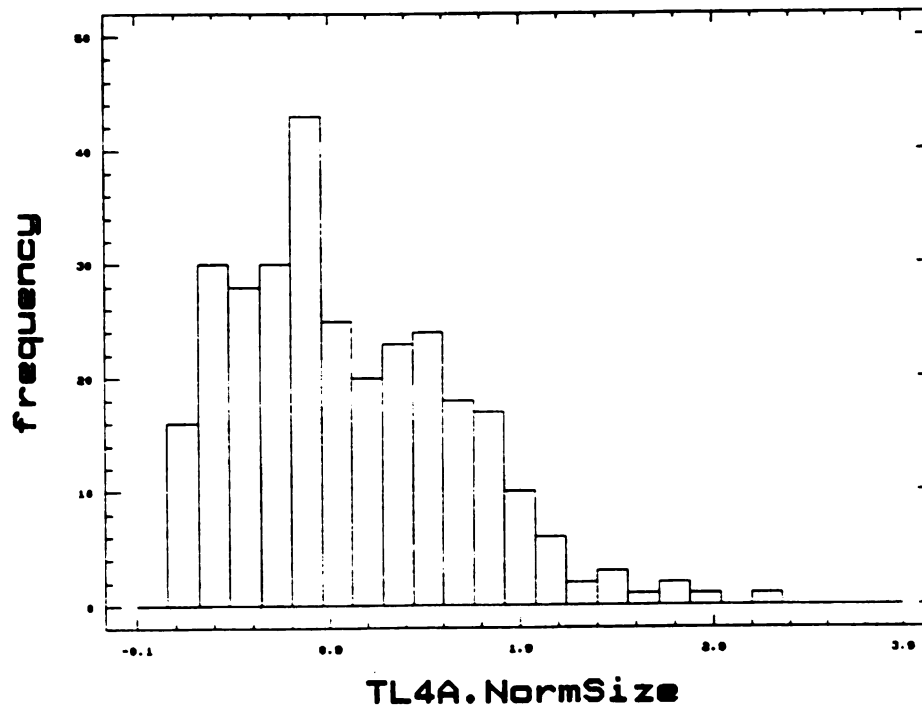


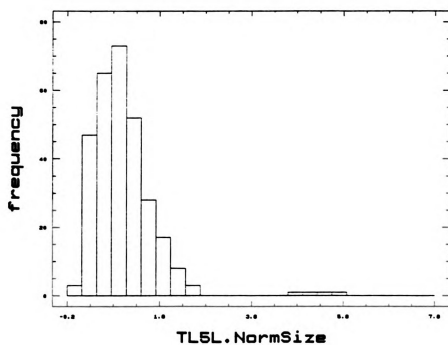
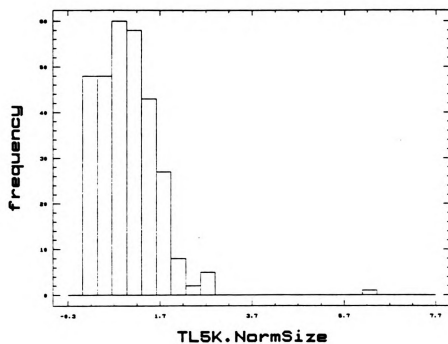


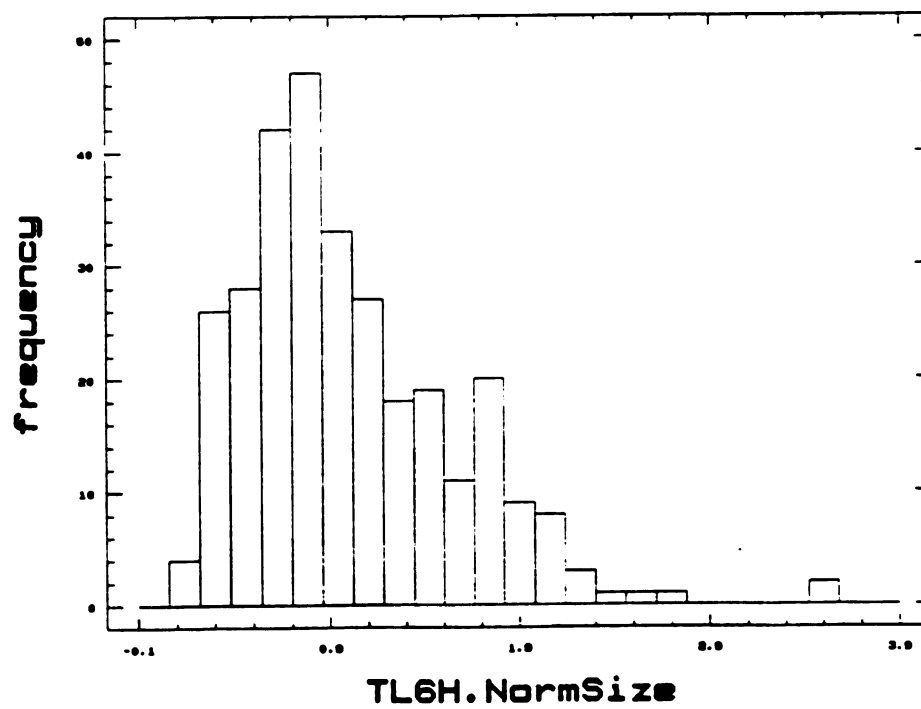
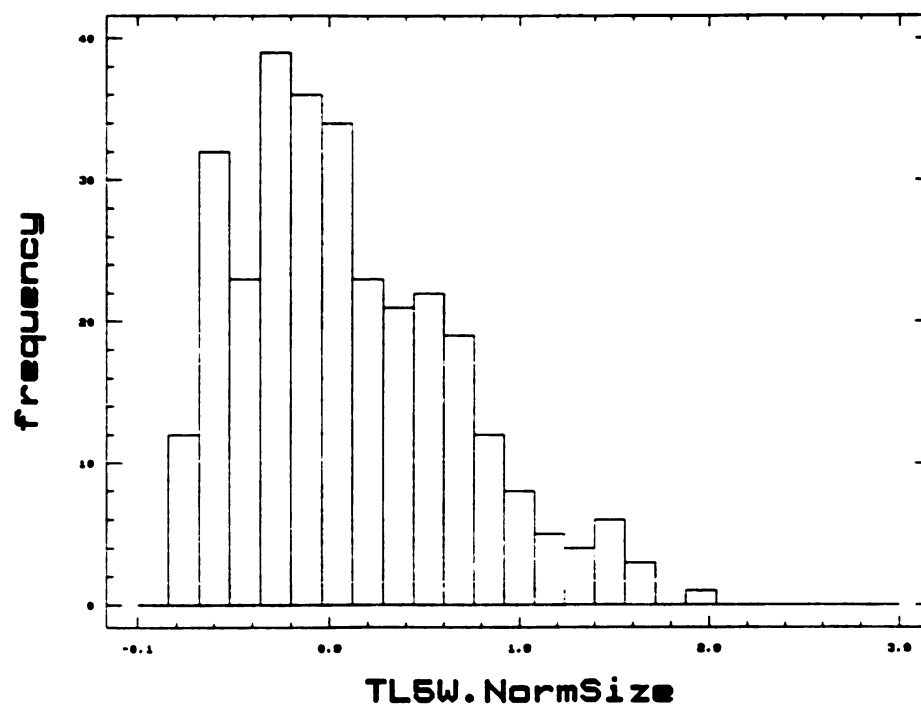


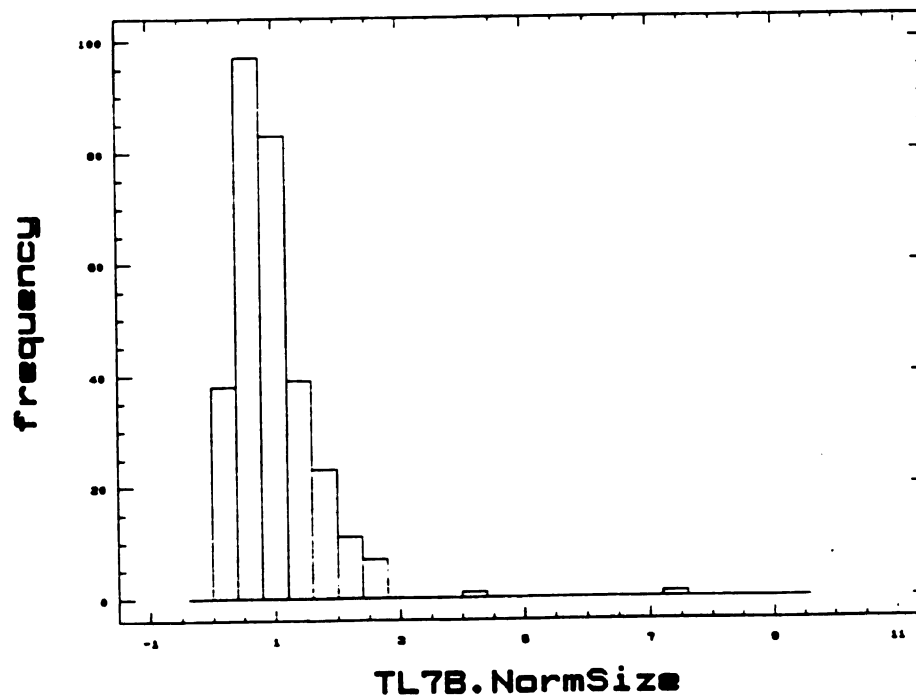
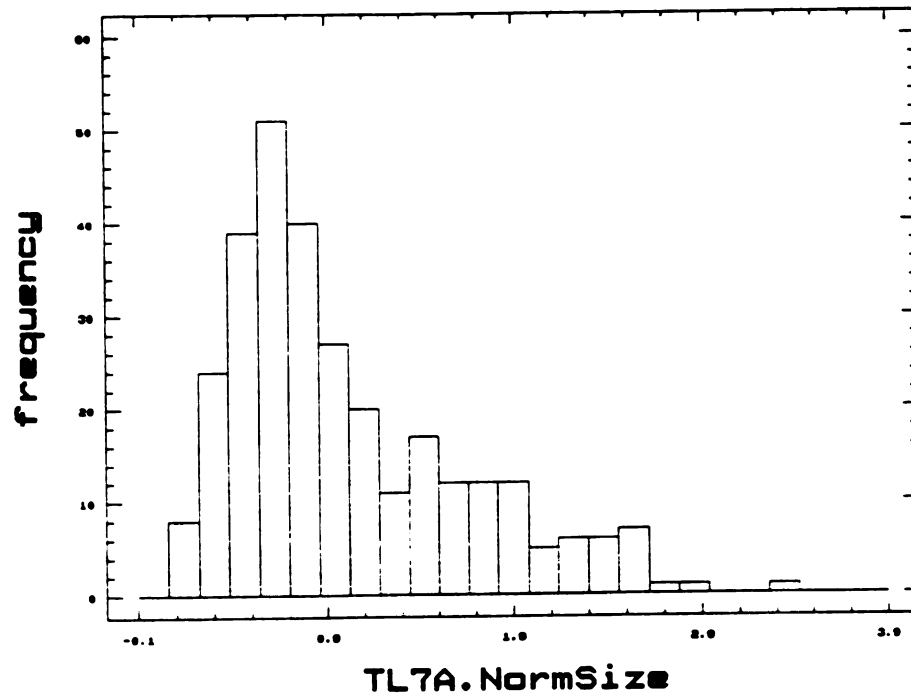


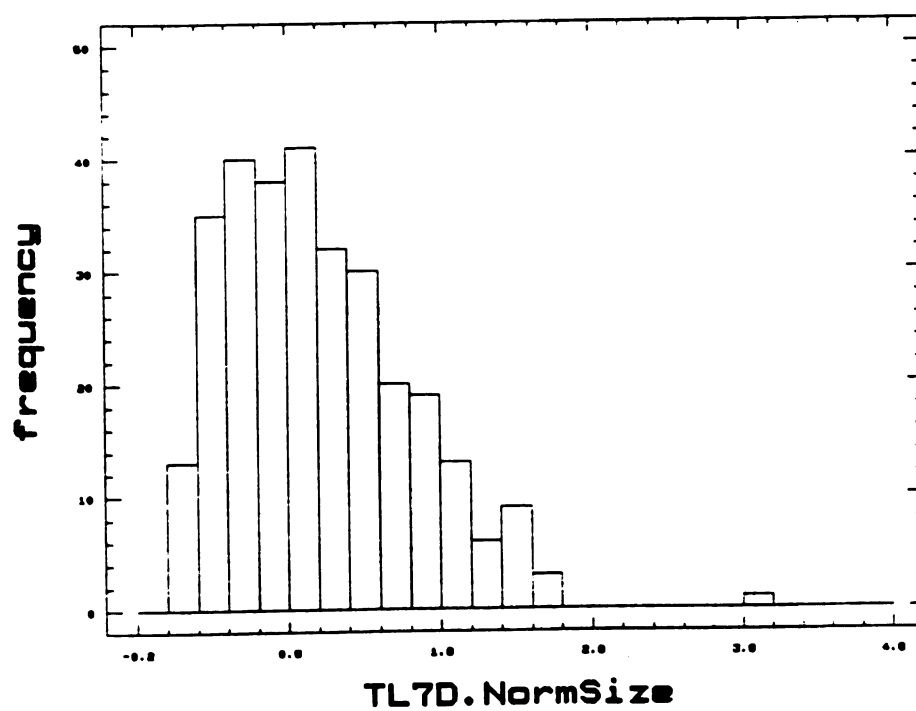
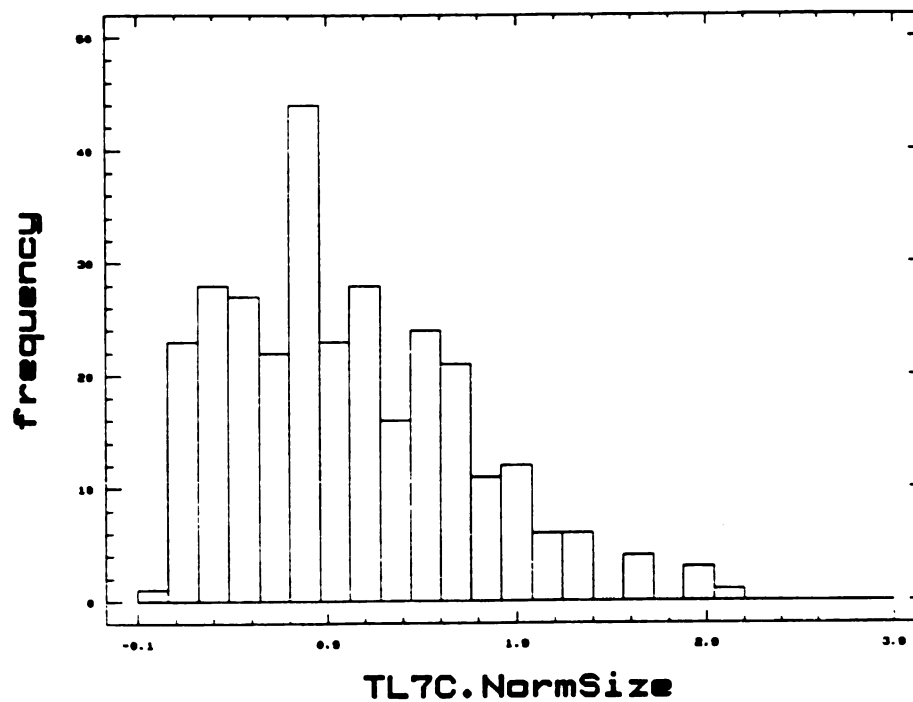


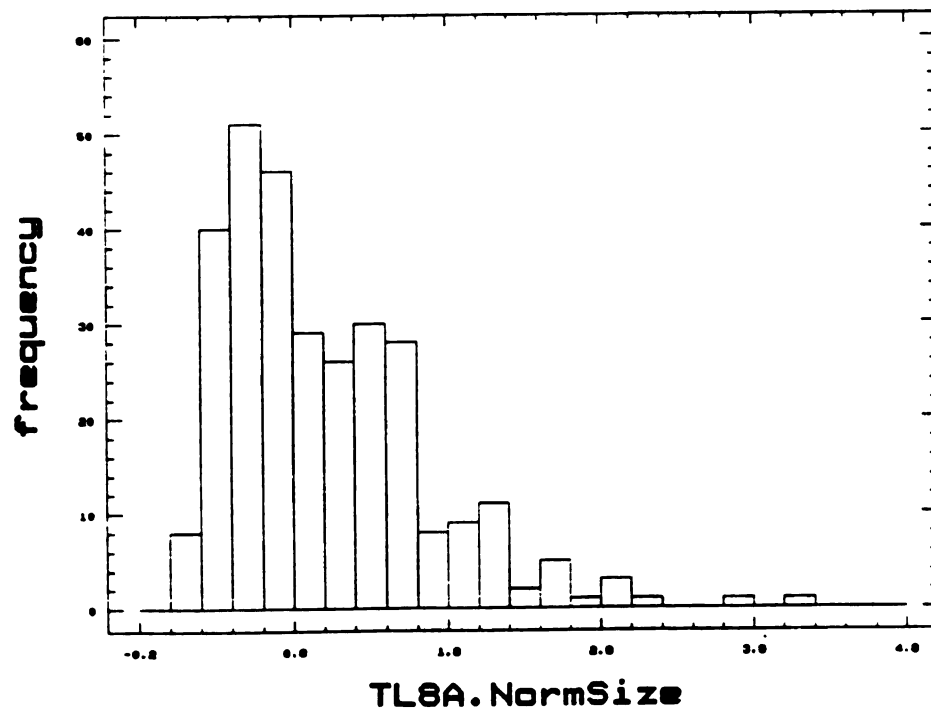
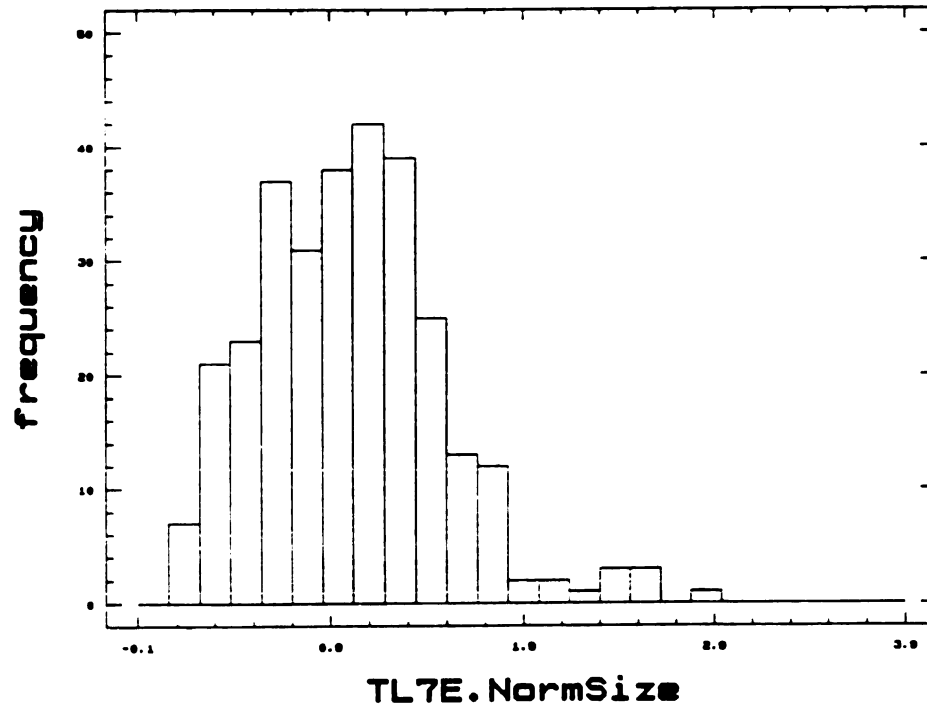




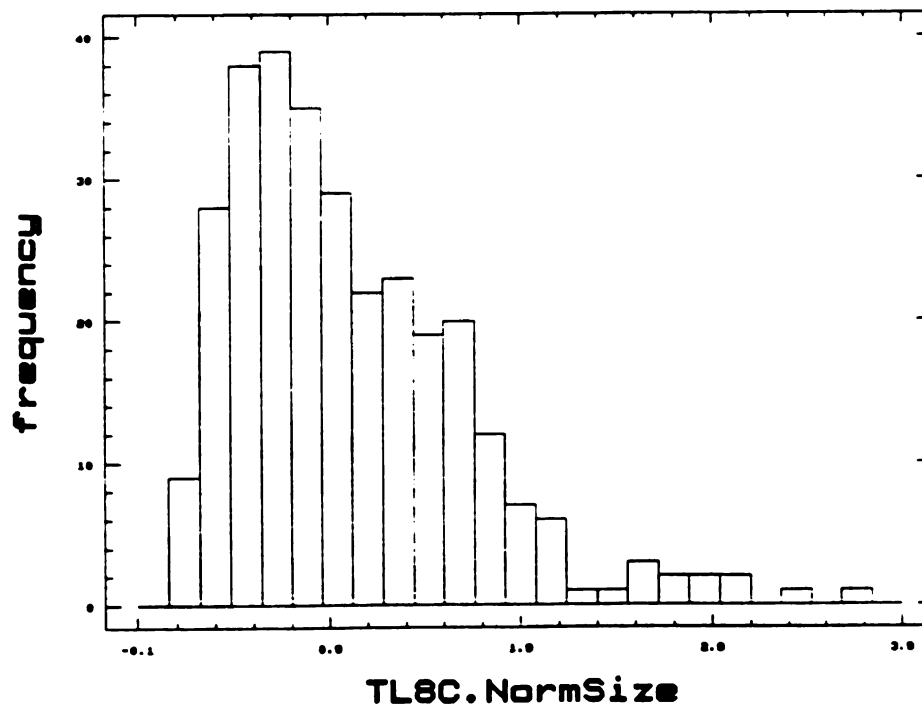
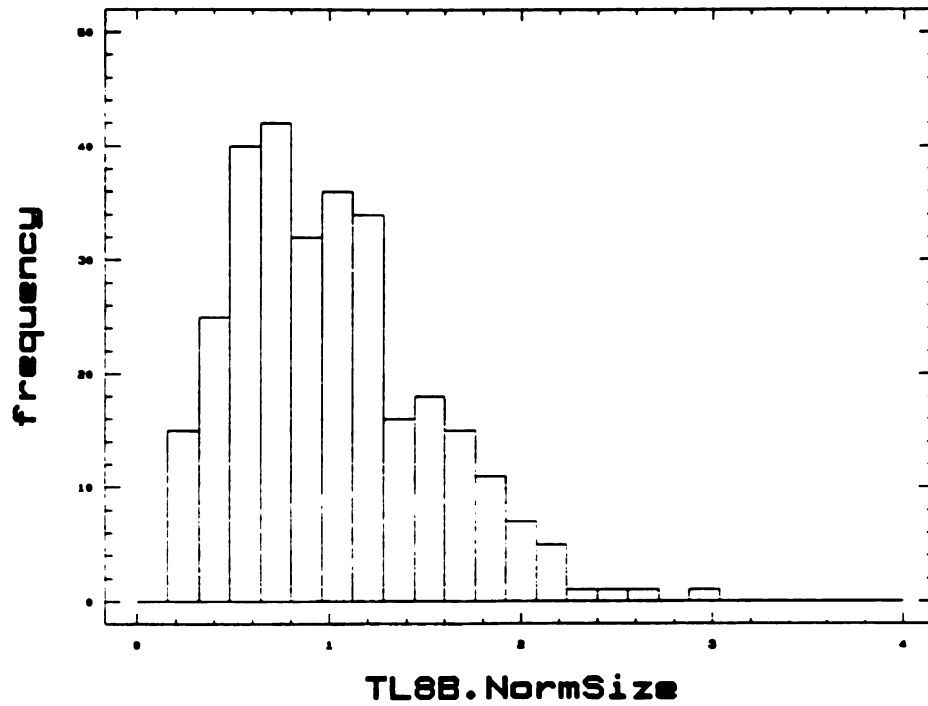


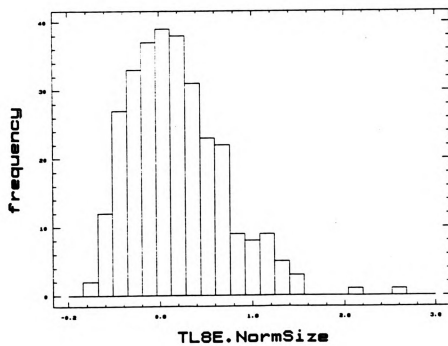
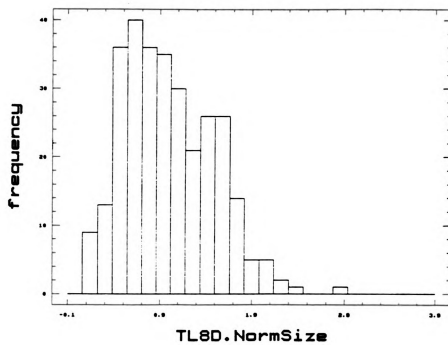


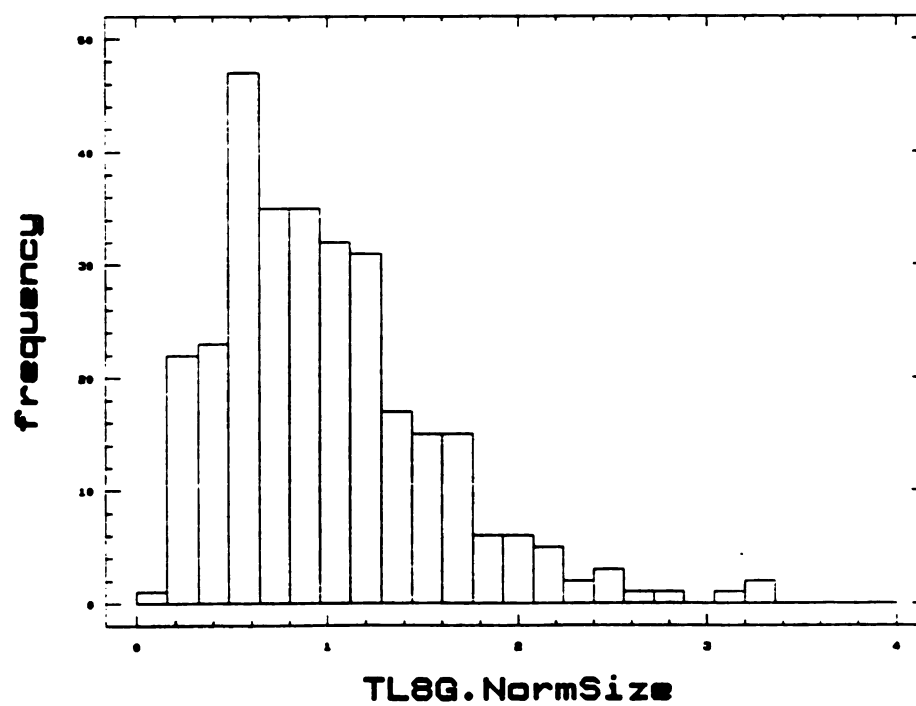
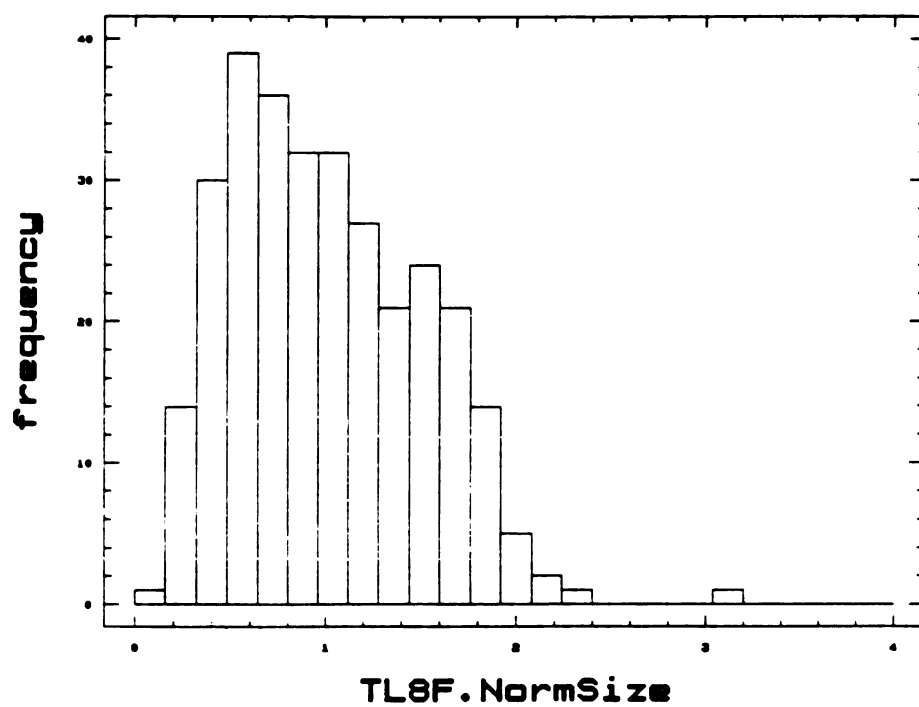


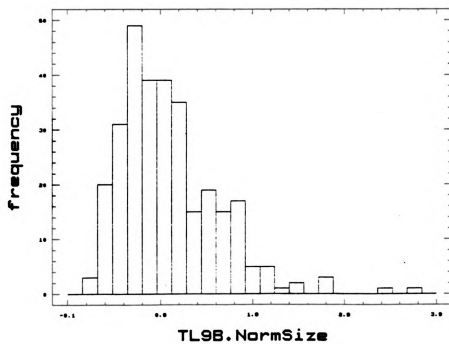
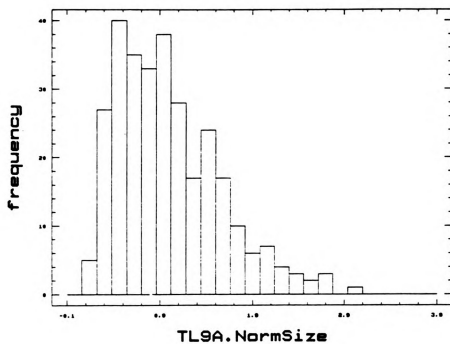


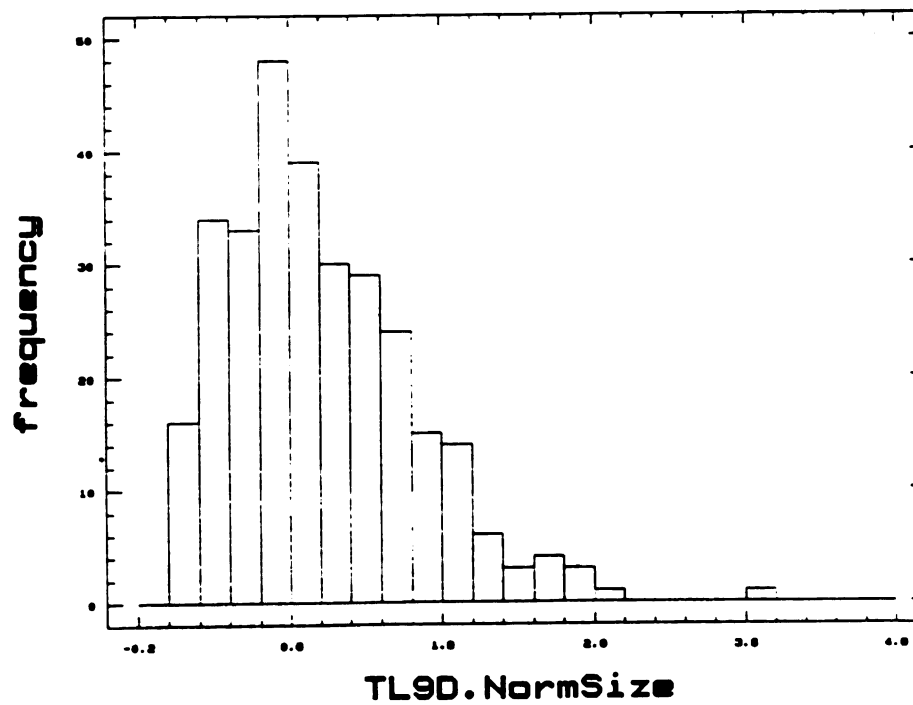
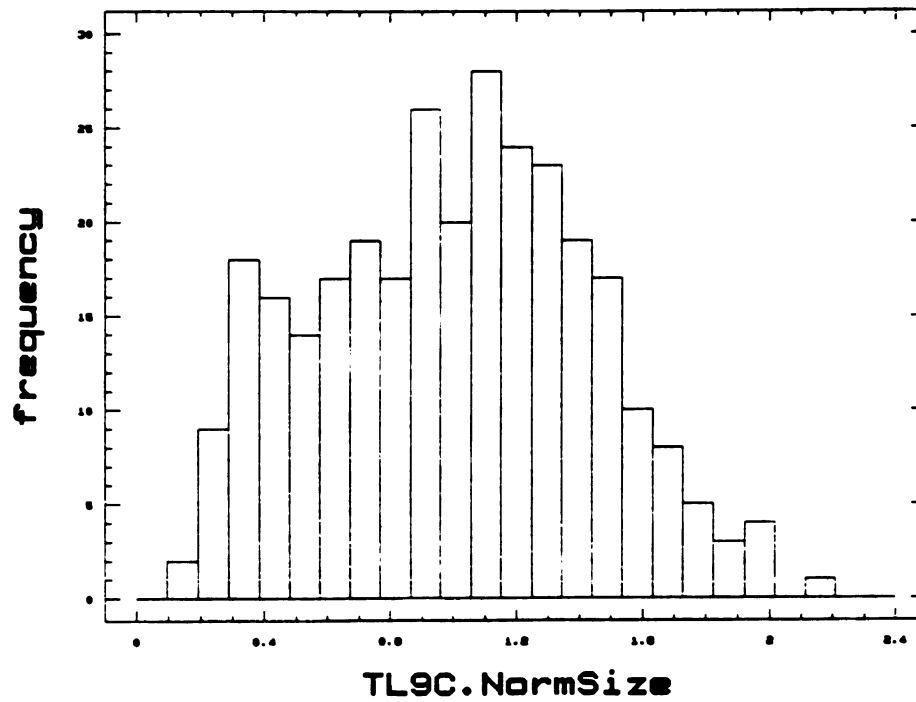


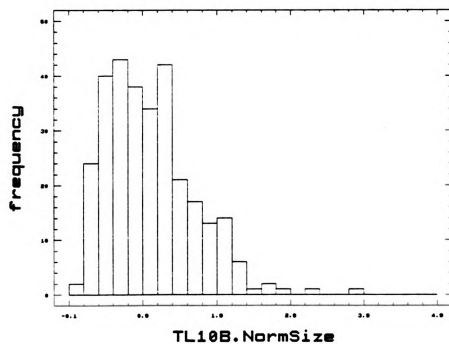
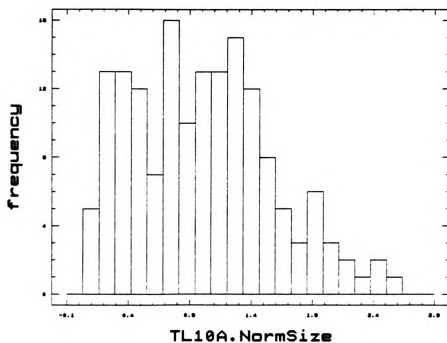


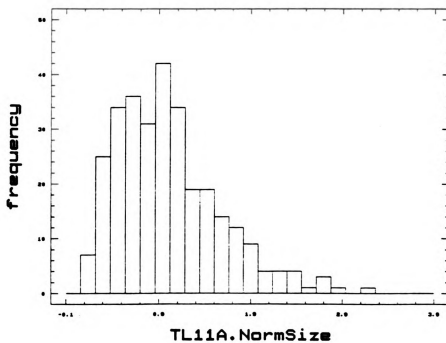
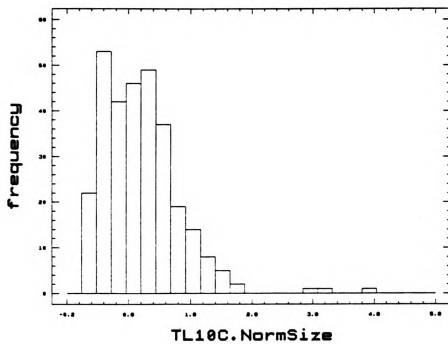


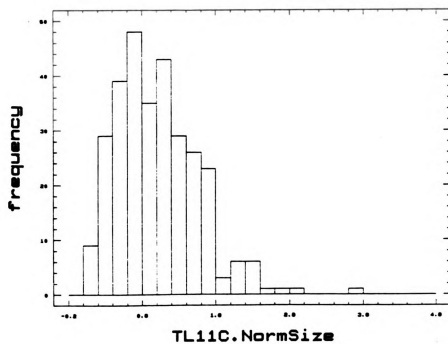
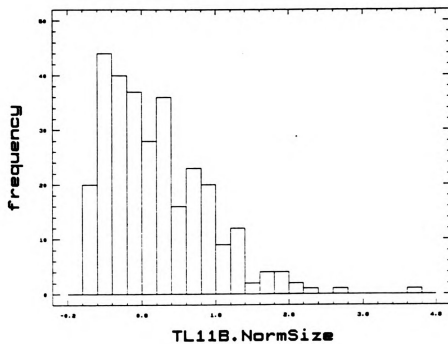




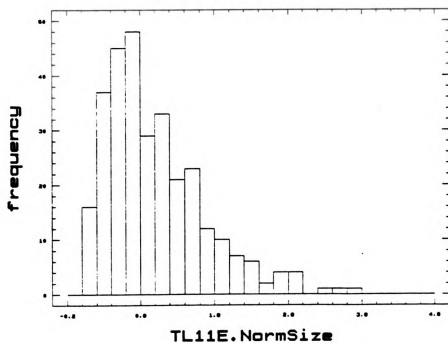
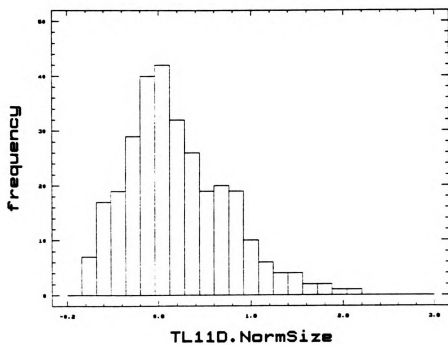


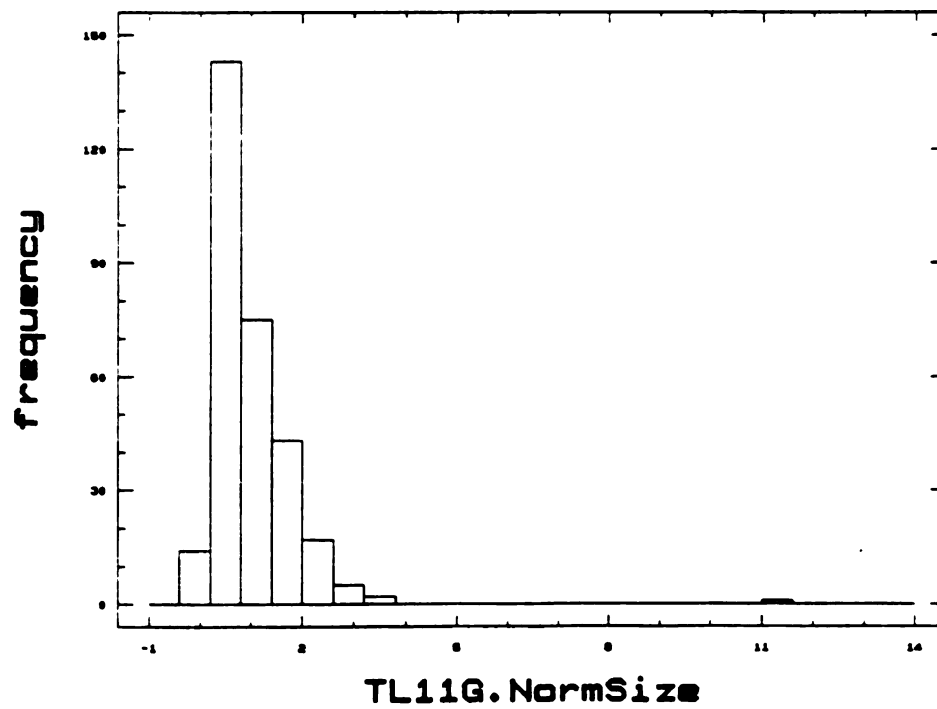
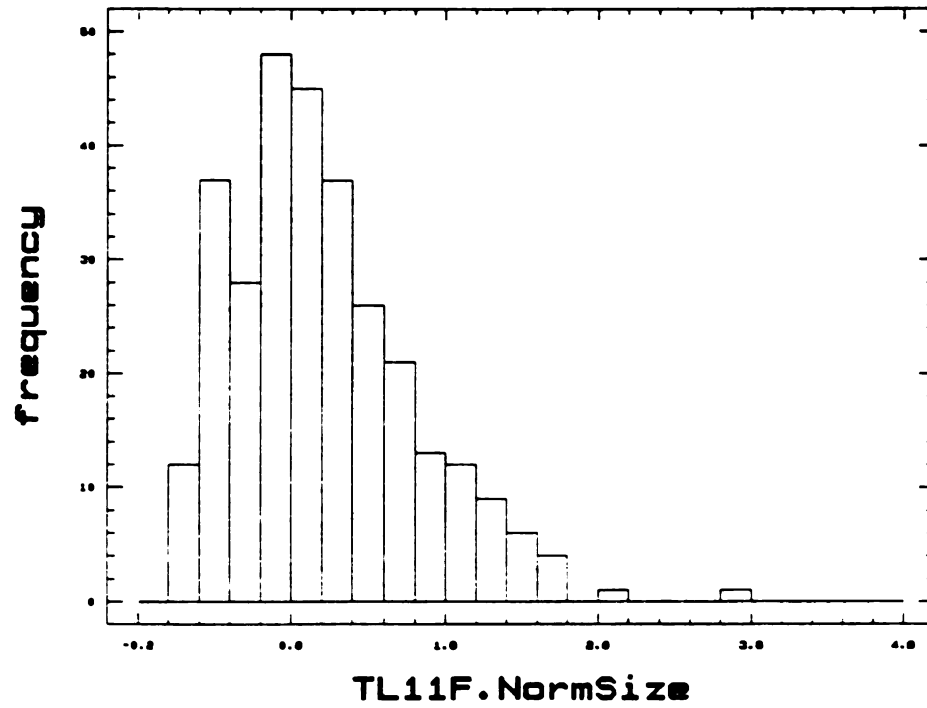


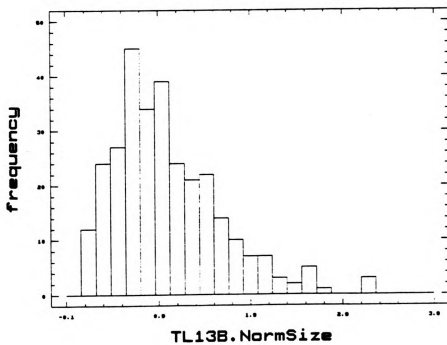
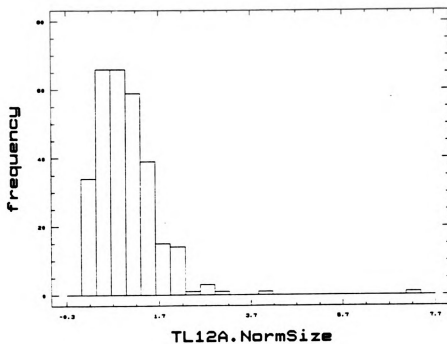


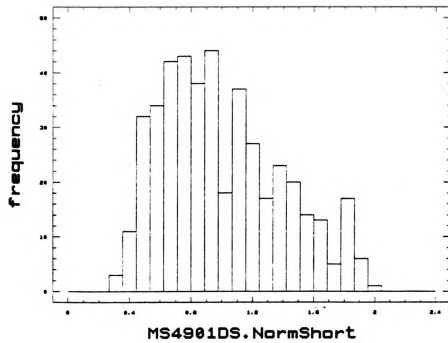
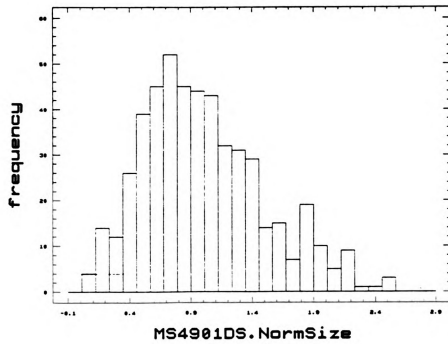


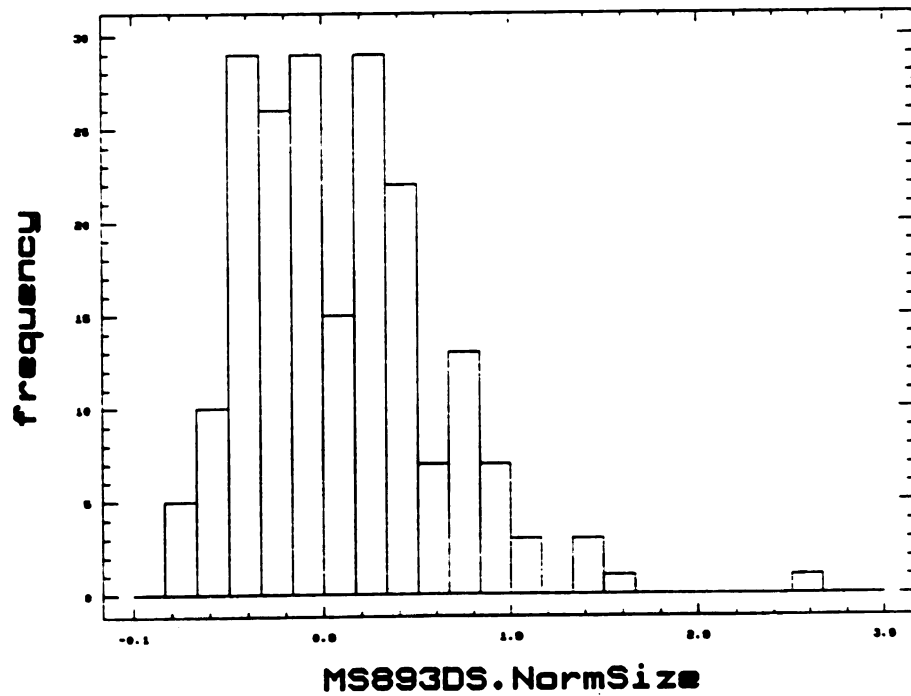
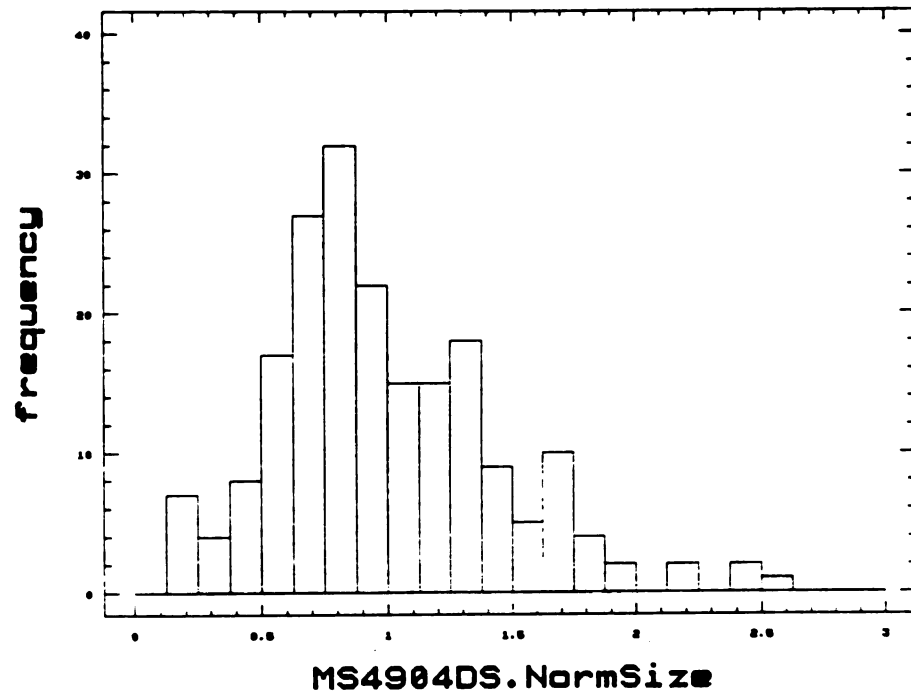


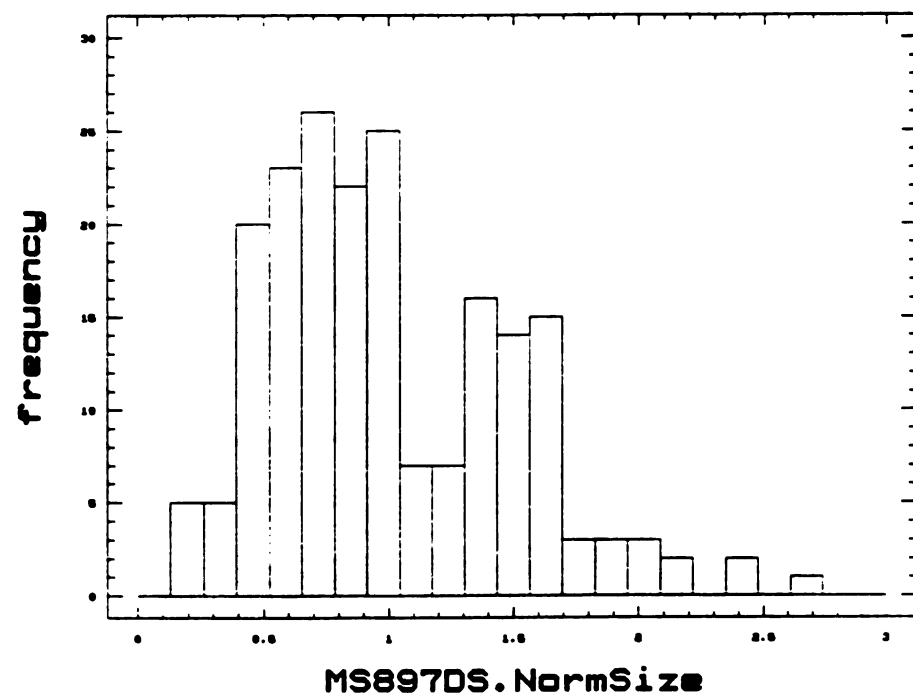
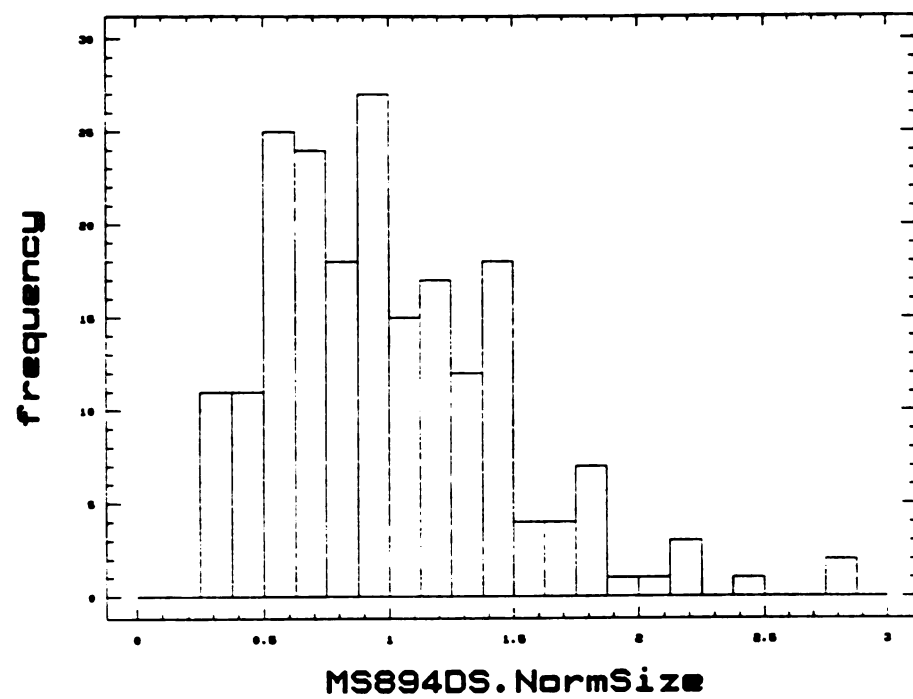


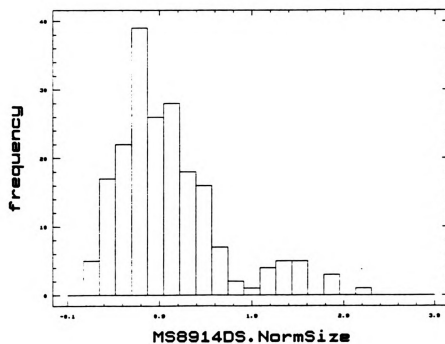
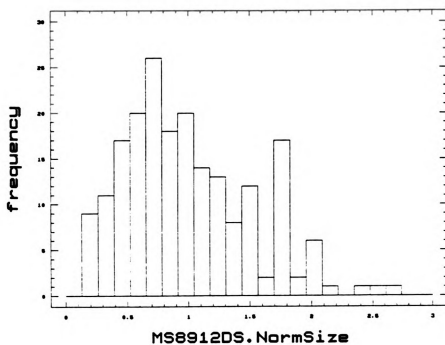


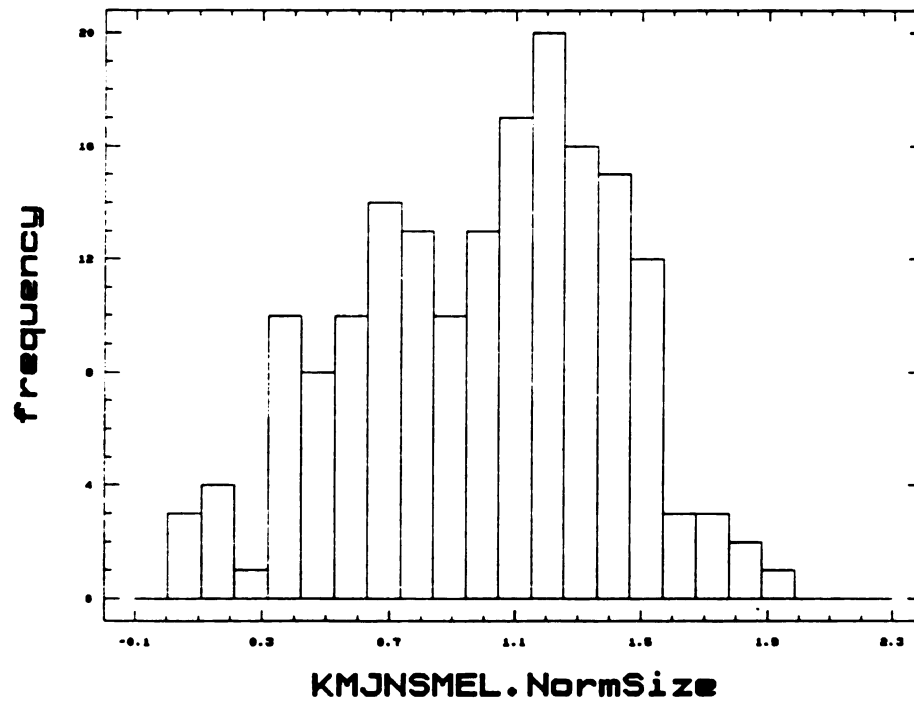
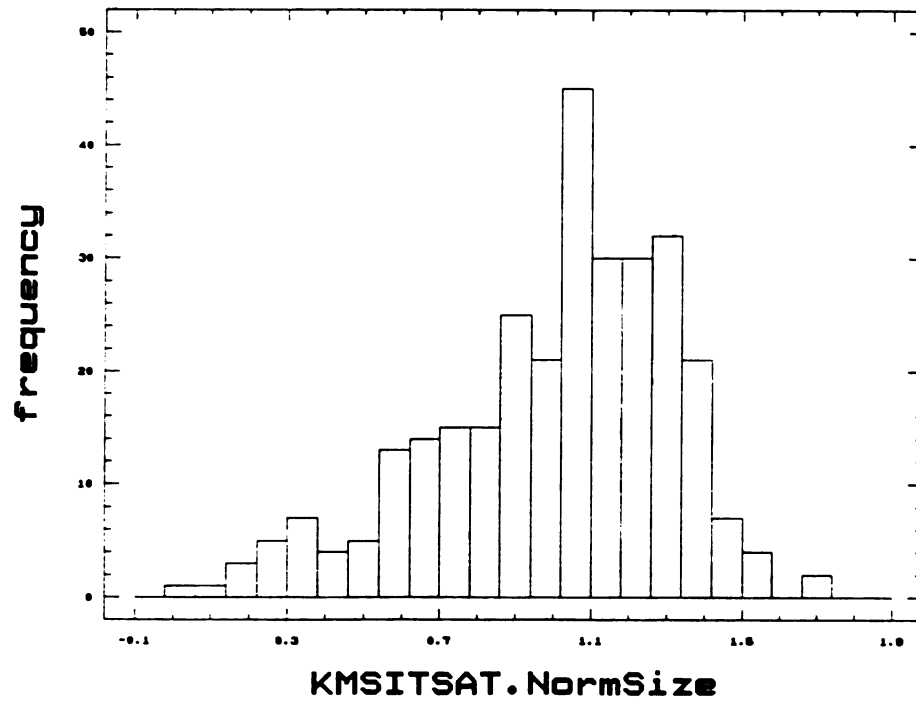




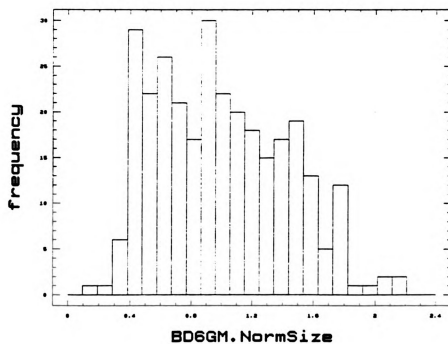
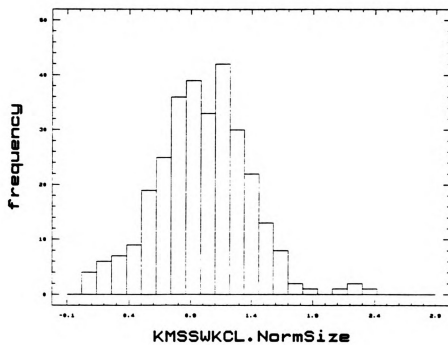


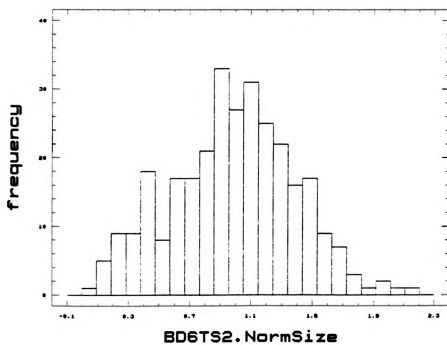
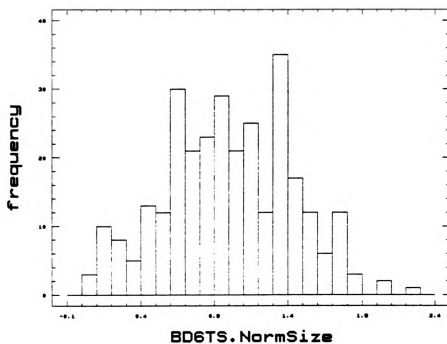












## **BIBLIOGRAPHY**

- Beaumont, C., Quinlan, G., and Hamilton, J., 1988  
Orogeny and Stratigraphy: Numerical models of the Paleozoic in the eastern interior of North America. *Tectonics*, 7 (3), 389-416.
- Breiman, Leo  
Statistics: With a View Toward Applications. Houghton Mifflin Co., Boston, MA, 1973.
- Brown, George D. Jr., and Lineback, Jerry A., 1966  
Lithostratigraphy of Cincinnati Series (upper Ordovician) in southeastern Indiana. *American Association of Petroleum Geologists Bulletin*, 50 (5) 1018-1032.
- Bury, Karl V.  
Statistical Models in Applied Science. John Wiley & Sons, New York, 1975.
- Carlson, W.D., 1989  
The significance of intergranular diffusion to the mechanisms and kinetics of porphyroblast crystallization. *Contributions to Mineralogy and Petrology*, 103 (1) pp. 1-24.
- Cashman, K.V., and Marsh, B.D., 1988  
Crystal Size Distribution (CSD) in Rocks and the Kinetics and Dynamics of Crystallization II: Makaopuhi lava lake. *Contributions to Mineralogy and Petrology*, 99, 292-305.
- Conover, W.J.  
Practical Nonparametric Statistics. John H. Wiley & Sons, Inc., New York, 1971.
- Cumings, E.R., 1908  
The stratigraphy and paleontology of the Cincinnati Series of Indiana. *Indiana Department of Geology and Natural Resources Annual Report*, 32, 607-1188.
- Davis, John C.  
Statistics and Data Analysis in Geology. 2nd edition, John Wiley & Sons, Inc., New York, 1986.

Davis, R.A., 1986

Cincinnati Region: Ordovician stratigraphy near the southwest corner of Ohio. In Geological Society of America Centennial Field Guide - Southeastern Section. Geological Society of America, 1986.

Folk, Robert L.

Petrology of Sedimentary Rocks. Hemphil Publishing Co., Austin, Texas, 1980.

Friedman, G.M., 1965

Terminology of crystallization textures and fabrics in sedimentary rocks. *Journal of Sedimentary Petrology*, 35, 643-655.

Fridy, J.M., Marthinsen, K., Rouns, T.N., Lippert, K.B., Nes, E., and Richmond, O., Characterization of 3-D particle distributions and effects on recrystallization studied by computer simulation. in *Proc. of ICAA3, Trondheim, Norway, June 22-26, 1992*.

Frost, H.J., and Thompson, C.V., 1987

The effect of nucleation conditions on the topology and geometry of two-dimensional grain structures. *Acta Metallurgica*, 35 (2), pp. 529-540

Gregg, J.M., and Gerdemann, P.E.

Sedimentary facies, diagenesis, and ore distribution in the Bonnetterre Formation (Cambrian), southeast Missouri. In: Field Guide to the Upper Cambrian of Southeastern Missouri: Stratigraphy, Sedimentology and Economic Geology. Eds. Gregg, J.M., Palmer, J.M. and Kurtz, V.E., 1989, 43-55.

Gregg, J.M., and Howard, S., 1990

Crystallographic and mineralogic studies of Recent, peritidal dolomites, Ambergris Cay, Belize. (Abstract). *Geological Society of America Annual Meetings*, 22, 179.

Gregg, J.M., and Shelton, K.L., 1990

Dolomitization and dolomite neomorphism in the back reef facies of the Bonnetterre and Davis Formations (Cambrian), southeastern Missouri.. *Journal of Sedimentary Petrology*, 60, 539-562.

Gregg, J.M., and Sibley, D.F., 1984

Epigenetic dolomitization and the origin of xenotopic dolomite texture. *Journal of Sedimentary Petrology*, 54, 908-934.

Groeneveld, Richard A., 1991

An influence function approach to describing the skewness of a distribution. *The American Statistician*, 45 (2), 97-102.

Hartmann, Daniel, 1988

The Goodness-of-fit to Ideal Gauss and Rosin Distributions: A new grain-size parameter. Discussion. *Journal of Sedimentary Petrology*, 58, 5, 913-917.

Hatfield, Craig Bond, 1968

Stratigraphy and paleoecology of the Saluda Formation (Cincinnatian) in Indiana, Ohio, and Kentucky. Geological Society of America, Special Paper Number 95.

Holland, S.M., 1993

Sequence Stratigraphy of a Carbonate-Clastic Ramp: The Cincinnatian Series (Upper Ordovician) in its type area. Geological Society of America Bulletin, 105, 306-322.

Keith, B., 1985

Facies diagenesis and the upper contact of the Trenton Limestone of northern Indiana. In: Ordovician and Silurian Rocks of the Michigan Basin. Cercone, K.R. and Judai, J.M. (Eds.), Michigan Basin Geological Society Special Publication No. 4, pp. 15-32.

Kretz, R., 1974

Some models for the rate of crystallization of garnet in metamorphic rocks. Lithos, 7, pp. 123-131.

Krumbein, W.C., 1935

Thin-section mechanical analysis of indurated sediments. Journal of Geology, 43, 482-496.

Lorenz, B., 1989

Simulation of grain-size distributions in nucleation and growth processes. Acta Metallurgica, 37 (10), pp. 2689-2692.

Larikov, L.N., Karpovich, V.V., and Dneprenko, V.N., 1989

Computer analysis of regularities of nucleation and crystal growth in a solid. Cryst. Res. Technol., 24 (6), 579-583.

Mahin, K.W., Hanson, K., and Morris, J.W., Jr.

The computer simulation of homogeneous nucleation and growth processes. In Computer Simulation for Materials Applications, 1976, (ed., Arsenault, R., Simmons, J., and Beeler, J.), National Bureau of Standards, Gaithersburg.

Mahin, K.W., Hanson, K., and Morris, J.W., Jr., 1980

Comparative analysis of the cellular and Johnson-Mehl microstructures through computer simulation. Acta Metallurgica, 28, 443-453.

Marsh, B.D., 1988

Crystal Size Distribution (CSD) in Rocks and the Kinetics and Dynamics of Crystallization I: Theory. Contributions to Mineralogy and Petrology, 99, 277-291.

Marthinsen, K., Lohne, O., and Nes, E., 1989

The development of recrystallization microstructures studied experimentally and by computer simulation. Acta Metallurgica, 37 (1), 135-145.

- Miller, Michael, 1988  
Dolomitization and Porosity Evolution. PhD. Disertation, Michigan State University, East Lansing, Michigan.
- Moore, P.G.  
Principles of Statistical Techniques, Second Edition, pp. 164-199. Cambridge University Press, 1969.
- Neave, H.R., and Worthington, P.L.  
Distribution-Free Tests. Unwin Hyman, London, 1988.
- Nordeng, S. and Sibley, D.F., 1990  
 Diffusion Limited Growth of Dolomite, Saluda Formation, (Ordovician, Indiana). (Abstract). Geological Society of America Annual Meeting, 22, A178.
- Pingitore, N.E., Jr., 1982  
 The Role of Diffusion During Carbonate Diagenesis. *Journal of Sedimentary Petrology*, 52, 27-40.
- Russ, J.C.  
 Size distributions. In Practical Stereology, Chapter 4, pp. 53-72, Plenum Press, 1986.
- Saetre, T.O., Hunderi, O., and Nes, E., 1985  
 Computer Simulation of Primary Recrystallization Microstructures: The effects of nucleation and growth kinetics. *Acta Metallurgica*, 34 (6), 981-987.
- Sibley, D.F., 1990  
 Unstable to stable transformations during dolomitization.. *Journal of Geology*, 98, 739-748.
- Sibley, D.F., and Gregg, J.M., 1987  
 Classification of dolomite rock textures. *Journal of Sedimentary Petrology*, 57, 967-975.
- Siegel, Sydney  
Nonparametric Statistics for the Behavioral Sciences. McGraw Hill, 1956.
- Taylor, T.R., and Sibley, D.F., 1986  
 Petrographic and geochemical characteristics of dolomite types and the origin of ferroan dolomite in the Trenton Formation, Ordovician, Michigan Basin, USA. *Sedimentology*, 33, 61-66.

**Tweed, Cherry J., Hanson, Niels, and Ralph, Brian, 1983**

**Grain growth in samples of aluminum containing alumina particles. Metallurgical Transactions A, 14A, 2235-2243.**

**Vaz, M.Fatima, and Fortes, M.A., 1988**

**Grain Size Distribution: The Lognormal and Gamma Distribution Functions. Scripta METALLURGICA, 22, 35-40.**

**Vernon, R.,**

**Reactions in microstructure development. In Metamorphic Processes, Halstead Press, John Wiley & Sons, N.Y., 1975**

**Walters, Sylvia J., 1988**

**The Sedimentology and Depositonal Environment of the Saluda Formation (Upper Ordovician) on Highway 421, Jefferson County, Indiana. unpublished Masters thesis, University of Cincinnati, Cincinnati, Ohio.**

**Wilson, J.L., and Sengupta, A., 1985**

**The Trenton Formation in the Michigan Basin and environs: Pertinent questions about its stratigraphy and diagenesis. In Cercone, K.R. and Budai, J.M. (Eds.), Ordovician and Silurian rocks of the Michigan Basin. Michigan Basin Geological Society Special Publication No. 4, pp. 1-13.**